Louisiana State University
LSU Digital Commons

LSU Master's Theses | Graduate School

2010

Itraconazole loaded poly (lactic-co-glycolic) acid nanoparticles for improved antifungal activity

Nipur Rajan Patel
Louisiana State University and Agricultural and Mechanical College, npate11@tigers.lsu.edu

Follow this and additional works at: https://digitalcommons.lsu.edu/gradschool_theses


Part of the Engineering Commons

Recommended Citation
Patel, Nipur Rajan, "Itraconazole loaded poly (lactic-co-glycolic) acid nanoparticles for improved antifungal activity" (2010). *LSU Master's Theses*. 1382.
https://digitalcommons.lsu.edu/gradschool_theses/1382

This Thesis is brought to you for free and open access by the Graduate School at LSU Digital Commons. It has been accepted for inclusion in LSU Master's Theses by an authorized graduate school editor of LSU Digital Commons. For more information, please contact gradetd@lsu.edu.

www.manaraa.com

ITRACONAZOLE LOADED POLY(LACTIC-*CO*-GLYCOLIC) ACID NANOPARTICLES FOR IMPROVED ANTIFUNGAL ACTIVITY

A Thesis
Submitted to the graduate faculty of the
Louisiana State University and
Agricultural and Mechanical College
in partial fulfillment of the
requirements for degree of
Master of Science in Biological
and Agricultural Engineering
In
The Department of Biological and Agricultural Engineering

By
Nipur Rajan Patel
B.S., Louisiana State University, 2007
August 2010

www.manaraa.com

I dedicate this to the relentless pursuit of living a dream…

www.manaraa.com

Acknowledgements

I would like to thank the LSU Biological and Agricultural Engineering Department for providing me the opportunity and resources in my graduate studies. The faculty of the BAE department has been instrumental in my success and shaped me be an integral part of the research world. Of the faculty, my major advisor Dr. Cristina Sabliov has been especially guiding in my studies. She has provided the resources, knowledge, and motivation for a successful graduate career. It was extremely comforting to have an advisor that made every effort to ensure my success for the present and future and it was greatly appreciated. I would also like to thank Dr. Kenneth Damann Jr. of my committee for providing valuable knowledge and extending the resources of his lab in conducting my studies. It was his assistance that greatly furthered my studies and much would not have been possible without his genuine interest and help. For that I am forever grateful and thankful. Lastly of my committee, but certainly not the least, I would like to thank Dr. Fred Enright for sticking with me along the way and knowing that he was a source of knowledge and assistance if the need arose. Many others were kind to me and lent me their expertise along my graduate studies. Many thanks to Carlos Astete for being a great teacher and source of knowledge in the field of nanotechnology. I would like to thank Cathy DeRobertis for being a wonderful aid in the fungal studies and graciously lending me any assistance when needed. Thanks to Matt Brown for his extensive knowledge and help in microscopy studies, Claudia Leonardi for statistical analysis, and Erica Muse for assistance in all studies conducted. Lastly, I would like to thank my family, friends, and colleagues that have been there for me from the very beginning. My parents deserve much credit for raising me and molding me to be an adult, and my success is a by-product of their support. Many thanks to my friends Abitha Murugeshu, Beatrice Terigar, Akanksha Kanitkar, Derek Brown, Quoc Nguyen and Keith Miller for being a source of support and laughter throughout my graduate career.

www.manaraa.com

Table of Contents

www.manaraa.com

www.manaraa.com

List of Tables

www.manaraa.com

List of Figures

www.manaraa.com

www.manaraa.com

www.manaraa.com

www.manaraa.com

www.manaraa.com

Abstract

PLGA (polylactic-*co*-glycolic acid) nanoparticles containing the hydrophobic antifungal Itraconazole (ITZ) were developed to address the need for more efficient means of treating fungal infections. PLGA-ITZ nanoparticles were synthesized using an oil-in-water emulsion evaporation method. The nanoparticles morphology (TEM), size and size distribution, zeta potential (DLS), encapsulation efficiency (UV-VIS), release profile, and antifungal activity were characterized. The blank NPs and loaded PLGA-ITZ NPs were spherical with diameters of 201±5 nm, 232±1 nm and 223±36 nm at 0%, 12.5% and 25% loadings, respectively. All synthesized particles measured a negative zeta potential ranging from -28 to -33 mV. The maximum encapsulation efficiency of ITZ was ~96% at 12.5% w/w theoretical loading. ITZ release showed an initial burst followed by a gradual release profile, with 75% ITZ released over 5 days. PLGA-ITZ nanoparticles inhibited *Aspergillus flavus* fungal growth more efficiently than free and emulsified ITZ. Quantitative fluorescence experiments performed with a GFP-expressing *A. flavus* verified that the PLGA-ITZ NPs had superior inhibitory activity at lower ITZ concentrations compared to free and emulsified ITZ drug formulations. PLGA-ITZ nanoparticles (232 nm) completely inhibited *Aspergillus flavus* growth over 11 days at 0.3 mg/ml ITZ, a concentration 100x less than free and emulsified ITZ. In nanoparticle uptake studies, 203 nm fluorescent PLGA nanoparticles containing coumarin-6 were seen associating with fungal cell surfaces and internalizing efficiently, while 1206 nm particle uptake was sporadic. Quantitative fluorescence experiments of PLGA-ITZ NPs of 232 nm, 630 nm, and 1060 nm showed inhibitory differences at the lowest ITZ concentration of 0.003 mg/ml, and no differences at higher concentrations. The PLGA-ITZ nanoparticle system is envisioned to increase bioavailability of ITZ by improving its aqueous solubility, controlling its release over

www.manaraa.com

time and especially increasing antifungal penetration at the cellular level by efficient nanoparticle uptake by cells, thereby elevating antifungal efficacy.

www.manaraa.com

Chapter 1. Introduction

The frequency of acquiring bacterial, viral, or fungal infectious diseases increases each year due to the ease of transmission from person to person [1]. Swift and effective treatment options are a necessity to avoid spreading of disease to peripheral organs and potential death [2-3].

Of the many forms of infection, fungal infections can be easily acquired and are known to persist over time, causing great discomfort. Approximately 1.5 million fungal species exist on earth and according to some this number is increasing [4]. Because a large number of species exist coming in contact with fungal species can occur from a range of locations, especially moist areas. Some common species known to result in infection are *Aspergillus*, *Candida*, *Tinea*, *Pneumocystis*, *Cryptococcus*, and *Histoplasma* [5]. Superficial infections, a subset of fungal infections, caused by such species include conditions such as athlete's foot, finger and toe nail infections, yeast infections, oral thrush, and ringworm. There are also systemic and opportunistic fungal infections which can enter the bloodstream and result in more serious disease, particularly in those with compromised immune systems [6-8]. *Aspergillus* species are among the more life threatening species that result in opportunistic mycoses and will be focused on in the present study [9-11]. Aspergillosis is one such disease of the lungs, where an aspergilloma, or fungal ball, forms in the preexisting cavity in the lung parenchyma [12-15]. Treating patients with underlying diseases tends to be difficult due to the lack of efficient pharmaceutical drugs. Treatment of most fungal infections/diseases occurs via oral formulation or intravenous injection; however, due to a wide bio-distribution of drugs to various tissues, the amount actually reaching the target site is limited. The body deals with ingested drugs by absorption, distribution, metabolization, and excretion [16-17]. Through these processes, much of the drug can be degraded, renally excreted, or transformed in the liver to an inactive metabolite, reducing the amount of active agent circulating through the

www.manaraa.com

bloodstream. Hence, high drug dosing is sometimes required for proper treatment translating into potential toxicity, and increased treatment costs. For example, Itraconazole, a broad spectrum triazole is normally prescribed as an oral formulation at dosages of 200 mg per day and 400 mg per day for serious infections, which can lead to potential toxicity [18]. A prescription of 180 generic capsules at 100 mg per dose can potentially cost patients $360 [19]. More efficient means of delivery are needed in order to combat fungal diseases and reduce treatment costs.

One solution increasingly investigated in the past decade is the use of nanoparticulate drug delivery systems of various types, including polymeric nanoparticles. These nano sized vesicles have shown to be effective vectors for drug delivery by being able to provide protection to active agents from premature degradation, increased retention times, increased bioavailability, controlled drug release, and penetration into certain pathologies [20-22]. Polymeric nanoparticles applications are wide spread in areas of gene therapy, protein delivery, and targeted cancer therapies due to their bio-friendly and tunable properties [23-25]. The characteristics that define the particle's behavior are dictated by the polymer type, size, and surface charge [26]. Smaller sized particles have shown great benefit by facilitating drug penetration into tissue through various sized fenestrations, while avoiding defense mechanisms [27-29]. However, if particles are large (~1µm) and surfaces contain strong polycationic or hydrophobic properties, opsonins and macrophages can be attracted, reducing retention times. The polymer type can play a large role in how the delivery system will react in various environments. A variety of polymers may be employed to synthesize nanoparticles intended for particular applications. Chitosan, for example, is a naturally occurring linear polysaccharide derived by the deacetylation of chitin. Its use comes predominantly in gene therapy as a non-viral vector due to its strong polycationic properties and complexation ability with DNA [30-32]. As an alternative to natural polymers, synthetic polymers have increasingly gained interest

www.manaraa.com

in drug delivery due to their biocompatible nature and controllable release characteristics. Polylactides (PLA), polyglycolides (PGA), polyanhidrides, and poly (lactide-co-glydolides) (PLGA), to name a few, are some commonly used polymers in drug delivery. PLGA, in particular, is an FDA approved co-polymer that has been used widely in drug delivery due to its controllable release characteristics (Figure 1.1) [33]. This can be achieved by varying the molar ratio of its monomers lactic and glycolic acid, altering its degradation rate. PLGA degradation occurs primarily through hydrolysis of the ester linkages, producing by-products of lactic acid and glycolic acid which are normally removed from the body. PLGA is particularly of use for entrapping hydrophobic compounds (i.e. Itraconazole), that otherwise have poor systemic bioavailability due to premature degradation, clearance, and specific solubility requirements [34-35]. Entrapment of hydrophobic drugs into polymeric nanoparticles improves drug dispersibility and allows adequate time for active agents to reach target/infected sites [36]. Synthesis of PLGA nanoparticles can be conducted by an emulsion-solvent evaporation technique in the presence of a surfactant (i.e. polyvinyl alcohol), providing stability and preventing aggregation (Figure 1.2) [37].

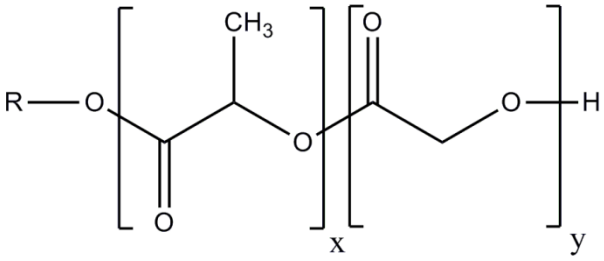

Figure 1.1: PLGA structure

The present study attempts to entrap Itraconazole in PLGA nanoparticles formed with PVA and improve the functionality of the antifungal compared to commercially available Itraconazole. The thesis is organized in 3 main chapters. Following Chapter 1- Introduction, Chapter 2 focuses on nanoparticle synthesis, characterization (size, zeta potential, morphology, encapsulation efficiency, release profile), and *in-vitro* qualitative and quantitative antifungal studies of PLGA nanoparticles with entrapped Itraconazole (PLGA-ITZ) against *Aspergillus flavus*. Chapter 3 will then present information on the effect of nanoparticle size on fungal uptake and antifungal activity.

www.manaraa.com

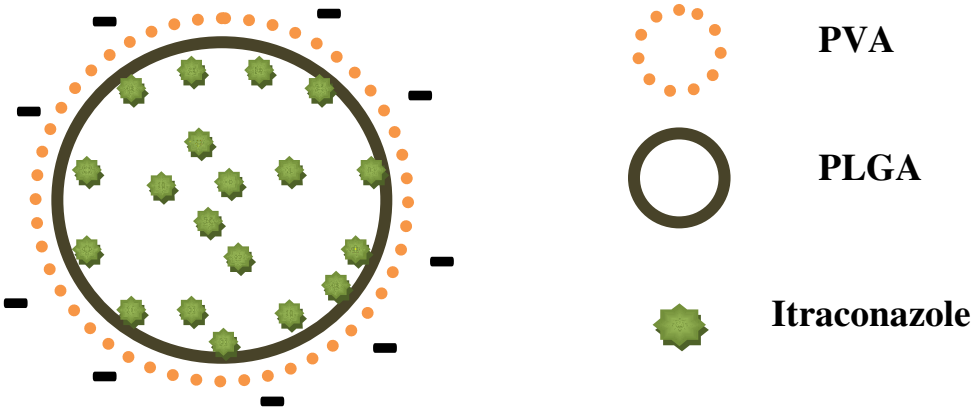

Figure 1.2: Schematic representing nanoparticle components, including the polymer (PLGA), surfactant (PVA), and drug (Itraconazole).

1.1 References

1. Pinner Rw, Teutsch Sm, Simonsen L *et al.*: Trends in infectious diseases mortality in the united states. *JAMA* 275(3), 189-193 (1996).

2. Armstrong Gl, Conn La, Pinner Rw: Trends in infectious disease mortality in the united states during the 20th century. *JAMA* 281(1), 61-66 (1999).

3. Morens Dm, Folkers Gk, Fauci As: The challenge of emerging and re-emerging infectious diseases. *Nature* 430(6996), 242-249 (2004).

4. L. Hawksworth D: The magnitude of fungal diversity: The 1·5 million species estimate revisited. *Mycological Research* 105(12), 1422-1432 (2001).

5. Peters Wag, H.M.: Colour atlas of tropical medicine and parasitology. Mosby-Wolfe, (1995).

6. Rolando N, Harvey F, Brahm J *et al.*: Fungal infection: A common, unrecognised complication of acute liver failure. *Journal of Hepatology* 12(1), 1-9 (1991).

7. Richardson Md: Changing patterns and trends in systemic fungal infections. *J. Antimicrob. Chemother.* 56(suppl_1), i5-11 (2005).

8. Degregorio Mw, Lee Wmf, Linker Ca, Jacobs Ra, A. Ries C: Fungal infections in patients with acute leukemia. *The American Journal of Medicine* 73(4), 543-548 (1982).

9. Anaissie E: Opportunistic mycoses in the immunocompromised host: Experience at a cancer center and review. *Clinical Infectious Diseases* 14(ArticleType: primary_article / Issue Title:

www.manaraa.com

Supplement 1. Focus on Fungal Infections: An Update on Diagnosis and Treatment / Full publication date: Mar., 1992 / Copyright © 1992 The University of Chicago Press), S43-S53 (1992).

10. Lass-Florl C, Kofler G, Kropshofer G *et al.*: In-vitro testing of susceptibility to amphotericin b is a reliable predictor of clinical outcome in invasive aspergillosis. *J. Antimicrob. Chemother.* 42(4), 497-502 (1998).

11. Tolkoff-Rubin N, Rubin R: Opportunistic fungal and bacterial infection in the renal transplant recipient. *J Am Soc Nephrol* 2(12), S264-269 (1992).

12. Denning Dw: Invasive aspergillosis. *Clinical Infectious Diseases* 26(4), 781-803 (1998).

13. Dutkiewicz R, Hage Ca: Aspergillus infections in the critically ill. *Proc Am Thorac Soc* 7(3), 204-209 (2010).

14. Denning Dw, Stevens Da: Antifungal and surgical treatment of invasive aspergillosis: Review of 2,121 published cases. *Reviews of Infectious Diseases* 12(6), 1147-1201 (1990).

15. Aisner J, Schimpff Sc, Wiernik Ph: Treatment of invasive aspergillosis: Relation of early diagnosis and treatment to response. *Annals of Internal Medicine* 86(5), 539 (1977).

16. Davis A: Medicines by design. *NIH* 6(474), 4-14 (2006).

17. Kopacek Kb: Administration and kinetics of drugs *The Merck Manuals*, (2007).

18. Gillies J, Hung Ka, Fitzsimons E, Soutar R: Severe vincristine toxicity in combination with itraconazole. *Clinical & Laboratory Haematology* 20(2), 123-124 (1998).

19. Bootman Jl: Cost-effectiveness of two new treatments for onychomycosis: An analysis of two comparative clinical trials. *Journal of the American Academy of Dermatology* 38(5, Supplement 2), S69-S72 (1998).

20. Soppimath Ks, Aminabhavi Tm, Kulkarni Ar, Rudzinski We: Biodegradable polymeric nanoparticles as drug delivery devices. *Journal of Controlled Release* 70(1-2), 1-20 (2001).

21. Rabinow Be: Nanosuspensions in drug delivery. *Nat Rev Drug Discov* 3(9), 785-796 (2004).

22. Leroux J-C, Allémann E, De Jaeghere F, Doelker E, Gurny R: Biodegradable nanoparticles -- from sustained release formulations to improved site specific drug delivery. *Journal of Controlled Release* 39(2-3), 339-350 (1996).

23. Hans Ml, Lowman Am: Biodegradable nanoparticles for drug delivery and targeting. *Current Opinion in Solid State and Materials Science* 6(4), 319-327 (2002).

www.manaraa.com

24. Nagarwal Rc, Kant S, Singh Pn, Maiti P, Pandit Jk: Polymeric nanoparticulate system: A potential approach for ocular drug delivery. *Journal of Controlled Release* 136(1), 2-13 (2009).

25. Fonseca C, Simões S, Gaspar R: Paclitaxel-loaded plga nanoparticles: Preparation, physicochemical characterization and in vitro anti-tumoral activity. *Journal of Controlled Release* 83(2), 273-286 (2002).

26. Mohamed F, Walle Cfvd: Engineering biodegradable polyester particles with specific drug targeting and drug release properties. *Journal of Pharmaceutical Sciences* 97(1), 71-87 (2008).

27. Desai Mp, Labhasetwar V, Amidon Gl, Levy Rj: Gastrointestinal uptake of biodegradable microparticles: Effect of particle size. *Pharmaceutical Research* 13(12), 1838-1845 (1996).

28. Brannon-Peppas L, Blanchette Jo: Nanoparticle and targeted systems for cancer therapy. *Advanced Drug Delivery Reviews* 56(11), 1649-1659 (2004).

29. Gaumet M, Vargas A, Gurny R, Delie F: Nanoparticles for drug delivery: The need for precision in reporting particle size parameters. *European Journal of Pharmaceutics and Biopharmaceutics* 69(1), 1-9 (2008).

30. Bozkir A, Saka Om: Chitosan nanoparticles for plasmid DNA delivery: Effect of chitosan molecular structure on formulation and release characteristics. *Drug Delivery* 11(2), 107 - 112 (2004).

31. Gan Q, Wang T: Chitosan nanoparticle as protein delivery carrier--systematic examination of fabrication conditions for efficient loading and release. *Colloids and Surfaces B: Biointerfaces* 59(1), 24-34 (2007).

32. Tiyaboonchai W: Chitosan nanoparticles : A promising system for drug delivery. *Naresuan University Journal* 11(3), 51-66 (2003).

33. Kim D-H, Martin Dc: Sustained release of dexamethasone from hydrophilic matrices using plga nanoparticles for neural drug delivery. *Biomaterials* 27(15), 3031-3037 (2006).

34. Sahana Dk, Mittal G, Bhardwaj V, Kumar Mnvr: Plga nanoparticles for oral delivery of hydrophobic drugs: Influence of organic solvent on nanoparticle formation and release behavior in vitro and in vivo using estradiol as a model drug. *Journal of Pharmaceutical Sciences* 97(4), 1530-1542 (2008).

35. Mainardes Rm, Evangelista Rc: Praziquantel-loaded plga nanoparticles: Preparation and characterization. *Journal of Microencapsulation: Micro and Nano Carriers* 22(1), 13 - 24 (2005).

المنارة للاستشارات
www.manaraa.com

36. Pandey R, Ahmad Z, Sharma S, Khuller Gk: Nano-encapsulation of azole antifungals: Potential applications to improve oral drug delivery. *International Journal of Pharmaceutics* 301(1-2), 268-276 (2005).

37. Pinto Reis C, Neufeld Rj, Ribeiro Aj, Veiga F: Nanoencapsulation i. Methods for preparation of drug-loaded polymeric nanoparticles. *Nanomedicine: Nanotechnology, Biology and Medicine* 2(1), 8-21 (2006).

www.manaraa.com

Chapter 2. In-vitro Antifungal Studies of Itraconazole Loaded PLGA Nanoparticles Against *Aspergillus flavus*

2.1 Introduction

The percentage of immune-compromised individuals vulnerable to fungal infections is constantly increasing due to the increase in HIV/AIDS, transplant surgeries, cancer, and various underlying diseases [1]. The high frequency of infections associated with increased cost, has placed a need for highly efficacious, less toxic drugs for treatment of fungal infections. Itraconazole (ITZ) is a broad spectrum triazole antifungal that is used in treating and preventing fungal infections, such as those commonly caused by *Candida albicans* and *Aspergillus* species. Amphotericin B is another common drug shown to be effective in treating endemic mycoses; although it is known to cause severe side effects such as nephrotoxicity [2-3]. Other azole antifungals, such as fluconazole, voriconazole, and ketoconazole, may be used; however ITZ shows better efficacy and less resistance by various fungal species [4].

The main drawback associated with ITZ is its low oral absorption. ITZ is a highly hydrophobic weak base with a low aqueous solubility of approximately 1 ng/ml at pH 7 [5]. An acidic medium, such as the gastric environment of the stomach, favors its solubilization (4 µg/ml at pH 1), which increases ITZ absorption [5]. It is recommended that ITZ be ingested with food to stimulate gastric secretion, which can increase ITZ bioavailability [6]. This can be troublesome for individuals that have underlying sicknesses as food intake may be limited due to nausea and vomiting, and GI tract complications that can hinder absorption, as is the case of those undergoing chemotherapy. An intravenous formulation is available that solubilizes Itraconazole by complexing with hydroxypropyl-β-cyclodextrin (HP-β-CD). However, the accumulation of HP-β-CD can potentially lead to toxicity limiting the frequency of intravenous doses [7]. This is most notably a concern for patients with renal complications, since the reduced clearance rate of HP-β-CD can

www.manaraa.com

reach toxic levels [8-9]. To address these limitations, there is a need for more efficient and effective means of delivery that maximizes ITZ bioavailability and increases its dispersibility at physiological pH.

Recently, many advances in nano drug delivery systems have been made to improve the efficacy of various drugs. Due to their small size, these nanosized structures are able to cross biological barriers, improving drug bioavailability in areas of interest [10]. Polymeric nanoparticles (NPs) composed of PLGA (polylactic-*co*-glycolic acid), have been used as a means of drug delivery due to their biodegradable and biocompatible nature, and controllable release characteristics [10-11]. Entrapping bioactive components such as ITZ into these particles protects the drug from premature degradation, increases drug dispersibility, and releases the contents gradually to reach therapeutic levels [12]. The combined effect of these factors can lead to increased bioavailability and effectiveness. PLGA has also been actively utilized as a vector for transporting chemotherapeutic and antibacterial drugs, attaining sustained and targeted drug concentrations at infected areas. Studies have shown cellular uptake of PLGA nanoparticles against various cancer cell lines, improving drug efficacy and minimizing deposition in peripheral tissue [13-17]. Esmaeili et al (2007) loaded PLGA NPs with the antibacterial rifampicin and showed four times greater antibacterial activity compared to free rifampicin; they surmised this could possibly be from enhanced penetration of bacterial cells [18]. Cellular uptake in fungal spores has not been completely elucidated, however, but studies have shown increased efficacy against fungal species when PLGA was used as a delivery vector. For example, Amphotericin B was entrapped into PLGA nanoparticles and showed improved oral bioavailability and minimized toxicity compared to a commercially available form [19]. Similarly, Peng et al (2008) showed the effects of voriconazole entrapped PLGA NPs against free voriconazole using tubes containing yeast cells in Sabouraud's

www.manaraa.com

dextrose broth [20]. Voriconazole NPs showed a more potent antifungal effect compared to free voriconazole. In each case, the underlying theme was the improved dispersibility, resulting in increased bioavailability and sustained drug concentrations compared to free drug formulations. These characteristics make PLGA an attractive polymer for drug delivery, as toxicity due to high drug dosing and the associated cost are problems that must be addressed [21-22].

The purpose of this study was to develop a nanocarrier drug delivery system for encapsulation of the hydrophobic drug ITZ into PLGA and to test the antifungal capability of the NPs with entrapped ITZ (PLGA-ITZ NPs) *in-vitro*. The ability of the ITZ entrapped nanoparticles to gradually release the drug and inhibit fungal growth over time was compared against two other treatments of ITZ in water (Water-ITZ), and an emulsion of ITZ in 0.03% Triton X-100 (Tx-ITZ) over eleven days. Growth inhibition of *Aspergillus* on culture plates and on microscope slides was observed to show the increased effect by PLGA-ITZ NPs, followed by a study on GFP- expressing *Aspergillus flavus* to quantify fungal inhibition using a fluorescent plate reader. Spores were treated at the time of seeding, and 12 hours later to show antifungal efficacy at different growth periods. *Aspergillus* species are among the more life threatening fungal infections with a 40% mortality rate, and thus was selected as a model fungus in this study [23-24]. The *in-vitro* results reported herein not only highlight visually the improved antifungal activity of entrapped ITZ, but also provide quantitative evidence of improved antifungal activity of the entrapped drug, adding to the available literature on antifungal nanoparticle delivery, predominantly conducted *in-vivo*.

2.2 Materials and Methods

2.2.1 Materials

Itraconazole, PLGA (50/50) 5-15 kDa, acetonitrile, dichloromethane, polyvinyl alcohol (31-50 kDa), and Triton X-100 were purchased from Sigma Chemical Co. (St. Louis, MO). Potato

www.manaraa.com

dextrose agar was made from potatoes according to the Bacteriological Analytical Manual [25]. *Aspergillus flavus 1298* and *Aspergillus flavus*70s GFP [26], were acquired from ARS USDA Southern Regional Research Center (New Orleans, LA). Corning Costar black clear bottom 96 well plates were acquired from Fisher Scientific (Pittsburgh, PA).

2.2.2 Polylactic-*co*-glycolic acid-Itraconazole Nanoparticle Synthesis

The unloaded PLGA nanoparticles and the ITZ loaded nanoparticles were synthesized by an emulsion-solvent evaporation method, purified by dialysis, and freeze-dried for further analysis. PLGA-ITZ nanoparticle synthesis was carried out by emulsion evaporation as follows. A 1% (w/v) PLGA solution was formed by dissolving 50:50 PLGA in Dichloromethane (DCM). ITZ (6.4 mg) was dissolved into 5 ml of 1% (w/v) PLGA in DCM to form an organic phase at 1:8 w/w Itraconazole:PLGA ratio. The organic phase was added to 50 ml of 0.3% (w/v) polyvinyl alcohol aqueous solution under mixing using an Ultra Turrax t-18 basic (IKA Works, Wilmington, NC). Sonication was then performed for 10 minutes with pulses of 2 seconds on and 2 seconds off, in order to form a (O/W) micro-emulsion using a Vibra Cell vc 750 (Sonics, Newton, CT). The DCM was then removed from the mixture by evaporation with a Rotovapor R-124 (Buchi, Switzerland). The evaporation of the organic solvent allowed for the formation of the nanoparticles and the encapsulation of ITZ within the polymeric matrix. Empty PLGA nanoparticles were synthesized following the same procedure, with the exception that no ITZ was added to the organic phase.

A dialysis step was applied immediately following synthesis to remove excess surfactant and associated ITZ from the solution. Any ITZ not removed by this method, whether entrapped or marginally associated with the surface of the particle, was considered entrapped. A Specrta/Por CE cellulose ester membrane (Spectrum, Rancho Dominquez, CA) with a molecular weight cut-off of 100 kDa was used. The nanoparticles underwent dialysis in a 2.5 L tank with nano-pure water, at a

www.manaraa.com

ratio of 100:1 nano-pure water to NP, for eight hours, changing the water after four hours to facilitate the dialysis process.

Following purification, a freeze-drying step was applied to remove the water from the nanoparticle suspension. The nanoparticle suspension was freeze-dried at -80°C at a reduced pressure of 0.13 Pa for a period of 48 hours using a Freezone 4.5 (Labconco, Kansas City, MO). After freeze drying, the nanoparticles were stored at -8°C prior to further analysis.

2.2.3 Nanoparticle Characterization

The morphology of the nanoparticles was studied by Transmission Electron Microscopy (TEM) using a JEOL 100-CX (JEOL USA Inc., Peabody, MA) system. One droplet of the nanoparticle suspension was placed on a polymer coated copper grid of 400 mesh with a carbon film, and the excess sample was removed with filter paper. Uranyl acetate 2% was used as a stain; the excess was removed after 1 min and the sample was dried before analysis by TEM.

Nanoparticles were tested for size, size distribution, and zeta potential by dynamic light scattering (DLS) using the Malvern Zetasizer Nano ZS (Malvern Instruments Inc., Southborough, MA). In all cases, a volume of 1.3 ml of each sample at a concentration of 0.3 mg/ml was placed in a polystyrene cuvette and measured at 25ºC at pH 6.5. The mean values of size and PDI were determined using a mono-modal distribution.

2.2.4 Encapsulation Efficiency

Encapsulation efficiency (EE) of ITZ was calculated by resuspending 3 mg of the freeze-dried nanoparticles in 1 ml of 95:5 (v/v) acetonitrile:water solution. Disruption of particles was assisted by 20 seconds sonication, and then the suspension centrifuged for 30 min at 30,000 rpm to remove the disrupted polymer. ITZ absorbance in the supernatant was measured at 300 nm with a

www.manaraa.com

Genesys 6 spectrophotometer (ThermoSpectronic Rochester, NY), and the concentration determined using a standard curve of Itraconazole in 95:5 (v/v) acetonitrile:water solution. The efficiency was reported as the ratio of the amount of ITZ entrapped in the recovered nanoparticles to the theoretically added.

2.2.5 Itraconazole Drug Release

The drug release profile was determined by resuspending the nanoparticles at 3mg/ml in PBS at pH 7. One ml aliquots of the suspension were pippetted into ten, 1.7 ml centrifuge tubes. The tubes, placed in an incubator shaker at 37ºC and 150 rpm, were removed at 0, 8, 24, 32, 48, 56, 72, 80, 96, 104 hours. Tubes were centrifuged at 30,000 rpm for 1 hour, the supernatant decanted and NPs recovered. NP pellets were disrupted by adding 95:5 acetonitrile in water and 20 seconds of sonication. Samples were centrifuged for 30 min at 30,000 rpm to remove the disrupted polymer, and ITZ in the supernatant was quantified via UV spectrophotometry at 300 nm, as done in the encapsulation efficiency method (see above).

2.2.6 Fungal Growth Inhibition Studies

The antifungal ability of the nanoparticles with entrapped ITZ was tested on fungal growth in three ways: growth inhibition on a lawn of conidia in a Petri plate; growth inhibition of mycelia growing into a treated area on a microscope slide; fluorescence inhibition of a GFP-expressing *A. flavus* in a 96-well plate assay. PLGA-ITZ NPs were compared against two drug formulations consisting of ITZ in water (Water-ITZ) and an emulsion of ITZ in 0.03% Tx-100 (Tx-ITZ).

2.2.6.1 *A. flavus* Petri Plate Culture

Potato dextrose agar plates were inoculated by spreading 10 µl of conidial suspension at $1x10^5$ spores/ml of *Aspergillus flavus* over the plate. Three different treatments (10 µl) were

www.manaraa.com

pippetted onto the plates: Water-ITZ at 0.3 mg/ml, Tx-ITZ emulsion at 0.3 mg/ml, and PLGA-ITZ NP suspensions at 10 and 1mg/ml (equivalent to 0.3, 0.03 mg/ml of ITZ respectively). The plates were incubated at 37ºC. Digital photos of the cultures were taken after treatments were initiated and on the third through the fifth day to assess the antifungal activity.

2.2.6.2 Microscope Slide Culture

Further qualitative evidence of the PLGA-ITZ NPs inhibiting *A. flavus* was acquired by observing the effects of the treatments on a line of fungus growing into treated areas. A mercerized cotton covered polyester thread (~4 inches) was dipped into ~1ml of 1% protamine sulfate in an Eppendorf tube, removed and allowed to air dry. The thread was then immersed in a conidial suspension ($1x10^5$ spores/ml) of *A.flavus* in an Eppendorf tube, removed and stretched across the center of a rectangular piece of potato dextrose agar on a 1.5x3 inch microscope slide. The ends of the thread were secured to the slide by tape. Treatments (2 µl) of Water-ITZ at 30, 3, and 0.3 mg/ml, Tx-ITZ emulsion at 30, 3, and 0.3 mg/ml, PLGA-blank NPs at 10 mg/ml and PLGA-ITZ NPs at 10 and 1mg/ml (equivalent to 0.3, 0.03 mg of ITZ respectively), were spotted 10 mm above the thread and the extent of inhibition beyond the point of application was observed over 5 days at 37ºC.

2.2.6.3 GFP-Expressing *A. flavus* Fluorescence Quantification

Quantification of growth inhibition was done by using a GFP expressing *Aspergillus flavus*, on the basis that biomass was directly proportional to fluorescence. Black clear bottom 96 well plates were inoculated with 50µl of a conidial suspension ($5x10^5$ spores/ml) containing 200 µl of 1.25x glucose salts medium [27]. Different concentrations of ITZ in water (30, 3, 0.3, 0.03 mg/ml), Tx-ITZ emulsion (at 30, 3, 0.3, 0.03 mg/ml ITZ), blank NPs at 10 mg/ml and PLGA-ITZ NPs at 10, 1, 0.1 mg/ml (equivalent to 0.3, 0.03, 0.003 mg/ml ITZ respectively) were tested. The four

www.manaraa.com

treatments (10 µl) were added immediately following inoculation (0 h) and 12 hours after inoculation (12 h) to the respective wells to assess the ability of the particles to inhibit growth. Fluorescent measurements were taken once a day for eleven days using a Synergy HT Multi-Mode Microplate Reader (BioTek, Winooski, VT), at excitation and emission wavelengths of 485 nm and 528 nm, respectively. Fluorescence drop off in latter parts of study were indicative of accumulation of waste-by product. Fluorescence values are the mean of 3 replications.

The natural log of fluorescence was analyzed using the MIXED procedure of SAS (SAS system, SAS Institute Inc., Cary, NC). The two treatment testings (0 h and 12 h) were analyzed separately. The two initial models included the fixed effects of treatment, concentration, time and their two- and three-way interactions. Time was analyzed as repeated measures using the covariance structure that best fitted the data based on the Akaike Information Criterion. The treatment by concentration by day interaction was significant ($P< 0.0001$) for both treatment testing (0h and 12 h); therefore treatments were compared over time separately at the various ITZ concentrations. For the 0 h treatment testing, day 0 was not included into the analysis because fluorescence was ≤ 1 for all treatments. The statistical analysis focused on days 1 to 5 for the 0 h testing (Appendix A-Tables S1 to S3) and the first 5 days for 12 h treatment testing (Appendix A-Tables S4 to S6), where most growth and antifungal activity occurred. Within each ITZ concentration the model included the fixed effects of treatment, time and their interaction. Time was analyzed as repeated measures using the covariance structure that best fitted the data based on the Akaike Information Criterion. When the treatment by day interaction was significant, comparisons between means were performed using the Tukey *post-hoc* multiple test adjustment. Statistical significance was declared at $P \leq 0.05$.

www.manaraa.com

2.3 Results

2.3.1 Nanoparticle (NP) Characterization: Size, Zeta Potential, Morphology, Encapsulation Efficiency, Release

Table 1 summarizes the size, PDI, zeta potential, and encapsulation efficiency (EE) for PLGA-blank NPs and loaded PLGA-ITZ NPs. Size measured via DLS reported blank PLGA nanoparticles of 201±5 nm and loaded PLGA-ITZ NPs at 12.5% and 25% loadings at 232±1 and 223±36 nm, respectively (Table 2.1). The PDI ranged from 0.01 to 0.213 and the zeta potential was negative for all particle types ranging from -28 to -33 mV. This negative charge helped in stabilizing the particles by charge repulsion.

Table 2.1: Summary of polylactic-*co*-glycolic acid-Itraconazole nanoparticle (PLGA-ITZ NP) characteristics: Size, PDI, zeta potential and encapsulation efficiency

NP Type	Theor. Loading (%w/w)	Size (nm)	PDI	Zeta (mV)	EE (%)
Empty PLGA	0	201 ± 5	0.010±0.031	-33 ± 8	N/A
PLGA-ITZ	12.5	232 ± 1	0.213±0.035	-31 ± 5	96 ±7
PLGA-ITZ	25.0	223 ± 36	0.175±0.112	-28 ± 6	46 ± 2

TEM pictures confirmed that particles were spherical in morphology with no visible aggregation (Figure 2.1). Size measured via DLS reported the hydrodynamic diameter, while that seen in the TEM photographs was the physical diameter of the dried particles (slightly smaller), hence the discrepancy between the two measurements. An encapsulation efficiency of approximately 96% was obtained at a theoretical loading of 12.5%. Increasing the theoretical loading to 25% decreased the efficiency to 46% for the given amount of polymer. For this reason, 12.5% PLGA-ITZ NPs were used in the subsequent studies.

www.manaraa.com

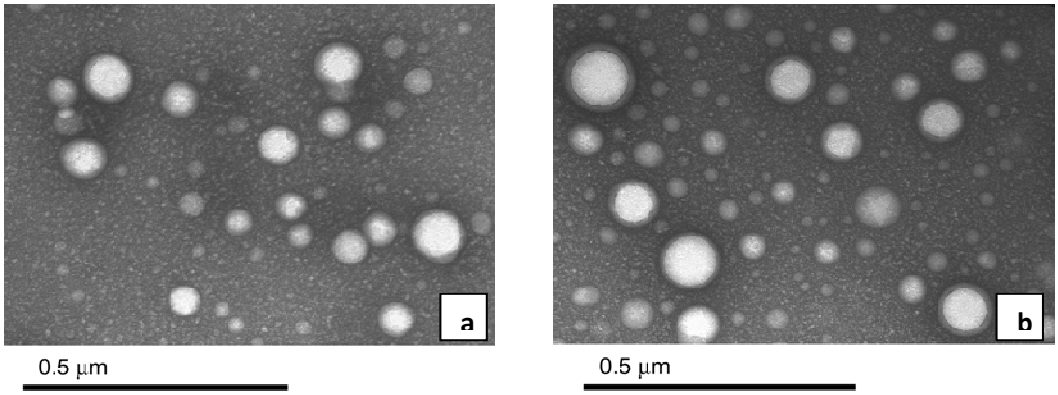

Figure 2.1: TEM pictures of (a) Blank polylactic-co-glycolic acid-Itraconazole nanoparticles and (b) loaded polylactic-co-glycolic acid-Itraconazole nanoparticles.

Itraconazole (ITZ) release from PLGA nanoparticles suspended in PBS at pH 7 was biphasic, with an initial jump of 20%, followed by a steady release over five days with 75% being released by the fifth day (Figure 2.2).

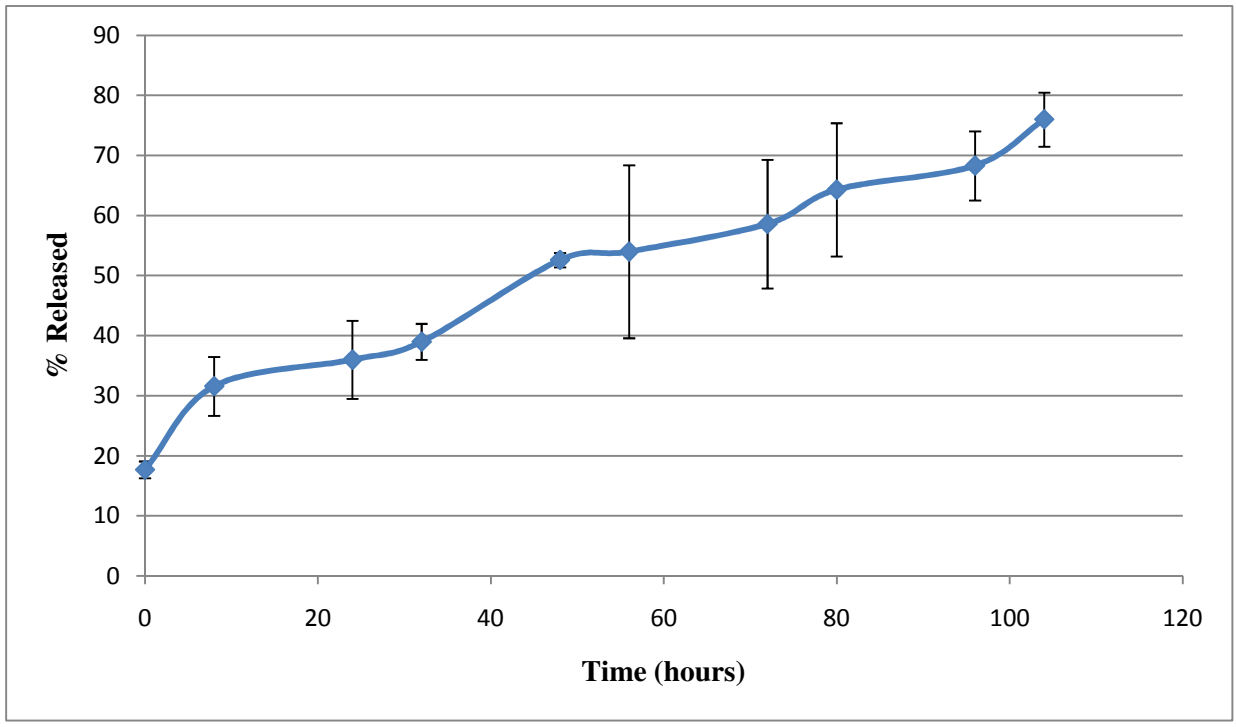

Figure 2.2: Release of ITZ from 12.5% (w/w ITZ:PLGA ratio) polylactic-*co*-glycolic acid-Itraconazole nanoparticles suspended in PBS pH 7 at 37ºC over 5 days (n=3). Release based on 85% encapsulation efficiency.

www.manaraa.com

2.3.2 *A. flavus* Growth Inhibition in Petri Plate Culture and Microscope Slide

Three treatments (Water-ITZ, Tx-ITZ emulsion, and PLGA-ITZ NPs) were tested on *Aspergillus flavus* (Figure 2.3); circled areas on culture plates indicate treatment placement.

The Water-ITZ and Tx-ITZ emulsion showed similar fungal inhibitory ability with Tx-ITZ having a slightly better effect (Figure 2.3a, 2.3b). Tx-ITZ showed moderate clearing near the applied drug at day three but as time progressed growth encroached the point of application (Figure 2.3b). In contrast, the PLGA-ITZ NPs showed greater inhibition compared to Water-ITZ and Tx-ITZ emulsion (Figure 2.4a, 2.4b). The PLGA-ITZ NP suspension (10mg/ml equivalent of 0.3 mg/ml ITZ) gave clear inhibition zones beyond the point of application (Figure 2.4a). Smaller inhibition zones were observed at lower NP concentration of PLGA-ITZ NPs (1mg/ml equivalent of 0.03 mg/ml of ITZ); however, even at this low particle concentration clear defined inhibition zones were seen rivaling what was observed in Water-ITZ and Tx-ITZ formulations. This indicated an enhanced antifungal capability of the PLGA-ITZ NPs in comparison to other formulations.

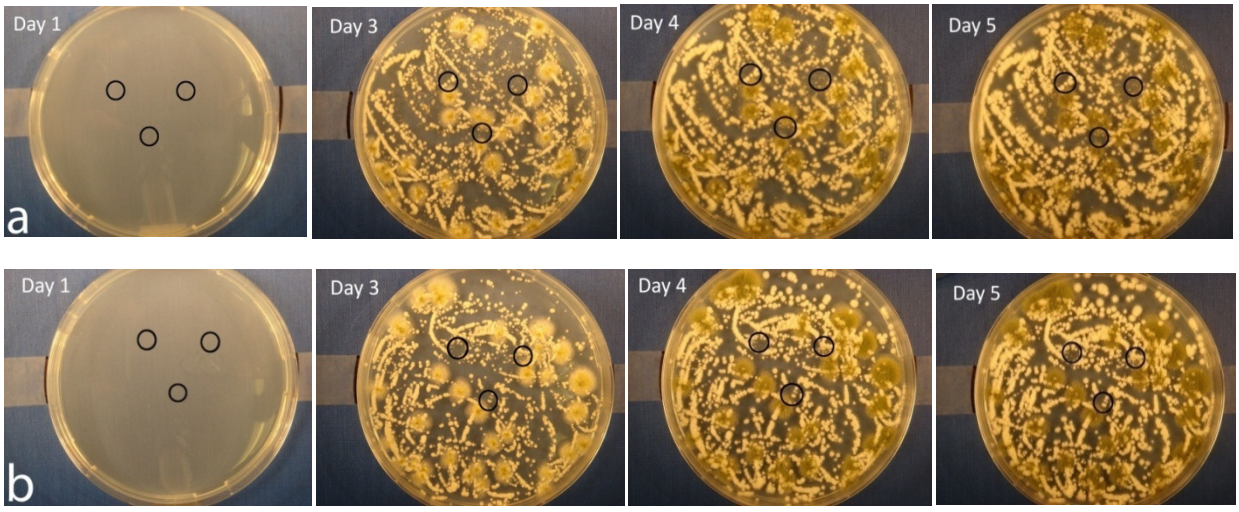

Figure 2.3: Plates inoculated with 50µl of *A. flavus* cells at $5x10^5$ cells per ml and incubated at 37°C, treated with 10 µl of (a) ITZ in water and (b) emulsion of ITZ in Tx-100 at 0.3 mg/ml. Circles represent location of applied treatments.

www.manaraa.com

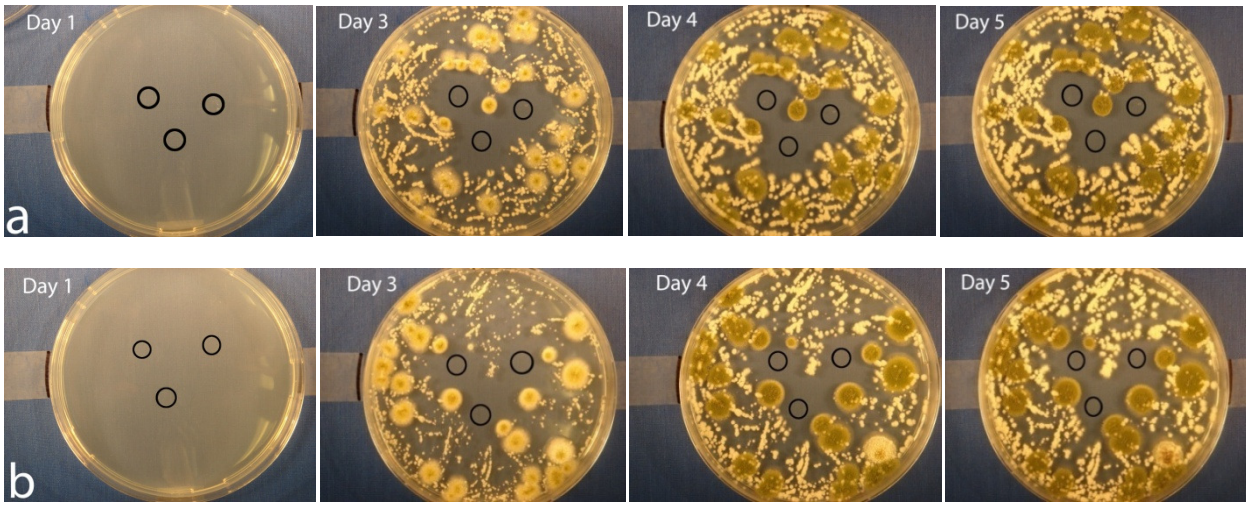

Figure 2.4: Plates inoculated with 50µl of *A. flavus* cells at $5x10^5$ cells per ml and incubated at 37ºC, treated with 10 µl of (a) polylactic-co-glycolic acid-Itraconazole Nanoparticles at 10 mg/ml (equivalent to 0.3 mg of ITZ), and (b) polylactic-co-glycolic acid-Itraconazole Nanoparticles at 1 mg/ml (equivalent to 0.03 mg/ml ITZ). Circles represent location of applied treatments.

The efficacy of the NP treatments compared to water-ITZ and Tx-ITZ emulsion were assessed by microscopically viewing the zone of inhibition on PDA on a microscope slide. A cotton thread with attached GFP fungal spores produced a line of growth into the treated areas (Figure 2.5). Similar to the culture plate experiment, the PLGA-ITZ NPs proved to be more effective in inhibiting growth, seen best at the highest concentration of 10 mg/ml and 1 mg/ml NP suspensions (equivalent to 0.3 and 0.03 mg/ml ITZ, respectively). The "growth front" shows a dip beyond the point of application of the PLGA-ITZ NPs at 10 mg/ml and 1 mg/ml. Inhibition zones of approximately 6 mm and 4 mm were observed, respectively. The NPs at 0.1 mg/ml and the blank NPs showed the least effect, with the blank NPs having no effect. Tx-ITZ had slightly better inhibition compared to water-ITZ seen by maximum inhibition zones of approximately 2 mm and 3 mm respectively at the highest concentration of 30 mg/ml ITZ.

www.manaraa.com

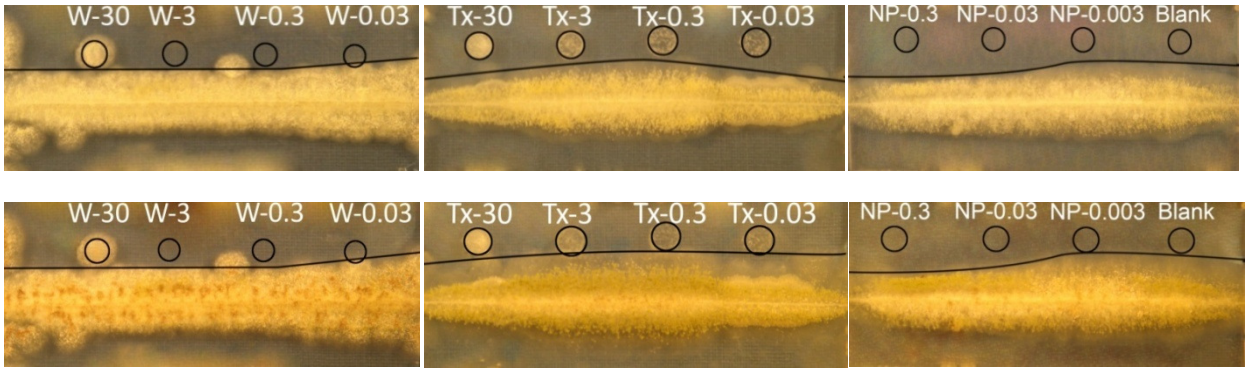

Figure 2.5: Cotton thread with attached *A. flavus* spores secured to PDA surface. Photos taken at 3 days(top row) and 5 days (bottom row) following placement of thread. Left to right: ITZ in water 30 mg/ml, 3 mg/ml, 0.3ml/ml and 0.03 mg/ml; emulsion of ITZ in Tx-100 at 30 mg/ml, 3 mg/ml, 0.3 mg/ml and 0.03 mg/ml; polylactic-co-glycolic acid-Itraconazole nanoparticles at 10 mg/ml, 1 mg/ml and 0.1 mg/ml (equivalent to 0.3, 0.03, 0.003 mg/ml ITZ, respectively).

2.3.3 GFP expressing *A. flavus* Fluorescence Quantification

2.3.3.1 Treated Immediately After Inoculation

A 96 well plate was inoculated with GFP expressing *Aspergillus flavus* and subjected to three treatments (Water-ITZ, TX-ITZ, and PLGA-ITZ NPs) which were compared to a control (no treatment) and blank NPs. Biomass was directly proportional to fluorescence and quenching of fluorescence was indicative of inhibition [26]. In general, at all concentrations of ITZ, NPs had a more immediate and superior effect compared to other treatments and lasted over the eleven day period (Figure 2.6). Statistical differences are shown in the appendix (Appendix A-Tables S1 to S3).

The effect of water-ITZ, Tx-ITZ emulsion, and PLGA-ITZ NPs on inhibiting *A.flavus* growth was least at the lowest concentrations of 0.003 mg/ml ITZ (Figure 2.6a). Treating the spores with blank NPs showed no significant decrease in fluorescence indicating that the particles themselves were not toxic (Appendix A-Table S1). Water-ITZ did not have a significantly different impact, reaching a maximum of 600 fluorescence units on day 2, compared to the *A.flavus* control

www.manaraa.com

which reached maximum fluorescence of approximately 800 units on day 2. Tx-ITZ showed a stronger effect, seen by lower fluorescence levels of 200 units on day 2 and a maximum of 350 units on day 3 compared to water-ITZ during the first three days. The PLGA-ITZ NPs had the greatest inhibitory effect seen on day 2, where fluorescence measured approximately 100 units, or 85% inhibition compared to the control. Because of the low ITZ concentrations, the inhibitory effect was limited and fluorescence increased to 350 units on day 3, however to levels still significantly lower than those of the control (Appendix A-Table S1).

At 0.03 mg/ml ITZ, water-ITZ again had minimal inhibition (Figure 2.6b) and followed what was seen at 0.003 mg/ml ITZ. The Tx-ITZ emulsion showed significant inhibition, measuring approximately 100 fluorescence units on day two, or 85% inhibition; fluorescence reached a maximum of 200 units on day three, and steadily declined in following days from the accumulation of waste by-products. The PLGA-ITZ NPs had considerable inhibition through the first 5 days seen by less than 2 fluorescence units (Appendix A-Table S2).

Increasing the ITZ concentration to 0.3 mg/ml increased inhibition (Figure 2.6c). Water-ITZ showed some inhibitory effect on day 2 seen by fluorescence of 250 units, or 65 % inhibition; however the effect diminished on day 3 before gradually declining and was not found significantly different from the control (Appendix A-Table S3). Tx-ITZ had a greater inhibitory effect during the first three days compared to water-ITZ and the control. On days 2 and 3, fluorescence was recorded at 50 units and 60 units, respectively, equivalent to 95% and 89% inhibition. Although, following day 3 the inhibitory effect decreased seen by an increase to approximately 400 fluorescence units on days 4 and 7, after which fluorescence declined. The PLGA-ITZ NPs maintained near zero fluorescence throughout the study, similar to what was seen at 0.03 mg/ml ITZ (Figure 2.6b), and

www.manaraa.com

was significantly different from all treatments and the control over the first four days (Appendix A-Table S3).

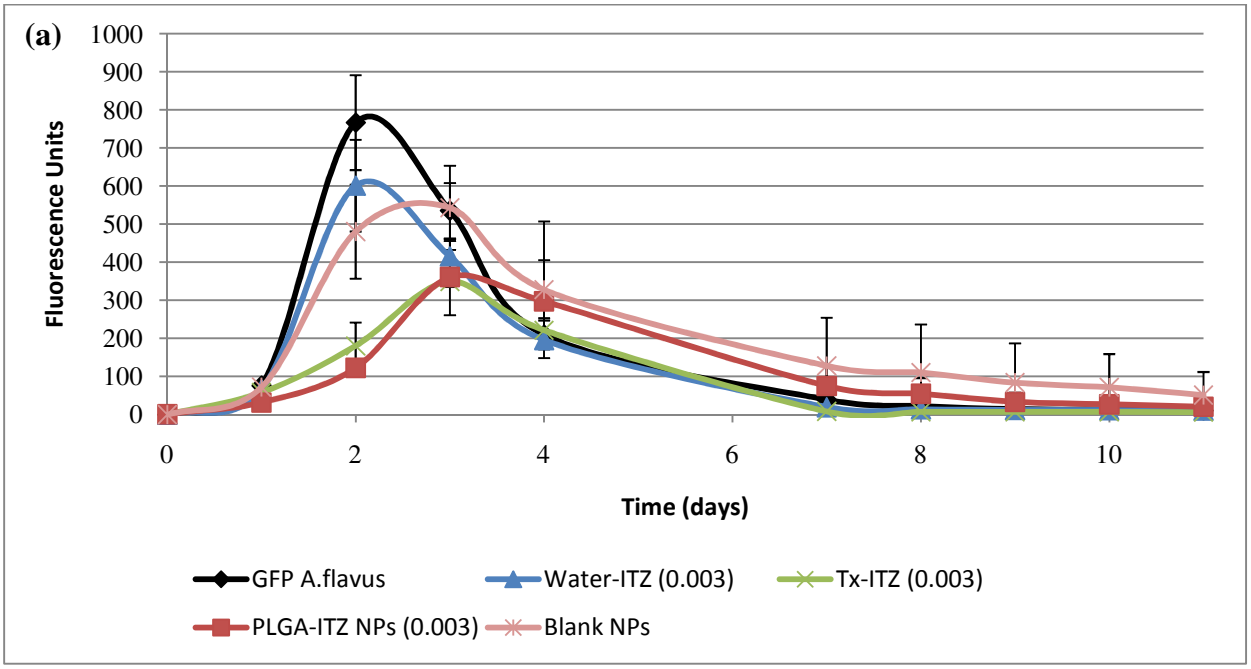

Figure 2.6a: GFP-expressing *A.flavus* at 5x10^5 spores/ml for each treatment, at 37ºC, in a 96 well plate seeded with glucose salts media and treated immediately following inoculation. Fluorescence comparison of ITZ in water, Tx-100 ITZ emulsion, and polylactic-co-glycolic acid nanoparticles with entrapped ITZ at 0.003 mg/ml ITZ (n=3 wells).

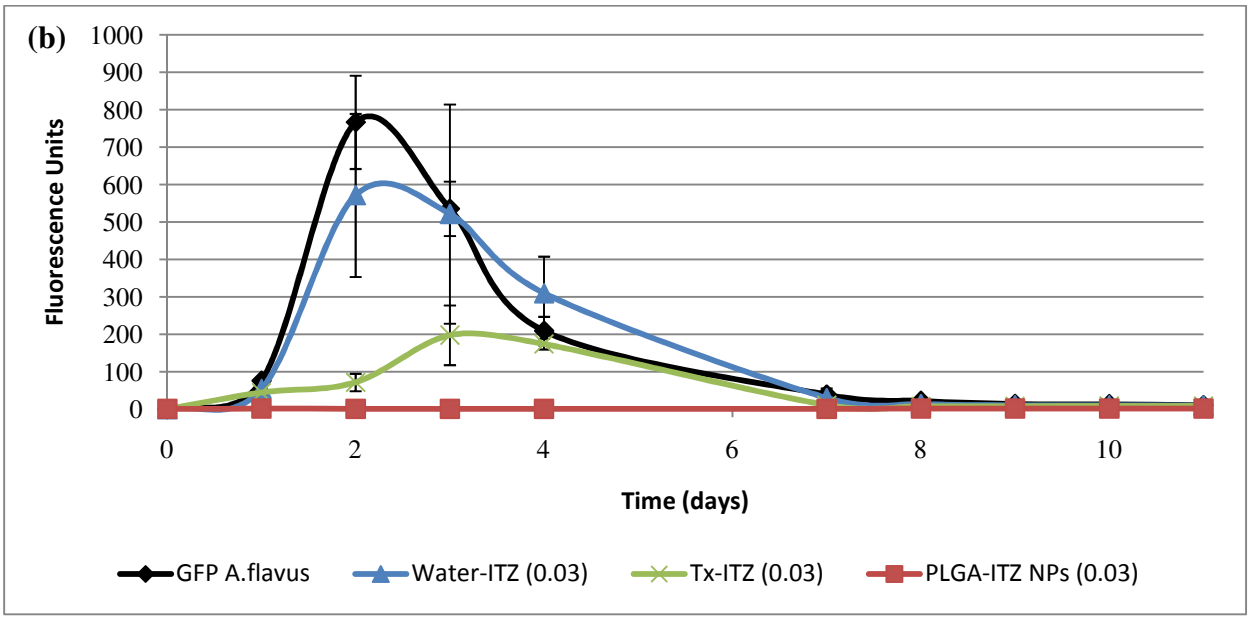

Figure 2.6b: Fluorescence comparison of ITZ in water, Tx-100 ITZ emulsion, and polylactic-co-glycolic acid nanoparticles with entrapped ITZ at 0.03 mg/ml ITZ (n=3 wells).

www.manaraa.com

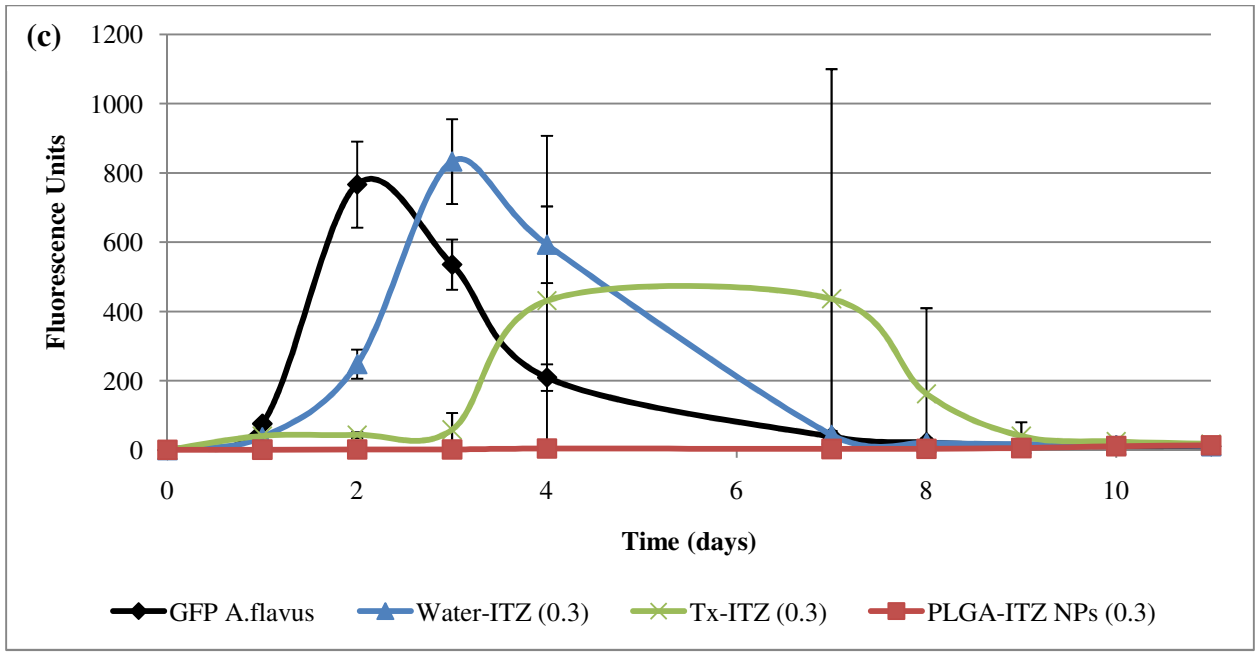

Figure 2.6c: Fluorescence comparison of ITZ in water, Tx-100 ITZ emulsion, and polylactic-co-glycolic acid nanoparticles with entrapped ITZ at 0.3 mg/ml ITZ (n=3 wells).

The antifungal effect of the three treatments was studied as a function of concentration and time (Figure 2.7). High ITZ concentrations of 3 and 30 mg/ml in free drug formulations were included in this study in order to observe where a considerable antifungal effect occurred in comparison to the NP treatments. The inhibitory effect was directly proportional to the ITZ concentration (Figures 2.7a and 2.7b). The water-ITZ graph shows that low fluorescence levels (~50 units) were maintained through day 2 at 3 mg/ml ITZ, after which an increase to ~400 fluorescence units on day 4 was observed (Figure 2.7a). At 30 mg/ml, a maximum of 100 fluorescence units was measured on day 2, followed by decreasing fluorescence levels. Tx-ITZ at 3 mg/ml showed fluorescence no higher than 70 units, and no greater than 100 units at 30 mg/ml (Figure 2.7b). Conversely, PLGA-ITZ NPs proved to have a superior antifungal effect even at 100 times less ITZ concentration (Figure 2.7c). It should be noted that while a concentration as high as 30 mg/ml would not be used in direct treatment, the results serve to show the point at which free ITZ formulations have an antifungal effect comparable to NP formulations.

www.manaraa.com

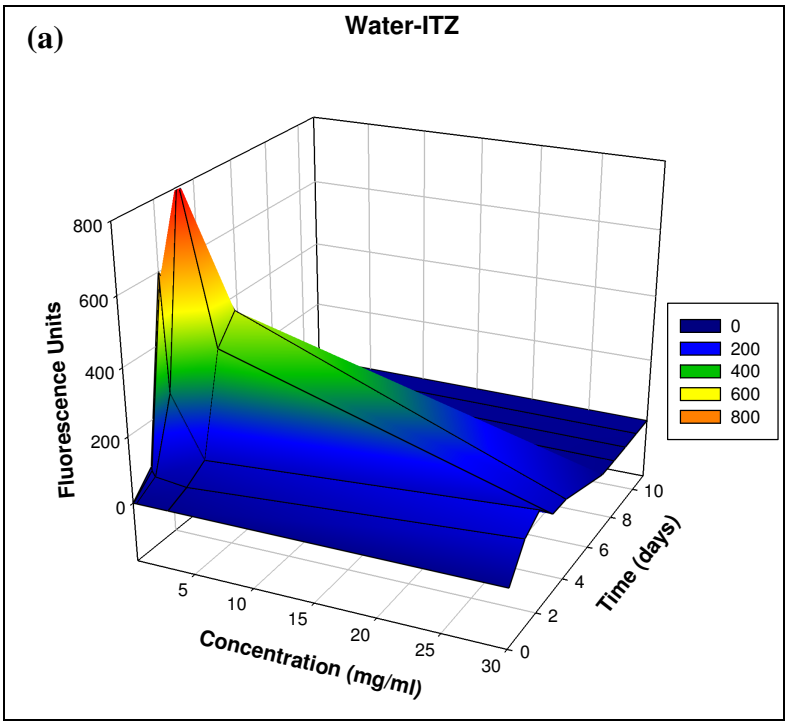

Figure 2.7a: Fluorescence of GFP-expressing *A.flavus* treated immediately after inoculation of ITZ in water (water-ITZ) at 30, 3, 0.3, 0.03, and 0.003 mg/ml ITZ,

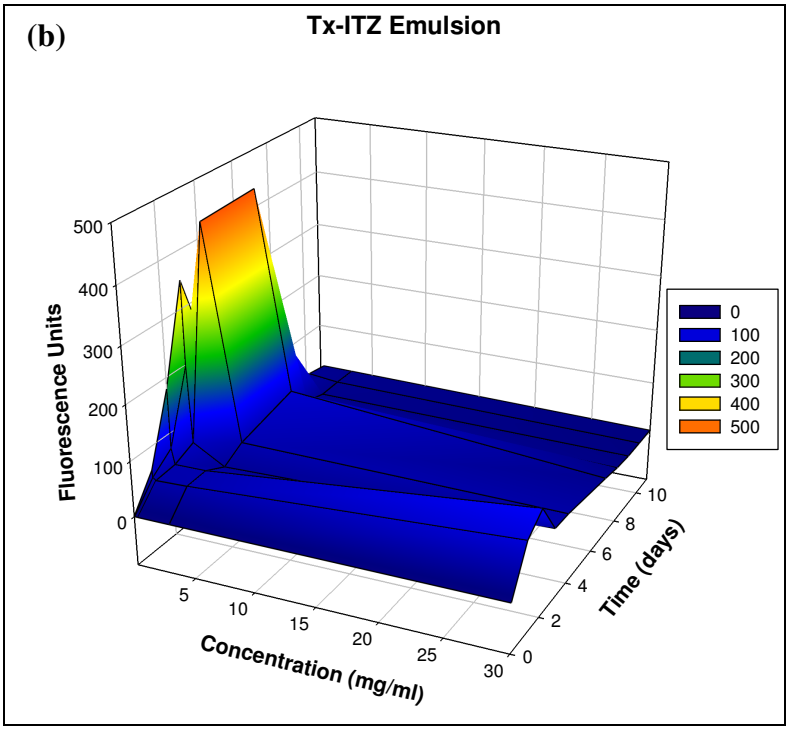

Figure 2.7b: Fluorescence of GFP-expressing *A.flavus* treated immediately after inoculation of emulsion of ITZ in Tx-100 (Tx-ITZ) at 30, 3, 0.3, 0.03, and 0.003 mg/ml ITZ.

www.manaraa.com

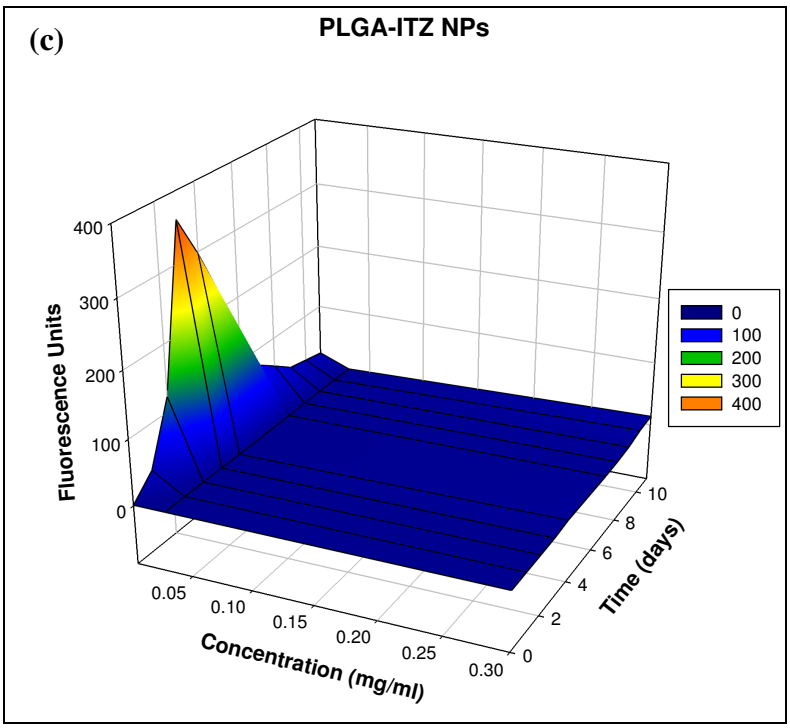

Figure 2.7c: Fluorescence of GFP-expressing *A.flavus* treated immediately after inoculation of polylactic-co-glycolic acid-Itraconazole nanoparticles at 10 mg/ml, 1 mg/ml and 0.1 mg/ml (equivalent to 0.3, 0.03, 0.003 mg/ml ITZ, respectively).

2.3.3.2 Treated 12 Hours After Inoculation

A second 96 well plate was inoculated with GFP *A.flavus* and treated 12 hours later to demonstrate efficacy after the spores germinated and began to grow. Figure 2.8 shows the fluorescence of the three treatments (Water-ITZ, TX-ITZ and PLGA-ITZ NPs) at 0.003, 0.03, and 0.3 mg/ml ITZ. It is evident that the PLGA-ITZ NPs still showed superior inhibitory activity at all ITZ concentrations followed by Tx-ITZ and water-ITZ. Water-ITZ had minimal inhibition, observed only during the first day at 0.3 mg/ml ITZ. Tx-ITZ exhibited a far greater effect over the eleven days than water-ITZ at higher ITZ concentrations; however this effect was limited at lower concentrations. Statistical differences are shown in Tables S4-S6 (Appendix A).

At the lowest ITZ concentration of 0.003 mg/ml, Water-ITZ showed the least inhibition, which occurred during the first two days (Figure 2.8a). Fluorescence on day 1 and 2 was 150 and

www.manaraa.com

400 units, respectively, yielding 40% inhibition compared to the control, which was found not significantly different (Appendix A-Table S4). In comparison, Tx-ITZ inhibited growth to a greater degree during the first two days, seen by fluorescence levels of approximately 50 and 100 units, or 75% and 85% inhibition, respectively. A large increase in fluorescence was observed following day 2 up to day 4, after which fluorescence dropped off. The PLGA-ITZ NPs inhibited *A.flavus* for the first 5 days considerably better than water-ITZ. On days 1 and 2, 20 and 30 fluorescence units were observed, equaling to 85% and 95% inhibition (Appendix A-Table S4)

At 0.03 mg/ml ITZ, water-ITZ followed a trend similar to what was seen at 0.003 mg/ml ITZ (Figure 2.8b). Minimal inhibition was observed and the fluorescence levels closely followed those of the control (Appendix A-Table S5). During the first three days Tx-ITZ fluorescence was no higher than 100 units, but spiked on day 4 before dropping off. PLGA-ITZ NPs had significant impact, seen by fluorescence units less than 1 during the first eight days (Appendix A-Table S5). Slight increases were seen latter, but fluorescence no higher than 50 units was observed.

At 0.3 mg/ml ITZ, water-ITZ delayed growth only to a certain degree (Figure 2.8c); the difference between water-ITZ and control was only found significant for day 1 (Appendix A-Table S6). Fluorescence was recorded at approximately 50 units on day 1 and 300 units on day 2, equivalent to 85% and 55% inhibition, respectively. Tx-ITZ exhibited significant inhibition, as can be seen by low fluorescence levels no higher than 50 units over the eleven days. PLGA-ITZ NPs still showed a superior antifungal effect seen by fluorescence units less than 2 for the majority of the study, with slight increases at the end of the 11 days. Even though Tx-ITZ had considerable inhibition, the PLGA-ITZ NPs maintained a significantly lower fluorescence profile (Appendix A-Table S6).

www.manaraa.com

The fluorescence effect of each treatment as a function of concentration and time showed that even at the highest concentration of 30 mg/ml ITZ, water-ITZ fluorescence increased as a function of time (Figure 2.9a). Tx-ITZ showed a much stronger effect with fluorescence no higher than 100 units (Figure 2.9b). Even so, the PLGA-ITZ NPs maintained the lowest fluorescence levels among the treatments over the 11 day period, seen by a predominantly flat fluorescence profile at 100 times less ITZ (Figure 2.9c).

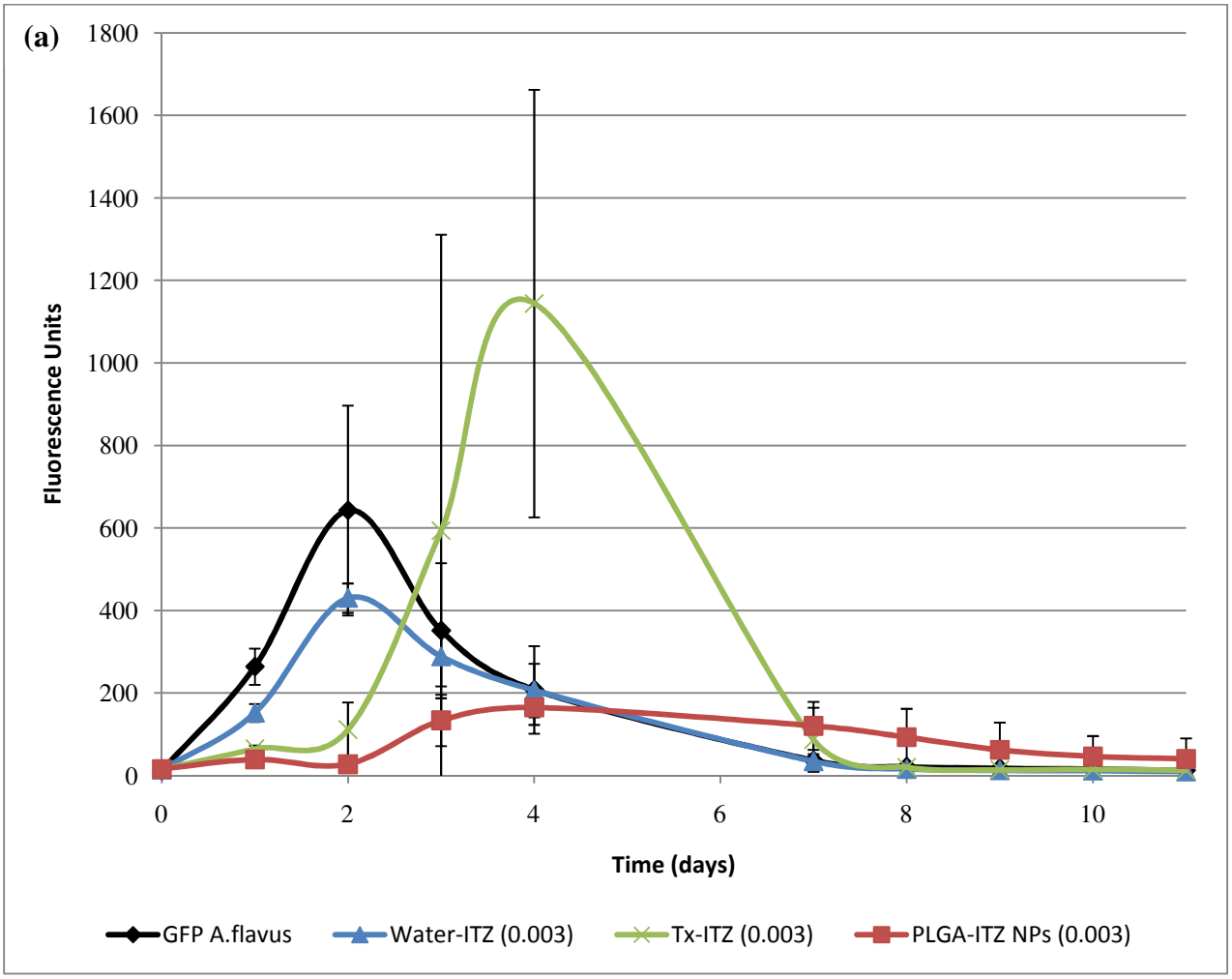

Figure 2.8a: GFP-expressing *A.flavus* at 5x10^5 spores/ml for each treatment, at 37°C, in a 96 well plate seeded with glucose salts media and treated 12 hours after inoculation. Fluorescence comparison of ITZ in water, Tx-100 ITZ emulsion, and polylactic-co-glycolic acid nanoparticles with entrapped ITZ at 0.003 mg/ml ITZ (n=3 wells).

www.manaraa.com

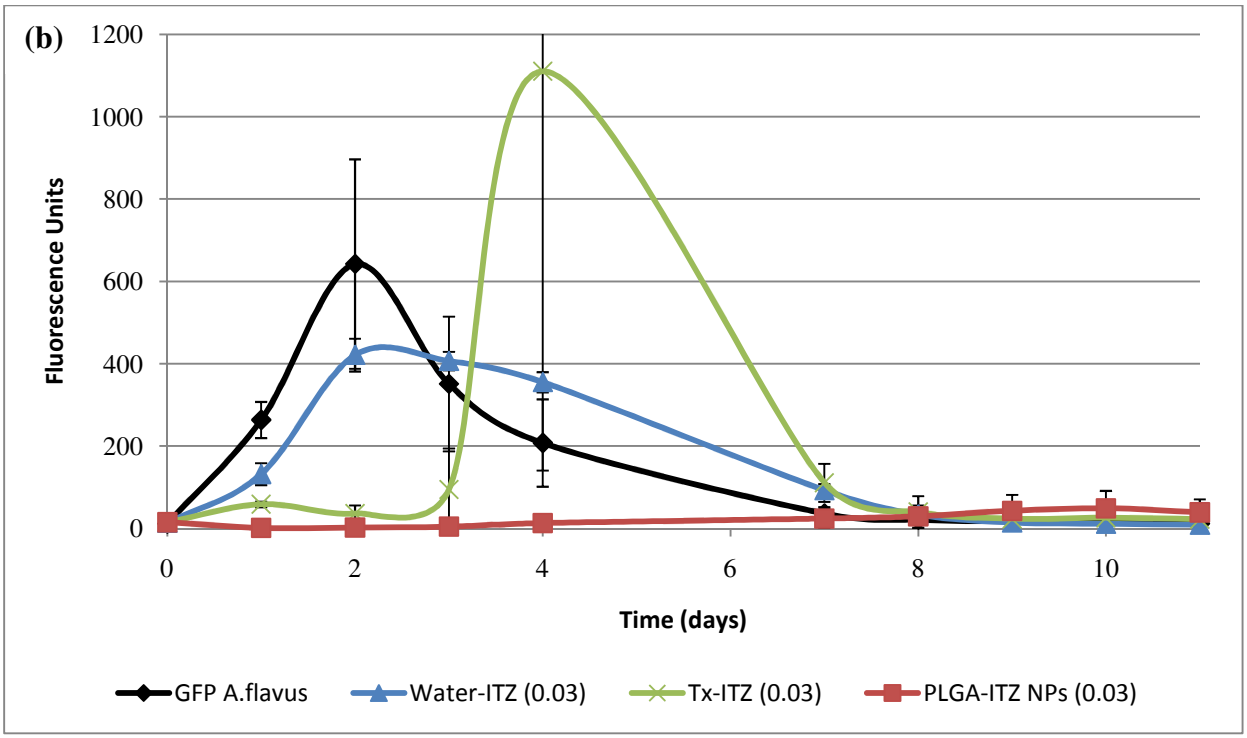

Figure 2.8b: Fluorescence comparison of ITZ in water, Tx-100 ITZ emulsion, and polylactic-co-glycolic acid nanoparticles with entrapped ITZ at 0.03 mg/ml ITZ (n=3 wells).

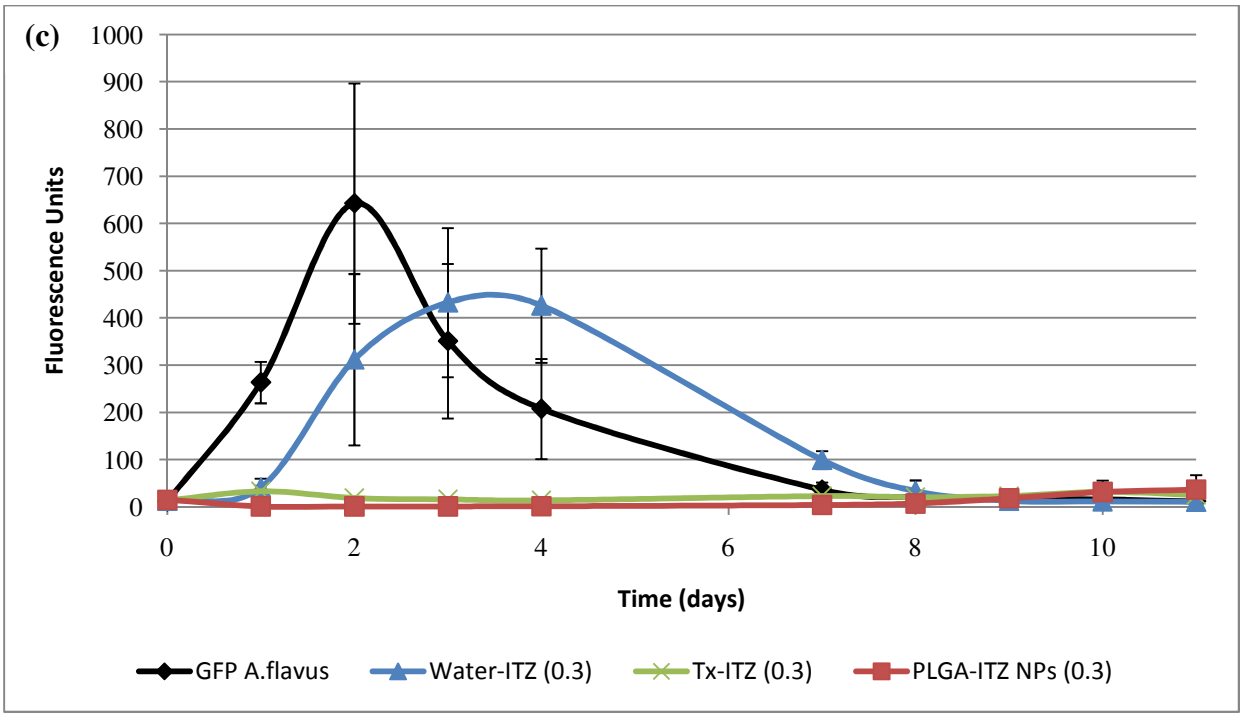

Figure 2.8c: Fluorescence comparison of ITZ in water, Tx-100 ITZ emulsion, and polylactic-co-glycolic acid nanoparticles with entrapped ITZ at 0.3 mg/ml ITZ (n=3 wells).

www.manaraa.com

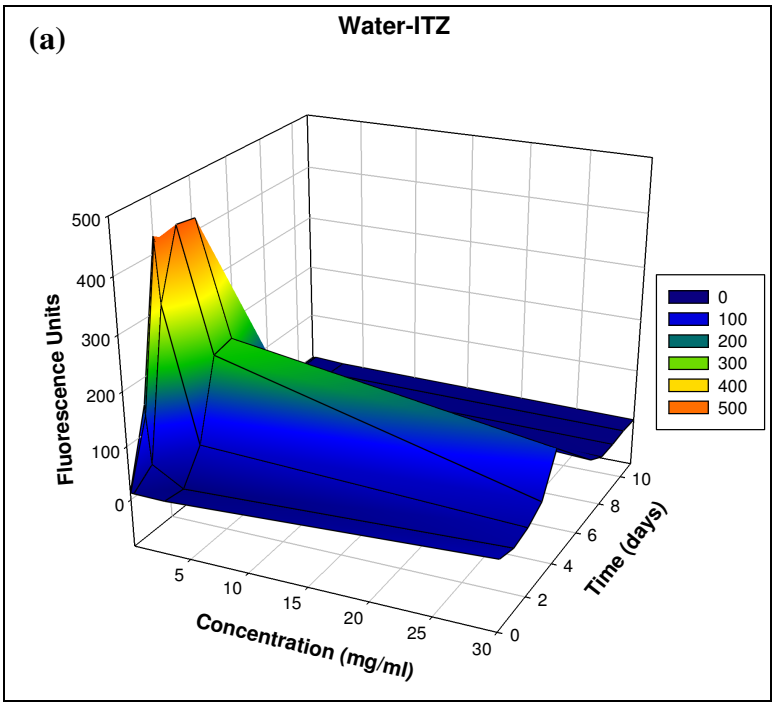

Figure 2.9a: Fluorescence of GFP-expressing *A.flavus* treated 12 hours after inoculation of ITZ in water (water-ITZ) at 30, 3, 0.3, 0.03, and 0.003 mg/ml.

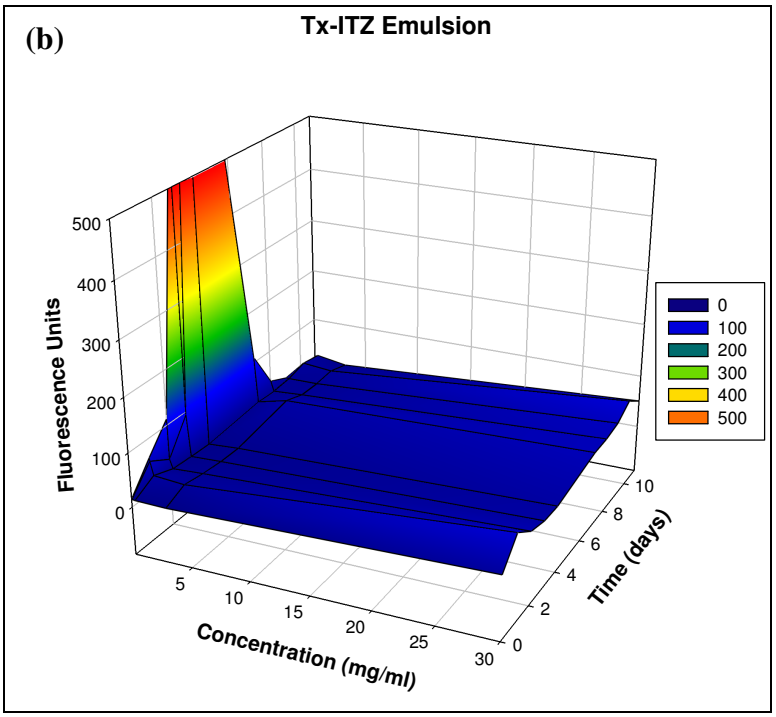

Figure 2.9b: Fluorescence of GFP-expressing *A.flavus* treated 12 hours after inoculation emulsion of ITZ in Tx-100 (Tx-ITZ) at 30, 3, 0.3, 0.03, and 0.003 mg/ml

www.manaraa.com

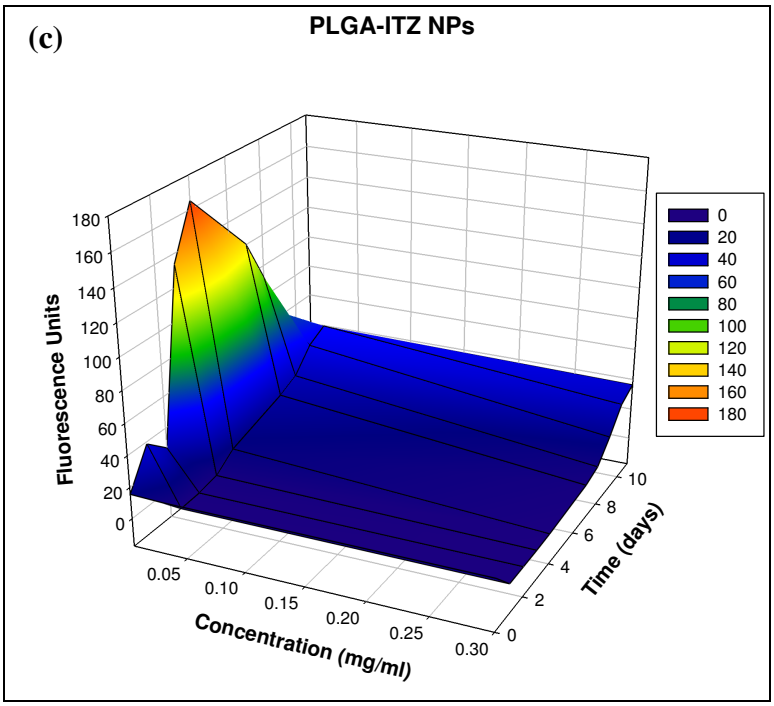

Figure 2.9c: Fluorescence of GFP-expressing *A.flavus* treated 12 hours after inoculation of polylactic-co-glycolic acid-Itraconazole nanoparticles at 10 mg/ml, 1 mg/ml and 0.1 mg/ml (equivalent to 0.3, 0.03, 0.003 mg/ml ITZ, respectively)

2.4 Discussion

In general, nanoparticles of small size (approximately 100-500 nm) can accumulate at and possibly be translocated across cell membranes, leading to increased drug efficacy [17, 28]. Loaded PLGA-ITZ NPs, approximately 232 nm with an entrapment efficiency of 96% at 12.5 % loading were used in the in-vitro studies.

ITZ release from the 12.5 % loaded PLGA-ITZ nanoparticles showed an initial jump, commonly known as the burst effect, due to the release of the drug present near the particle surface (Figure 2.2). Thereafter, the drug was released by a combination of diffusion and particle degradation [29-30]. From this profile, it was apparent that a steady dose of ITZ could be administered over five days, and consequently increase the efficacy of the drug over this time period.

www.manaraa.com

In addition to providing a time-release profile, PLGA nanoparticles were expected to aid in dispersing ITZ in water and improving its cellular uptake. ITZ functions by inhibiting the cytochrome P450-dependent 14-α-sterol demethylase synthesis of ergosterol, a vital component of fungal cell membranes [31]. Ergosterol synthesis occurs in the mitochondria and endoplasmic reticulum, requiring internalization of ITZ to inhibit synthesis [31-32]. Because the inoculated medium surface is hydrophilic and the drug is hydrophobic, a barrier exists between the two surfaces limiting contact. However, fungi possess small secreted surface active proteins known as hydrophobins that self assemble at hydrophilic-hydrophobic interfaces [33]. When hyphae are submerged in media, these hydrophobins are secreted into the surrounding medium from the hyphae apical tip [33]. Once they encounter a hydrophobic environment, such as ITZ, they self assemble with the hydrophilic side facing the aqueous environment and hydrophobic side toward the drug, forming an amphipathic membrane [34]. In this manner contact between the drug and fungal surface is enhanced allowing some inhibitory effect of water-ITZ (Figure 2.3a). However, the effect is minimized as time progresses, as seen by increased growth near the drug.

Since the nanoparticles are water soluble, contact with the fungal spores on the plate surface occurs to a greater degree compared to other treatments. This event is also facilitated by the particle size. It has been reported that smaller sized NPs (100 to 500 nm) accumulate at cell wall surfaces and are internalized with greater ease compared to larger sized particles [10, 17, 28]. These characteristics can aid in delivering ITZ by two mechanisms: first by releasing ITZ near the cell surface resulting in a quicker internalization, and second by cellular uptake of the particle followed by release of ITZ in the cytosol, however recent literature suggests the former is a more likely mechanism [35]. In combination to these mechanisms, the sustained release of ITZ explains the larger inhibition zones observed over time with the PLGA-ITZ NPs compared to water-ITZ and Tx-

www.manaraa.com

ITZ (Figure 2.4). Water-ITZ and the Tx-ITZ emulsion provide an initial high dose of antifungal resulting in some inhibitory effect, however as the drug is consumed by the spores or degraded the concentration decreases. This gradual decrease allowed surrounding spores to grow and invade the point of application. On the other hand, due to the gradual release of ITZ from the NPs, the surrounding spores sensed unfavorable and stressful conditions, causing the hyphae branches to not grow into the point of application, indicated by the large zones of clearing [36].

The limited inhibitory effect of water-ITZ and Tx-ITZ was also observed in the GFP 96-well quantitative experiments (Figures 2.6 through 2.9). Compared to water-ITZ, the Tx-ITZ emulsion showed a greater inhibitory effect during the first two days; an effect which was not clearly seen in the culture plates (Figure 2.3 and Figure 2.4). In the culture plates, a decrease in inhibitory effect was observed as time progressed, attributed to decreasing levels of ITZ. In the GFP study, the acidity of the microenvironment in the well increased as growth progressed and waste by-products accumulated. It is possible that the increased acidity resulted in higher ITZ solubility, and inhibited fungal growth. Figures 2.6 through 2.9 showed that in the first 4 days, when spores were treated immediately or 12 hours after inoculation, Tx-ITZ had more success in inhibiting *A.flavus* growth, with higher concentrations having the greatest effect. This could be expected since solubilizing ITZ in Tx-100 facilitated ITZ internalization. The inhibitory effect at lower concentrations was limited to the first four days and spores that survived from the harsh conditions of the drug were able to grow later on.

In contrast, PLGA-ITZ NPs demonstrated an enhanced inhibitory effect. As mentioned, since the NPs are small in size and water soluble, it is believed that the particles have increased contact with the cells, leading to faster drug internalization [20, 37]. The steady release of ITZ maintained low fluorescence levels, seen best at particle concentrations of 1 and 10 mg/ml (0.03 and

www.manaraa.com

0.3 mg/ml ITZ) (Figures 2.6 and 2.8). These results paralleled what was seen in the culture plates, where larger inhibition zones were noticed when PLGA-ITZ NPs were applied, due to the ability of the NP suspension to penetrate the surrounding media and spores (Figure 2.4). Figure 2.5 further showed that when 2 µl of PLGA-ITZ NPs were applied away from an inoculated surface, inhibition of spores 6 mm away from the point of application was observed at 10 mg/ml NPs (0.3 mg/ml ITZ). Water-ITZ and Tx-ITZ were not capable of producing significant inhibition zones which could possibly be a result of limited diffusibility. The stressful conditions produced by the constant ITZ concentrations forced spores to not grow into the treated area. The growth of fungi can be split into phases where the initial lag phase is preparation for growth/adaptation, followed by an exponential phase with accelerated growth [38]. Combining the NPs small size and their ability to gradually release ITZ, the exponential phase was prevented from beginning and growth was inhibited (Figure 2.6). Twelve hours after seeding, an immediate effect was also observed, however as the drug was released and consumed, any surviving spores flourished, as seen by slight increases in fluorescence towards the end of the study (Figure 2.8). However, even compared to higher ITZ concentrations of 3 and 30 mg/ml of water-ITZ and Tx-ITZ emulsion, the NPs still showed a stronger antifungal result at 100 times less ITZ. This reinforces our claim that the PLGA-ITZ NPs improve drug penetration into the spores and increase the antifungal effect.

PLGA NPs as an antifungal delivery vector has shown to be greatly effective in this study, however concerns regarding the particular method of delivery *in vivo* should not be overlooked. For example in oral delivery, nanoparticles can potentially cross the epithelial wall of the intestine, but the percentage of particles that actually reach the bloodstream is crucial [39-41]. This can be dictated by the properties of the mucus layer and nanoparticle, as well as what occurs in the stomach prior to entering the GI tract [42]. Intravenous injection is also a common delivery option

www.manaraa.com

where nanoparticles can provide protection from premature drug clearance, however, clearance of nanoparticles themselves and whether they reach target/infected sites are major points of interest [43-44]. Other direct routes such as pulmonary delivery can be implemented and provide a localized therapeutic effect [45-47]. Although, similar concerns of particle clearance and depth of penetration in the lungs are important issues to be studied closely. Nonetheless, the benefits provided by polymeric nanoparticles, as seen in this study, can greatly improve therapeutic efficacy, warranting further in-depth investigation.

2.5 Conclusions

Entrapment of ITZ in PLGA NPs has proven to be an effective means of improving delivery of this antifungal agent. Strong visual evidence of large inhibition zones were observed in PLGA-ITZ NP treated areas compared to free ITZ formulations in Petri plate studies. GFP quantitative studies revealed that when nanoparticles were added as a pre-germination and 12 hours post growth treatment, low fluorescence profiles were maintained over the span of the study at 100 times less antifungal as compared to other treatments studied. These results suggested that the extracellular release of ITZ near the cell surface can lead to expedited drug internalization, and steady release of ITZ can maintain concentrations, preventing further fungal growth. The ability to utilize 100 times less ITZ and produce greater inhibition can alleviate the concerns related to high costs and toxicity of many oral drugs. This becomes important for those having underlying illnesses such as cancer, HIV, Aspergillosis, etc., where a compromised immune system puts patients at risk, and swift recovery is desired. The antifungal effect demonstrated here can help in preventing and treating those that may be predisposed to infection. To further elucidate how this occurs, additional studies must be conducted to verify the mechanism of action.

www.manaraa.com

2.6 Future Perspectives

Nanotechnology is at the forefront of developing efficient drug delivery systems and is beginning to address many of the shortcomings of traditional drugs on the market. Biocompatible techniques for treating numerous diseases and infections are a goal that polymeric nanoparticles can achieve. What has been determined in this paper is that PLGA nanoparticles aid in delivery of antifungal agents to fungal cells and can provide for a more efficient antifungal treatment. It is envisioned that targeted antifungal delivery will be developed to reduce side effects from excess dosing, and expedite treatment and recovery in all aspects of medicine. Further studies on particle tracking and particle-cell interactions, and the antifungal capability of PLGA-ITZ NPs at other growth periods of *A.flavus* are intended. In addition, the effect of particle properties (i.e. size and composition) and their impact on ITZ release rates shall provide more clarity on the antifungal effect being observed. As a whole, these further studies are expected to give more insight on the mechanism of action. This may provide ideas on more direct and efficient routes of antifungal drug delivery. As more information becomes available, how nanodelivery systems function on a fundamental level will be revealed. This shall open the door for nanomedicine to be a more integral part of not only actively treating fungal diseases, but also preventing fungal and other debilitating diseases from occurring.

2.7 References

1. Kauffman Ca: Fungal infections in immunocompromised hosts: Focus on epidemiologic aspects of infection. *National Foundation for Infectious Diseases* 1(4), (1998).

2. Jung Sh, Lim Dh, Lee Je, Jeong Ks, Seong H, Shin Bc: Amphotericin b-entrapping lipid nanoparticles and their in vitro and in vivo characteristics. *Eur. J. Pharm. Sci.* 37(3-4), 313-320 (2009).

3. Odds Fc, Brown Ajp, Gow Nar: Antifungal agents: Mechanisms of action. *Trends in Microbiology* 11(6), 272-279 (2003).

www.manaraa.com

4. Willems L, Van Der Geest R, De Beule K: Itraconazole oral solution and intravenous formulations: A review of pharmacokinetics and pharmacodynamics. *J. Clin. Pharm. Ther.* 26(3), 159-169 (2001).

5. Peeters J, Neeskens P, Tollenaere Jp, Remoortere Pv, Brewster Me: Characterization of the interaction of 2-hydroxypropyl-beta-cyclodextrin with itraconazole at ph 2, 4, and 7. *Journal of Pharmaceutical Sciences* 91(6), 1414-1422 (2002).

6. Debeule K: Itraconazole: Pharmacology, clinical experience and future development. *Int. J. Antimicrob. Agents* 6(3), 175-181 (1996).

7. Akkar A, Müller Rh: Intravenous itraconazole emulsions produced by solemuls technology. *European Journal of Pharmaceutics and Biopharmaceutics* 56(1), 29-36 (2003).

8. Chen W, Gu B, Wang H, Pan J, Lu W, Hou H: Development and evaluation of novel itraconazole-loaded intravenous nanoparticles. *International Journal of Pharmaceutics* 362(1-2), 133-140 (2008).

9. Yi Y, Yoon Hj, Kim Bo *et al.*: A mixed polymeric micellar formulation of itraconazole: Characteristics, toxicity and pharmacokinetics. *Journal of Controlled Release* 117(1), 59-67 (2007).

10. Panyam J, Labhasetwar V: Biodegradable nanoparticles for drug and gene delivery to cells and tissue. *Advanced Drug Delivery Reviews* 55(3), 329-347 (2003).

11. Bala I, Hariharan S, Kumar M: Plga nanoparticles in drug delivery: The state of the art. *Critical Reviews in Therapeutic Drug Carrier Systems* 21(5), 387-422 (2004).

12. Pandey R, Ahmad Z, Sharma S, Khuller Gk: Nano-encapsulation of azole antifungals: Potential applications to improve oral drug delivery. *International Journal of Pharmaceutics* 301(1-2), 268-276 (2005).

13. Brannon-Peppas L, Blanchette Jo: Nanoparticle and targeted systems for cancer therapy. *Advanced Drug Delivery Reviews* 56(11), 1649-1659 (2004).

14. Desai Mp, Labhasetwar V, Walter E, Levy Rj, Amidon Gl: The mechanism of uptake of biodegradable microparticles in caco-2 cells is size dependent. *Pharmaceutical Research* 14(11), 1568-1573 (1997).

15. Panyam J, Zhou W-Z, Prabha S, Sahoo Sk, Labhasetwar V: Rapid endo-lysosomal escape of poly(dl-lactide-co-glycolide) nanoparticles: Implications for drug and gene delivery. *FASEB J.* 16(10), 1217-1226 (2002).

16. Vicari L, Musumeci T, Giannone I *et al.*: Paclitaxel loading in plga nanospheres affected the in vitro drug cell accumulation and antiproliferative activity. *BMC Cancer* 8(1), 212 (2008).

www.manaraa.com

17. Win Ky, Feng Ss: Effects of particle size and surface coating on cellular uptake of polymeric nanoparticles for oral delivery of anticancer drugs. *Biomaterials* 26(15), 2713-2722 (2005).

18. Esmaeili F, Hosseini-Nasr M, Rad-Malekshahi M, Samadi N, Atyabi F, Dinarvand R: Preparation and antibacterial activity evaluation of rifampicin-loaded poly lactide-co-glycolide nanoparticles. *Nanomed.-Nanotechnol. Biol. Med.* 3(2), 161-167 (2007).

19. Italia Jl, Yahya Mm, Singh D, Kumar Mnvr: Biodegradable nanoparticles improve oral bioavailability of amphotericin b and show reduced nephrotoxicity compared to intravenous fungizonea (r). *Pharmaceutical Research (Dordrecht)* 26(6), 1324-1331 (2009).

20. Peng Hs, Liu Xj, Lv Gx *et al.*: Voriconazole into plga nanoparticles: Improving agglomeration and antifungal efficacy. *International Journal of Pharmaceutics* 352(1-2), 29-35 (2008).

21. Yang W, Wiederhold Np, Williams Ro: Drug delivery strategies for improved azole antifungal action. *Expert Opinion on Drug Delivery* 5(11), 1199-1216 (2008).

22. Kramer Mr, Merin G, Rudis E *et al.*: Dose adjustment and cost of itraconazole prophylaxis in lung transplant recipients receiving cyclosporine and tacrolimus (fk 506). *Transplantation Proceedings* 29(6), 2657-2659 (1997).

23. Lass-Florl C, Nagl M, Speth C, Ulmer H, Dierich Mp, Wurzner R: Studies of in vitro activities of voriconazole and itraconazole against aspergillus hyphae using viability staining. *Antimicrob. Agents Chemother.* 45(1), 124-128 (2001).

24. Maschmeyer G, Ruhnke M: Update on antifungal treatment of invasive candida and aspergillus infections. *Mycoses* 47(7), 263-276 (2004).

25. Fda: Potato dextrose agar. *Bacteriological Analytical Manual*, (2008).

26. Rajasekaran K, Cary Jw, Cotty Pj, Cleveland Te: Development of a gfp-expressing aspergillus flavus strain to study fungal invasion, colonization, and resistance in cottonseed. *Mycopathologia* 165(2), 89-97 (2008).

27. Wicklow Dt, Bobell Jr, Palmquist De: Effect of intraspecific competition by aspergillus flavus on aflatoxin formation in suspended disc culture. *Mycological Research* 107(5), 617-623 (2003).

28. Swayam Prabhaa W-Zz, Jayanth Panyama and Vinod Labhasetwar: Size-dependency of nanoparticle-mediated gene transfection: Studies with fractionated nanoparticles *International Journal of Pharmaceutics* 244(1-2), 105-115 (2002).

29. Mccarron Pa, Donnelly Rf, Marouf W: Celecoxib-loaded poly(d,l-lactide-co-glycolide) nanoparticles prepared using a novel and controllable combination of diffusion and

www.manaraa.com

emulsification steps as part of the salting-out procedure. *Journal of Microencapsulation* 23(5), 480-498 (2006).

30. Mittal G, Sahana Dk, Bhardwaj V, Ravi Kumar Mnv: Estradiol loaded plga nanoparticles for oral administration: Effect of polymer molecular weight and copolymer composition on release behavior in vitro and in vivo. *Journal of Controlled Release* 119(1), 77-85 (2007).

31. Yoshida Y: Cytochrome p450 of fungi: Primary target for azole antifungal agents. *Curr Top Med Mycol* 2, 388-418 (1988).

32. Vanden Bossche H, Marichal P, Le Jeune L, Coene Mc, Gorrens J, Cools W: Effects of itraconazole on cytochrome p-450-dependent sterol 14 alpha-demethylation and reduction of 3-ketosteroids in cryptococcus neoformans. *Antimicrob. Agents Chemother.* 37(10), 2101-2105 (1993).

33. Wosten Hab, De Vocht Ml: Hydrophobins, the fungal coat unravelled. *Biochimica Et Biophysica Acta-Reviews on Biomembranes* 1469(2), 79-86 (2000).

34. Wessels Jgh: Hydrophobins, unique fungal proteins. *Mycologist* 14(4), 153-159 (2000).

35. Xu Ps, Gullotti E, Tong L *et al.*: Intracellular drug delivery by poly(lactic-co-glycolic acid) nanoparticles, revisited. *Molecular Pharmaceutics* 6(1), 190-201 (2009).

36. *The growing fungus.* Neil A.R. Gow Gmg (Ed.^(Eds). Chapman & Hall, London, UK (1995).

37. Amaral Ac, Bocca Al, Ribeiro Am *et al.*: Amphotericin b in poly(lactic-co-glycolic acid) (plga) and dimercaptosuccinic acid (dmsa) nanoparticles against paracoccidioidomycosis. *J. Antimicrob. Chemother.* 63(3), 526-533 (2009).

38. Griffin Dh: Fungal physiology. (Second Edition). Wiley-Liss, (1994).

39. Italia Jl, Bhatt Dk, Bhardwaj V, Tikoo K, Kumar Mnvr: Plga nanoparticles for oral delivery of cyclosporine: Nephrotoxicity and pharmacokinetic studies in comparison to sandimmune neoral®. *Journal of Controlled Release* 119(2), 197-206 (2007).

40. Lamprecht A, Ubrich N, Yamamoto H *et al.*: Biodegradable nanoparticles for targeted drug delivery in treatment of inflammatory bowel disease. *Journal of Pharmacology and Experimental Therapeutics* 299(2), 775-781 (2001).

41. Takeuchi H, Yamamoto H, Kawashima Y: Mucoadhesive nanoparticulate systems for peptide drug delivery. *Advanced Drug Delivery Reviews* 47(1), 39-54 (2001).

42. Jung T, Kamm W, Breitenbach A, Kaiserling E, Xiao Jx, Kissel T: Biodegradable nanoparticles for oral delivery of peptides: Is there a role for polymers to affect mucosal uptake? *European Journal of Pharmaceutics and Biopharmaceutics* 50(1), 147-160 (2000).

www.manaraa.com

43. Avgoustakis K, Beletsi A, Panagi Z *et al.*: Effect of copolymer composition on the physicochemical characteristics, in vitro stability, and biodistribution of plga-mpeg nanoparticles. *International Journal of Pharmaceutics* 259(1-2), 115-127 (2003).

44. Panagi Z, Beletsi A, Evangelatos G, Livaniou E, Ithakissios Ds, Avgoustakis K: Effect of dose on the biodistribution and pharmacokinetics of plga and plga-mpeg nanoparticles. *International Journal of Pharmaceutics* 221(1-2), 143-152 (2001).

45. Bailey Mm, Berkland Cj: Nanoparticle formulations in pulmonary drug delivery. *Medicinal Research Reviews* 29(1), 196-212 (2009).

46. Beck-Broichsitter M, Gauss J, Packhaeuser Cb *et al.*: Pulmonary drug delivery with aerosolizable nanoparticles in an ex vivo lung model. *International Journal of Pharmaceutics* 367(1-2), 169-178 (2009).

47. Sung Jc, Pulliam Bl, Edwards Da: Nanoparticles for drug delivery to the lungs. *Trends in Biotechnology* 25(12), 563-570 (2007).

www.manaraa.com

Chapter 3. Size Dependency on PLGA Nanoparticle Uptake and Antifungal Activity against *Aspergillus flavus*

3.1: Introduction

Polymeric nanoparticles (NPs) composed of poly(lactic-co-glycolic) acid (PLGA) have been extensively investigated in various forms for drug delivery due to their biocompatible characteristics, protection of entrapped bioactive agents, and controllable drug release characteristics [1-4]. Applications of PLGA NPs are broad, in areas such as gene therapy, targeted drug delivery, and delivery of active agents such as proteins, vitamins, and pharmaceutical drugs [5-13]. In antifungal therapy, a major concern with current available antifungal drugs is the low systemic bioavailability stemming from low aqueous solubility and premature drug degradation. Itraconazole (ITZ), a broad spectrum triazole, is one such antifungal with a bioavailability of only ~40% to ~50% due to its low aqueous solubility [14-15]. For individuals infected with opportunistic mycoses, particularly those who are immunosuppressed, this shortcoming can extend treatment times allowing further spreading of infections. Entrapping antifungal drugs in PLGA NPs can address some these concerns and improve treatment efficacy.

In recent studies, PLGA nanoparticles have proven to be a powerful tool in antifungal delivery compared to commercially available drugs [16-17]. Amaral et al (2009) formulated PLGA and dimercaptosuccinic (DMSA) blend nanoparticles with entrapped Amphotericin B in an attempt to minimize the dose frequency when treating mycoses [18]. Compared to conventional Amphotericin B, results showed a 3-fold decrease in dosing frequency. In a previously conducted study, we have also shown strong antifungal activity with ITZ entrapped PLGA NPs at 100x less drug concentrations compared to free ITZ [19]. Similarly, Peng et al (2008) studied Voriconazole entrapped PLGA nanoparticles and showed, *in-vitro* and *in-vivo*, more potent antifungal efficacy compared to free Voriconazole [20]. While these studies show a potent antifungal effect by drug

www.manaraa.com

entrapment in PLGA nanoparticles, in general a mechanism of action is not yet well understood. Many studies exist in literature showing superior antifungal effect of nanoencapsulated drugs, however to our knowledge, cellular uptake and antifungal activity based on nanoparticle size in fungal cells has not yet been investigated.

Cellular uptake of nanoparticles based on particle size is believed to be a contributing factor alongside with sustained drug concentrations resulting in therapeutic levels for extended periods of time [21-22]. In general, it is postulated that smaller nanoparticles are uptaken more effectively by cells. For example, in studying nanoparticle uptake in the gastrointestinal track, Desai et al (1996) showed 100 nm PLGA nanoparticle uptake to be more efficient than 500 nm, 1 µm, and 10 µm particles [23-24]. It is believed that nanoparticle uptake could be based on endocytosis by intestinal enterocytes or lymphatic uptake of small particles [25]. Likewise, Qaddoumi et al (2004) demonstrated that PLGA nanoparticles measuring 100 nm were uptaken better than 800 nm and 10µm particles by rabbit conjunctival epithelial cells [26]. Also, in various cancer cell lines, studies showed that particles ranging from 50-500 nm were internalized effectively depending on the cell type [27-29]. Zauner et al (2001) studied different particle sizes and the impact on internalization in different cell types [30]. Findings showed that while Hepatic cell lines had internalization with particles of 90 nm, 220 nm, and only marginally at 560 nm, other endothelial cell lines showed uptake of particles as large as 1000 nm. Numerous endocytic pathways have been suggested as potential uptake mechanisms.

The present study was designed to understand the effect of PLGA nanoparticle size on uptake and the respective antifungal activity of entrapped ITZ. PLGA nanoparticles with entrapped Itraconazole (PLGA-ITZ NP) of ~200 nm, ~600 nm, and ~1000 nm were tested on GFP-expressing *Aspergillus flavus* for differences in inhibitory activity against two other ITZ formulations, ITZ in

www.manaraa.com

water (Water-ITZ) and emulsified ITZ in 0.03% Triton X-100 (Tx-ITZ). In order to understand the treatment effect at different fungal growth stages, the antifungal capability was tested at the time of seeding and 12 hours after spore germination. In parallel, nanoparticle uptake by *A.flavus* was studied with ~200 nm (small) and ~1000 nm (large) nanoparticles entrapped with the fluorescent lipophilic marker coumarin-6 (PLGA-C6). Coumarin-6 is known to be non-toxic and released minimally at acidic pHs from PLGA nanoparticles, and was therefore chosen as an appropriate marker for nanoparticle tracking [28, 31-32].

3.2 Materials and Methods

3.2.1 Materials

Itraconazole, PLGA (50/50) 5-15 kDa, dichloromethane, polyvinyl alcohol (31-50 kDa),Triton X-100, and Coumarin-6 were purchased from Sigma Chemical Co. (St. Louis, MO). *Aspergillus flavus*70s and *Aspergillus flavus*70s GFP were acquired from ARS USDA Southern Regional Research Center (New Orleans, LA). Corning Costar black clear bottom 96 well plates were acquired from Fisher Scientific (Pittsburgh, PA).

3.2.2 PLGA-Itraconazole Nanoparticle Synthesis

The unloaded PLGA nanoparticles and the ITZ loaded nanoparticles were synthesized by an emulsion-solvent evaporation method, purified by dialysis, and freeze-dried for further analysis. PLGA-ITZ nanoparticles of 232 nm, 630 nm and 1060 nm range were synthesized by emulsion evaporation as follows. A 1% (for 232 nm NPs), 12% (for 630 nm NPs) and 15 % (for 1060 nm NPs) (w/v) PLGA solution was formed by dissolving 50:50 PLGA in Dichloromethane (DCM). ITZ (1.6 mg, 15 mg, and 19 mg) was dissolved into 1.25 ml of 1%, 12% and 15% (w/v) PLGA in DCM to form an organic phase at 1:8 w/w Itraconazole:PLGA. NPs measuring 232 nm were synthesized by adding the organic phase to 12.5 ml of 0.3% (w/v) polyvinyl alcohol aqueous

www.manaraa.com

solution under mixing using an Ultra Turrax t-18 basic (IKA Works, Wilmington, NC). Sonication was then performed for 10 minutes with pulses of 2 seconds on and 2 seconds off, in order to form a (O/W) micro-emulsion using a Vibra Cell vc 750 (Sonics, Newton, CT). The DCM was next removed from the mixture by evaporation with a Rotovapor R-124 (Buchi, Switzerland). NPs measuring 630 nm and 1060 nm were synthesized by adding the organic phase to 12.5 ml aqueous solution of 0.3% (w/v) polyvinyl alcohol under continuous sonication at 35% amplitude for 1 minute, and then pulsed for 1.5 minutes with pulses of 2 seconds on and 2 seconds off to form the (O/W) emulsion. DCM was then removed by evaporation. The evaporation of the organic solvent allowed for the formation of the nanoparticles and the encapsulation of ITZ. It should be noted that obtaining particles of 630 nm and 1060 nm was accomplished by an additional fractionation step by centrifuging synthesized samples at 5000 rpm (12% PLGA-ITZ NPs) and 3500 rpm (15% PLGA-ITZ NPs) for 10 min. Empty PLGA nanoparticles were synthesized following the same procedure, with the exception that no ITZ was added to the organic phase.

A dialysis step was applied to remove excess surfactant and associated ITZ from the solution following NP synthesis. Any ITZ not removed by this method, whether entrapped or marginally associated with the surface of the particle, was considered entrapped. A Specrta/Por CE cellulose ester membrane (Spectrum, Rancho Dominquez, CA) with a molecular weight cut-off of 100 kDa was used in the dialysis step. The nanoparticles underwent dialysis in a 2.5 L tank with nano-pure water, for eight hours, changing the water after four hours to facilitate the dialysis process. A final freeze drying step was applied for 48 hours at -80^{o}C using a Freezone 4.5 (Labconco, Kansas City, MO).

www.manaraa.com

3.2.3 Coumarin-6 Loaded PLGA Nanoparticle Synthesis

The lipophilic fluorescent marker coumarin-6 was used to synthesize fluorescent NPs of 203 nm and 1206 nm. Particles of 203 nm were formed by dissolving coumarin-6 into a 1% PLGA-DCM solution, and added to an aqueous solution of 0.3% PVA under mixing. Sonication was then performed for 10 minutes with pulses of 2 seconds on and 2 seconds off, followed by evaporation of DCM. Before freeze drying, particles were centrifuged at 20,000 rpm for 10 minutes and washed with deionized water to remove any free coumarin-6.

Nanoparticles measuring 1206 nm with entrapped coumarin-6 were synthesized by dissolving coumarin-6 into a 15% PLGA-DCM solution and added to an aqueous solution of 0.3% (w/v) polyvinyl alcohol under continuous sonication at 35% amplitude for 1 minute, and then pulsed for 1.5 minutes with pulses of 2 seconds on and 2 seconds off. DCM was then removed by evaporation, and particles were fractionated into the specified size by centrifuging at 3500 rpm for 10 min, and then freeze dried.

3.2.4 Nanoparticle Size Determination

Nanoparticles were tested for size and size distribution by dynamic light scattering (DLS) using the Malvern Zetasizer Nano ZS (Malvern Instruments Inc., Southborough, MA). A volume of 1.3 ml of each sample at a concentration of 0.3 mg/ml was placed in a polystyrene cuvette and measured at 25ºC at pH 6.5. The mean values of size and PDI were determined using a mono-modal distribution.

3.2.5 Nanoparticle Uptake Studies

PLGA nanoparticle uptake by fungal cells as a function of size was determined by visualizing the interaction between coumarin-6 entrapped PLGA NPs (PLGA-C6) nanoparticles and *Aspergillus flavus* in two manners: immediate interaction upon particle and hyphae contact, and in

www.manaraa.com

a time dependent manner. Cellular uptake of small (203 nm) and large (1206 nm) particles were tested, and compared against free coumarin-6 in 5% alcohol and emulsified coumarin-6 in 0.03% Triton X-100 (Tx-C6). A dye concentration of 0.3 mg/ml, equivalent to the maximum treatment concentration of PLGA-ITZ NPs (see Section 3.2.6), was used in all cases. The extreme particle sizes (203 and 1206 nm) were to observe the upper and lower limit differences in nanoparticle uptake.

A.flavus was grown for 24 hours in a microcentrifuge tube containing 1.25x glucose salts media at 37°C. A small section of grown hyphae were taken from the visible lawn and placed on a microscope slide. A 1 µl aliquot of PLGA-C6 nanoparticles at 10 mg/ml was added to the hyphae, covered with a coverslip, and immediately visualized using a Leica CTRMIC deconvolution fluorescence microscope (Leica Microsystems, Bannockburn, IL) at 100x magnification. Similarly, 1 µl of free coumarin-6 and Tx-C6 were spotted onto the hyphae and visualized under the microscope. A GFP filter cube was used with excitation and emission wavelengths of 389 nm and 509 nm, respectively.

A timed study was then conducted to determine if incubation of fluorescence nanoparticles and *A.flavus* promoted particle internalization. 200 µl of glucose salts media, 50 µl of *A.flavus* spores at $5x10^5$ spores/ml, and 10 µl of PLGA-C6 nanoparticles at 10 mg/ml were incubated in a microcentrifuge tube for 0, 1, 12, and 24 hours at 37°C. 1 µl of each time point was placed on a microscope slide, covered with a coverslip, and photographed. Time points represented various fungal growth stages. All images were shown in differential interference contrast (DIC) and fluorescence, and then overlayed.

www.manaraa.com

3.2.6 Size Impact on Antifungal Activity of PLGA-ITZ NPs on GFP Expressing *A.flavus*

Different sized particles were tested to determine if particle size (232 nm, 630 nm and 1206 nm) played a role in the antifungal capability of entrapped ITZ. Quantification of fungal growth inhibition was accomplished using GFP-expressing *A.flavus*, on the basis that biomass was directly proportional to fluorescence [33]. Black clear bottom 96 well plates were inoculated with 50µl of a conidial suspension ($5x10^5$ spores/ml) containing 200 µl of 1.25x glucose salts medium. Free ITZ formulations of ITZ in water (0.3, 0.03, 0.003 mg/ml) and Tx-ITZ emulsion (0.3, 0.03, 0.003 mg/ml ITZ) were tested against NP formulations. Different sized PLGA-ITZ NPs equaling 0.3, 0.03, 0.003 mg/ml ITZ and blank NPs at weights equivalent to max treatment concentrations were compared to free ITZ formulations. Treatments (10 µl) were added immediately following inoculation (0 h) and 12 hours after inoculation (12 h) to the respective wells and inhibition was quantified. Fluorescent measurements were taken once a day for eleven days using a Synergy HT Multi-Mode Microplate Reader (BioTek, Winooski, VT), at excitation and emission wavelengths of 485 nm and 528 nm, respectively. Fluorescence drop off in latter parts of study were indicative of accumulation of waste-by product. Fluorescence values are the mean of 3 replications.

The natural log of fluorescence was analyzed using the MIXED procedure of SAS (SAS system, SAS Institute Inc., Cary, NC). The two treatment time exposure testings (0 h and 12 h) were analyzed separately. Furthermore, treatments were compared over time separately at the various ITZ concentrations. The statistical analysis focused on days 0 to 5 for both the 0 h and 12 h testing (Appendix B-Tables B1 to B6), where most growth and antifungal activity occurred. Within each ITZ concentration the model included the fixed effects of treatment, time and their interaction. Time was analyzed as repeated measures using the covariance structure that best fitted the data based on the Akaike Information Criterion. When the treatment by day interaction was significant,

www.manaraa.com

comparisons between means were performed using the Tukey *post-hoc* multiple test adjustment. Statistical significance was declared at $P \leq 0.05$.

3.3 Results

3.3.1 Nanoparticle Characterization: Size and Size Distribution

1%, 12% and 15% PLGA-ITZ NPs used in the antifungal studies measured a size of 232 nm and 0.213±0.035 PDI, 630 ± 22 nm and 0.29±.057 PDI, and 1060 ±146 nm and 0.45± 0.1 PDI, respectively. Smallest and largest sized particles only were studied in the nanoparticle uptake studies to observe the upper and lower limits of nanoparticle uptake by *A.flavus*. Hence, 1% and 15% PLGA-C6 nanoparticles measuring 203 ±16 nm with a 0.17 ±0.019 PDI, and 1206 ±15 nm and 0.5± 0.14 PDI were used in the *A. flavus* uptake studies.

3.3.2 Size Dependency of Nanoparticle Uptake at Different *A.flavus* Growth Stages

Fluorescent pictures of 203 nm and 1206 nm PLGA-C6 nanoparticles and *A.flavus* were taken to determine if particles were internalized and if the event was dependent on particle size. Uptake of 203 nm particles was carried out as a function of time as well, to identify if the growth stage had an impact on nanoparticle uptake. Particle interaction with fungal cells was compared visually against free coumarin-6 in 5% alcohol and Tx-C6.

The free coumarin-6 control showed minimal dye being internalized (Figure 3.1a), however, the Tx-C6 emulsion showed accumulation of coumarin-6 inside hyphae (Figure 3.1b). This was expected since the activity of Itraconazole emulsified in 0.03% Tx-100 (Tx-ITZ) observed in a previous antifungal study (Chapter 2, section 2.3.3) showed an inhibitory effect similar to that of PLGA NPs with entrapped Itraconazole at high concentrations.

In comparison, small nanoparticles, measuring an average of 203nm were internalized immediately and effectively when dropped onto pre-grown hyphae (Figure 3.2). Small fluorescent

www.manaraa.com

spherical vesicles were observed inside the hyphae, indicating the presence of PLGA-C6 NPs inside the cells.

In order to understand if the particle uptake was affected by different growth stages, 203 nm nanoparticles were incubated with *A.flavus* spores and observed over time at 0, 1, 12, and 24 hours (Figure 3.3). At 0 hours (immediately after application), photos showed small fluorescent nanoparticles in the vicinity of the spores, however no interaction or uptake was observed (Figure 3.3a). This changed as incubation time increased. After 1 hour incubation particles began to associate with the spore surface, however, only surface association was seen and no internalization (Figure 3.3b). As hyphae extension occurred at 12 hours, higher particle density was seen at cell surfaces and greater internalization was observed (Figure 3.3c). Similarly at 24 hours, more coumarin-6 accumulated in the cells, seen by fluorescence extending to the cell's septa (Figure 3.3d). Leaching and background of coumarin-6 from PLGA nanoparticles was not observed, supporting the fact that dye accumulation inside hyphae was a result of nanoparticle uptake.

Uptake of larger PLGA-C6 nanoparticles of 1206 nm was studied to see if internalization was size dependent. Upon adding the large particles onto grown hyphae, accumulation of coumarin-6 inside the hyphae was still apparent (Figure 3.4a); however, the phenomenon was sporadic. Figure 3.4b showed that at a different photographed section of the same sample, while particle uptake was observed, the fluorescent intensity was lower than that observed with smaller nanoparticles (Figure 3.3). During incubation at 1 hour, a similar association of the particle to spore surface was still present (Figure 3.5a). After 12 and 24 hour incubation, an increased accumulation of particles on cell surfaces and internalization of coumarin-6 was observed (Figure 3.5b and 3.5c). At 12 hours especially, some extremely large particles were seen localized at the hyphae surface, signifying that while there is an upper limit of particle size where internalization may decrease, the localizing

www.manaraa.com

effect of the nanoparticles on the hyphae surface could aid in transporting coumarin-6 into cells. After 24 hours incubation, dye accumulation inside the hyphae was observed as well (Figure 3.5c); however this event was again sporadic, similar to what was seen in Figure 3.4 (Figure 3.5d). Obviously, size was a determinant factor which dictated interaction of nanoparticles with the fungal cells. Regardless of size, however it was evident that a physical interaction between the particles and fungal cells occurred and factors other than size were also involved in this event.

3.3.3 Size Impact on Antifungal Activity of PLGA-ITZ NPs on GFP Expressing *A.flavus*

While large particles (1206 nm) were internalized differently than smaller particles (203 nm) as shown in the uptake studies, it was necessary to investigate the impact of PLGA-ITZ nanoparticle uptake on antifungal activity. To determine the effect of nanoparticle size on antifungal activity, welled plates were inoculated with GFP expressing *Aspergillus flavus* and subjected to five treatments (Water-ITZ, TX-ITZ, and PLGA-ITZ NPs of 232 nm, 630 nm, and 1060 nm). ITZ concentrations of 0.3, 0.03, 0.003 mg/ml were tested for all treatments. Results were compared against a control (no treatment) and blank NPs. Plates were treated immediately after inoculation with *A.flavus* and 12 hours after incubation to investigate treatment effect at different growth periods. Biomass was directly proportional to fluorescence and quenching of fluorescence was indicative of inhibition. Statistical differences are shown in the appendix (Appendix B-Tables B1 to B6).

3.3.3.1 Antifungal Activity of Treatments Immediately After *A.flavus* Inoculation`

In general, water-ITZ showed minimal inhibition, while Tx-ITZ had a better inhibitory activity (Figure 3.6). In comparison, 232 nm, 630 nm, and 1060 nm particles showed superior antifungal activity compared to free ITZ formulations with no significant difference being observed between the sizes at high ITZ concentrations.

www.manaraa.com

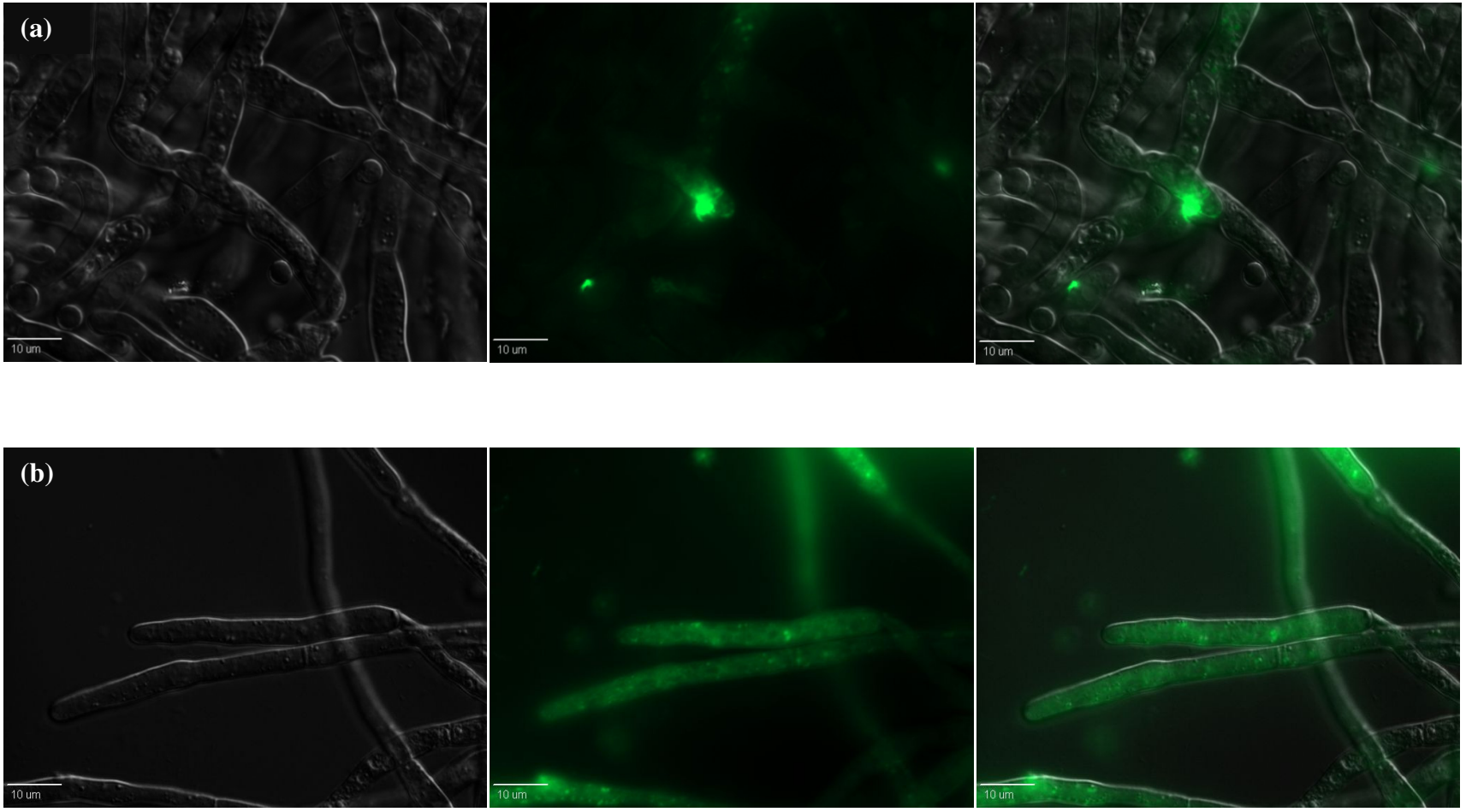

Figure 3.1: Fluorescent pictures of (a) free coumarin-6 at 0.3 mg/ml in 5% alcohol, and (b) 0.3% Tx-100 and coumarin-6 emulsion at 0.3 mg/ml. 1 µl pipetted onto *A.flavus* grown for 24 hours and photographed immediately at 100x magnification. From left to right, photos shown as differential interference contrast (DIC), fluorescence, and DIC and fluorescence overlay.

www.manaraa.com

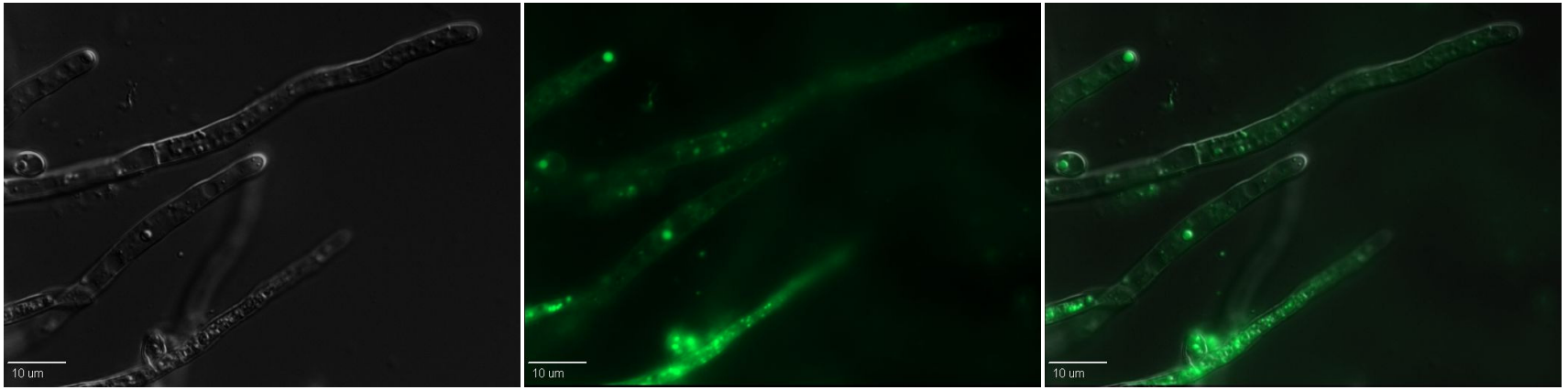

Figure 3.2: Fluorescent pictures of 203 nm PLGA-coumarin-6 NPs at 0.3 mg/ml of dye were added to 24 hour grown *A.flavus* hyphae. 1 µl of nanoparticle suspension pipetted onto *A.flavus* and photographed immediately at 100x magnification. From left to right, photos shown as differential interference contrast (DIC), fluorescence, and DIC and fluorescence overlay.

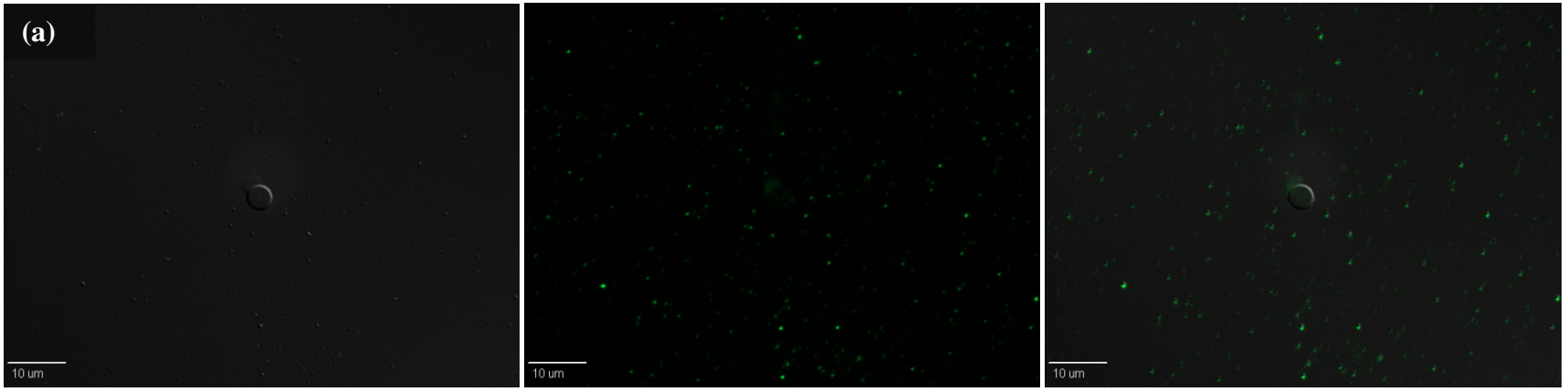

Figure 3.3a: Fluorescent pictures of 203 nm PLGA-coumarin-6 NPs at 0.3 mg/ml of dye and *A.flavus* spores incubated at (a) 0 hours, (b) 1 hour, (c) 12 hours, and (d) 24 hours at 37°C hours at 37°C. 1 µl pipetted onto microscope slide and taken at 100x magnification. From left to right, photos shown as differential interference contrast (DIC), fluorescence, and DIC and fluorescence overlay.

www.manaraa.com

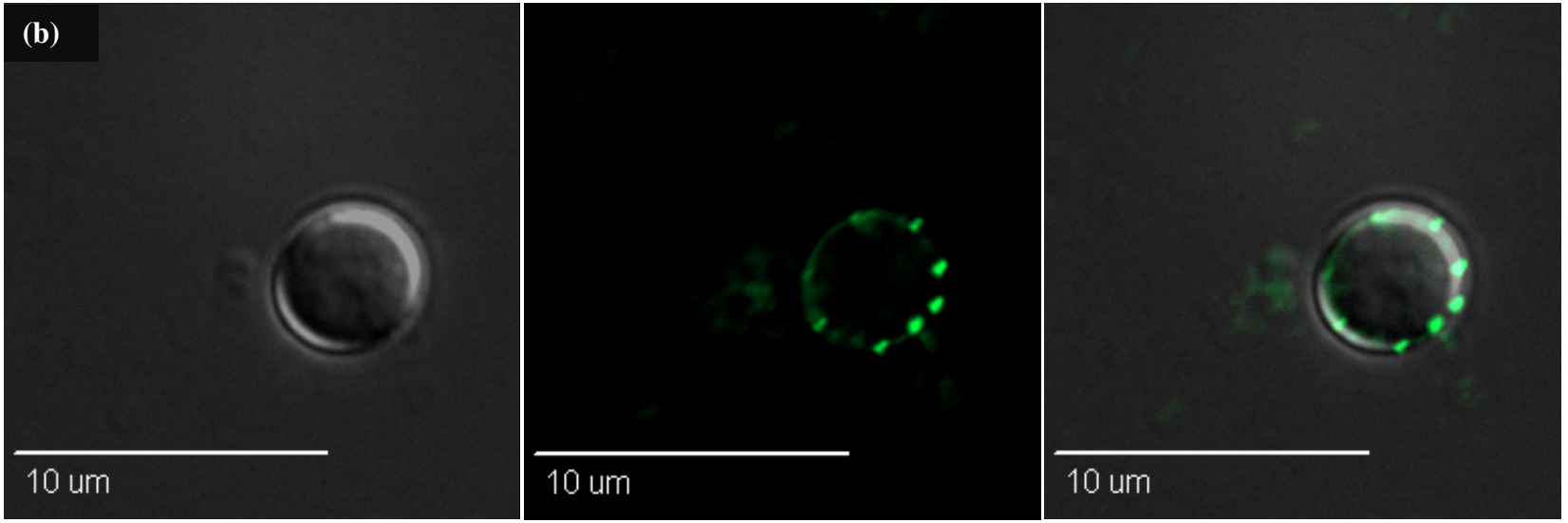

Figure 3.3b: Fluorescent pictures of 203 nm PLGA-coumarin-6 NPs and *A.flavus* spores incubated 1 hour at 37°C. From left to right, photos shown as differential interference contrast (DIC), fluorescence, and DIC and fluorescence overlay.

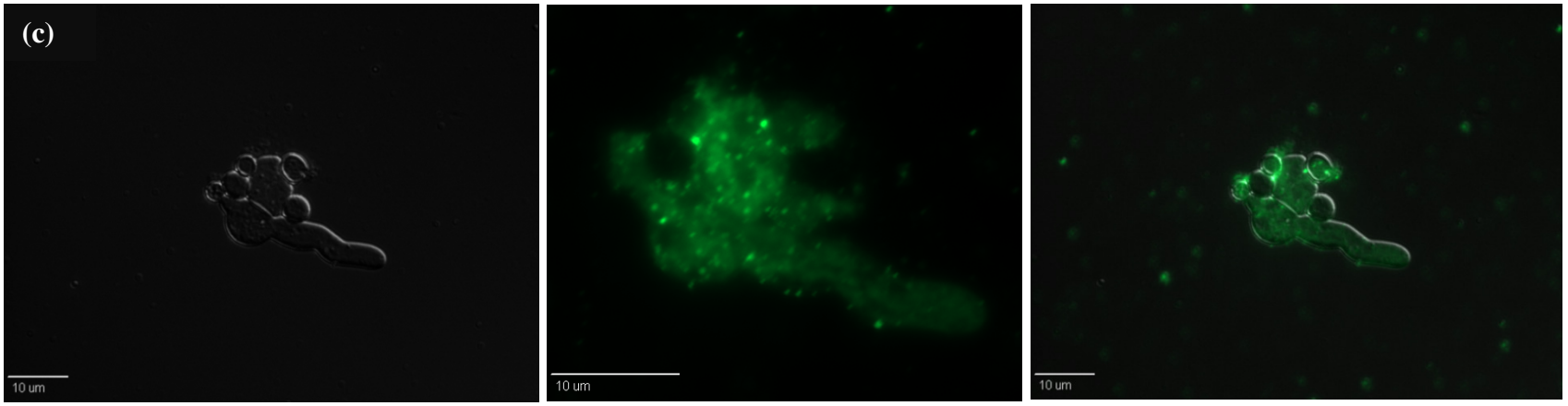

Figure 3.3c: Fluorescent pictures of 203 nm PLGA-coumarin-6 NPs and *A.flavus* spores incubated 12 hours at 37°C. From left to right, photos shown as differential interference contrast (DIC), fluorescence, and DIC and fluorescence overlay.

www.manaraa.com

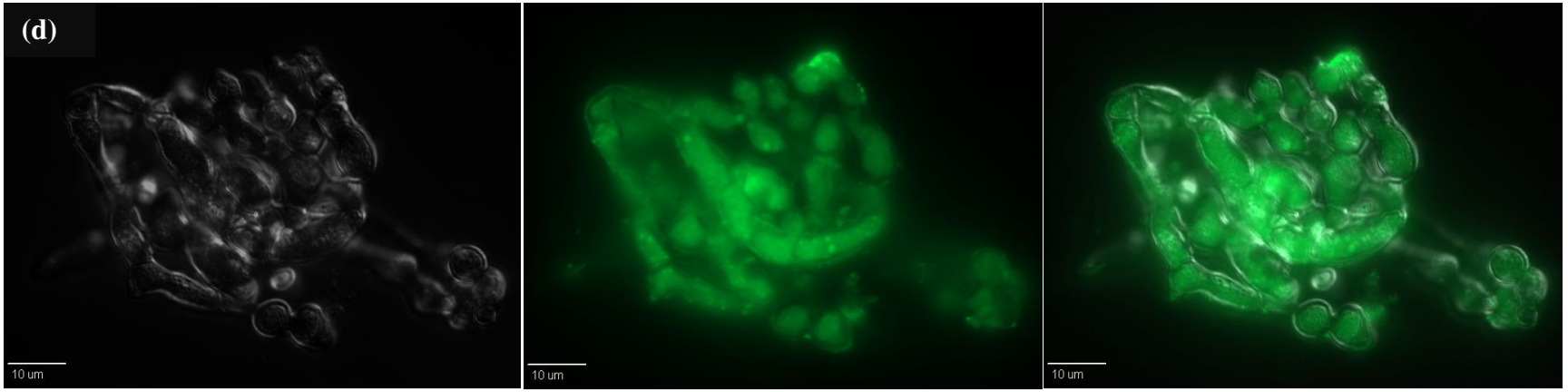

Figure 3.3d: Fluorescent pictures of 203 nm PLGA-coumarin-6 NPs and *A.flavus* spores incubated 24 hours at 37°C. From left to right, photos shown as differential interference contrast (DIC), fluorescence, and DIC and fluorescence overlay.

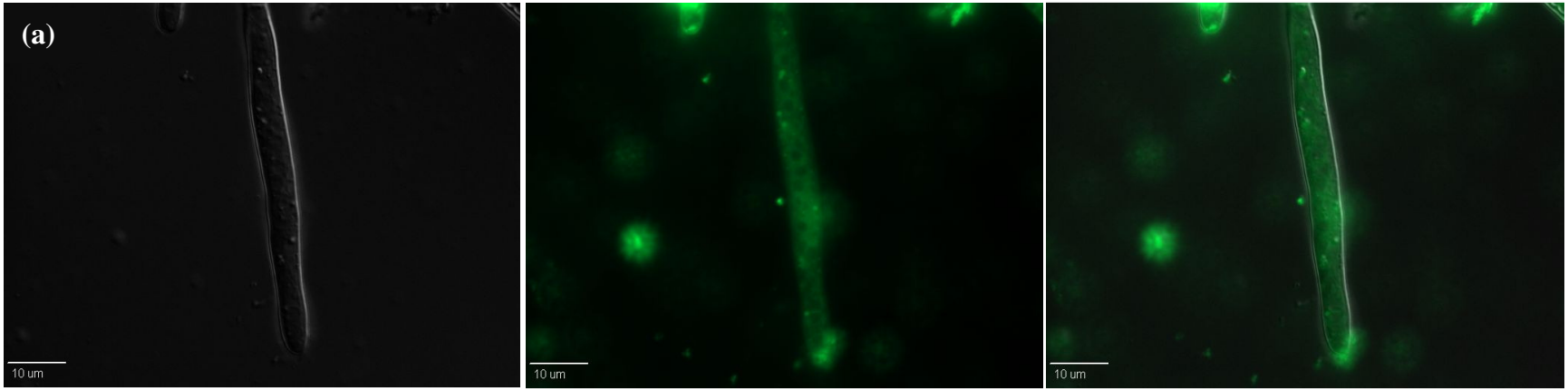

Figure 3.4a: Fluorescent pictures of 1206 nm PLGA-coumarin-6 NPs at 0.3 mg/ml of dye added to 24 hour grown *A.flavus*. 1 µl of nanoparticle suspension pipetted onto *A.flavus* and photographed immediately at 100x magnification. Pictures shown represent two different photographed locations of sample; (a) location 1, and (b) location 2. From left to right, photos shown as differential interference contrast (DIC), fluorescence, and DIC and fluorescence overlay.

www.manaraa.com

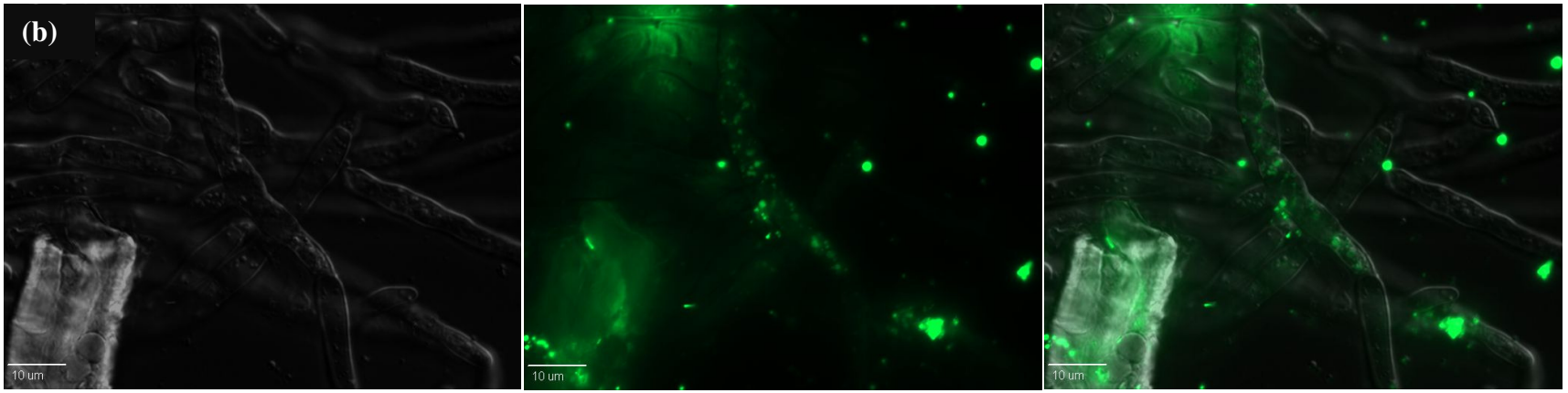

Figure 3.4b: Fluorescent pictures of location 2 of 1206 nm PLGA-coumarin-6 NPs added to 24 hour grown *A.flavus*. From left to right, photos shown as differential interference contrast (DIC), fluorescence, and DIC and fluorescence overlay.

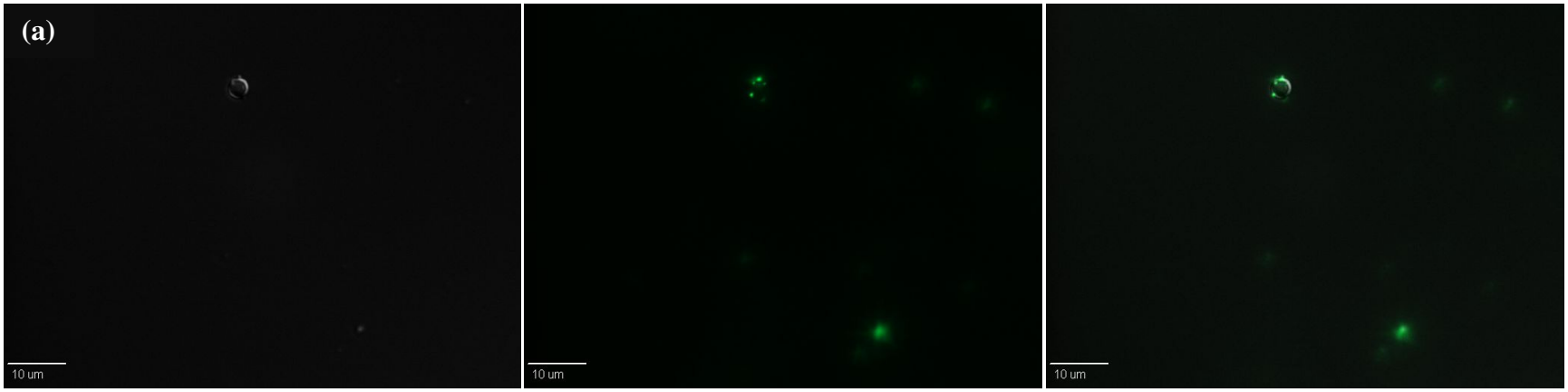

Figure 3.5a: Fluorescent pictures of 1206 nm PLGA-coumarin-6 NPs at 0.3 mg/ml of dye and *A.flavus* spores incubated at (a) 1 hour, (b) 12 hours, (c) 24 hours, and (d) location 2 of 24 hours at 37°C. 1 µl pipetted onto microscope slide and taken at 100x magnification. From left to right, photos shown as differential interference contrast (DIC), fluorescence, and DIC and fluorescence overlay.

www.manaraa.com

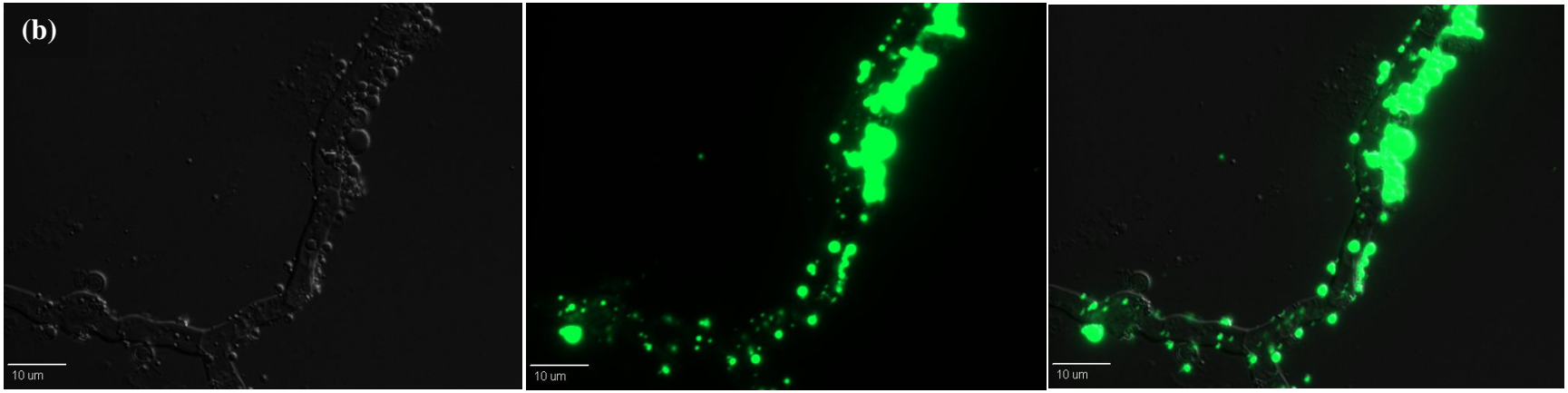

Figure 3.5b: Fluorescent pictures of 1206 nm PLGA-coumarin-6 NPs and *A.flavus* spores incubated at 12 hours. From left to right, photos shown as differential interference contrast (DIC), fluorescence, and DIC and fluorescence overlay.

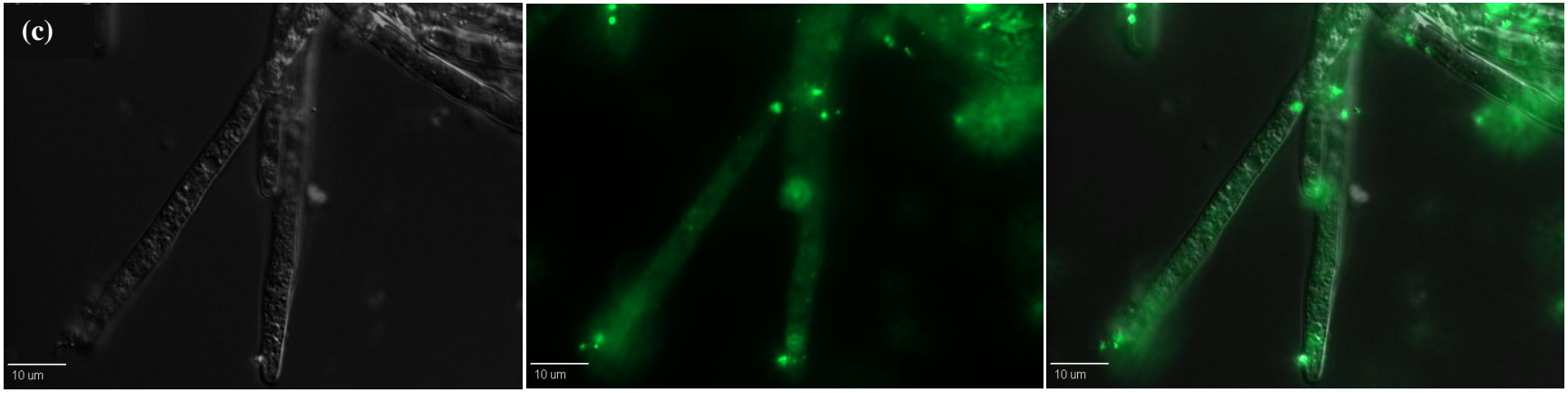

Figure 3.5c: Fluorescent pictures of 1206 nm PLGA-coumarin-6 NPs and *A.flavus* spores incubated at 24 hours. From left to right, photos shown as differential interference contrast (DIC), fluorescence, and DIC and fluorescence overlay.

www.manaraa.com

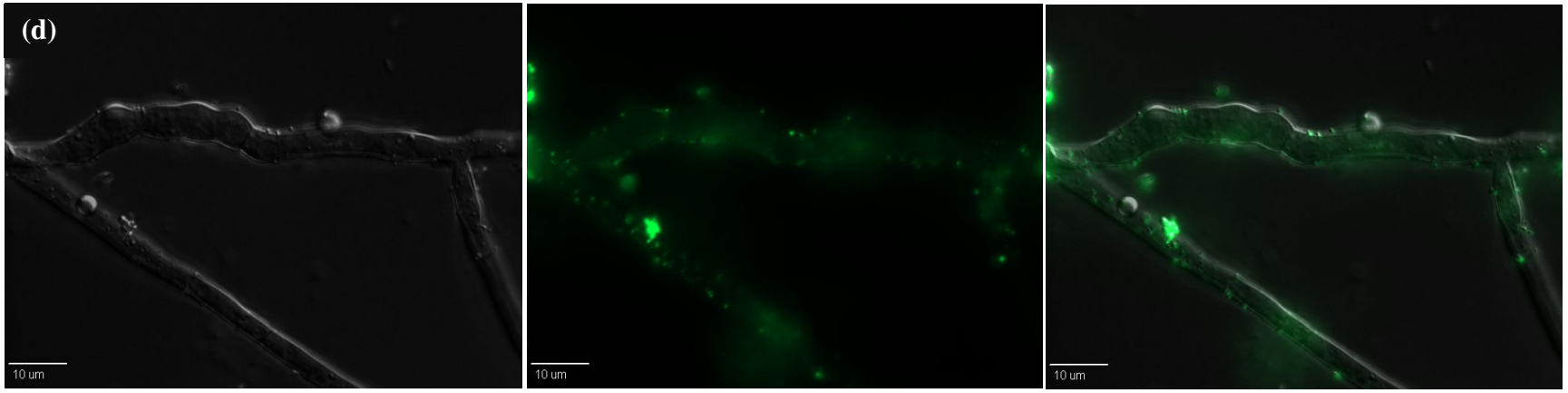

Figure 3.5d: Fluorescent pictures of location 2 of 1206 nm PLGA-coumarin-6 NPs and *A.flavus* spores incubated at 24 hours. From left to right, photos shown as differential interference contrast (DIC), fluorescence, and DIC and fluorescence overlay.

www.manaraa.com

At the lowest ITZ concentration of 0.003 mg/ml, minimal inhibition was observed (Figure 3.6a) with all treatments. Blank NPs of 232 nm, 630 and 1060 nm showed no significant inhibitory activity and followed trends similar to those of the control. Similarly, water-ITZ showed very low inhibitory activity and even exceeded fluorescence levels of the control, while Tx-ITZ showed greater inhibition during days 2 and 3, or 37% and 47%, relative to the control. PLGA-ITZ NPs measuring 232 nm had the greatest inhibitory effect on day 2 (81% inhibition); however the effect was limited as seen by an increase in fluorescence to 350 units on day 3, before declining on day 4. PLGA-ITZ NPs of 630 nm and 1060 nm, showed a similar inhibitory effect of 80% on day 2, however following day 2, fluorescence values remained above the control and gradually declined in the latter, following similar trends. Compared to 232 nm particles, the decline in fluorescence units occurring with larger particles from day 3 through day 11 was a more gradual process. This was the most significant difference observed between large and small particles, and was not observed at the other ITZ concentrations (Appendix B-Table B1).

At 0.03 mg/ml, water-ITZ showed some inhibitory effect on day 2 at 67% relative to the control, but fluorescence increased on day 3 and stayed at levels above the control in the following days (Figure 3.6b). Tx-ITZ showed significant inhibition maintaining fluorescence below 100 units through day 4. However, a spike in fluorescence was seen on days 7 and 8 to 230 and 250 fluorescence units, respectively, before declining from the accumulation of waste-by product. Both mid-sized and large PLGA-ITZ NPs showed considerable inhibitory activity throughout the eleven day study. 1060 nm particles did show a slight increase in fluorescence units towards the end of the study; however levels did not exceed 100 fluorescence units. Compared to 232 nm particles, no significant difference was seen between the nanoparticle sizes (Appendix B-Table B2).

www.manaraa.com

At the highest ITZ concentration of 0.3 mg/ml, water-ITZ showed an increase in inhibition which was best seen on day 2 by fluorescence levels of 155 units, or 76% relative to the control (Figure 3.6c). This effect was again limited and on day 3 fluorescence levels increased above the control. Tx-ITZ had a greater inhibitory effect with fluorescence values no higher than 60 units through day 4; however fluorescence again spiked on day 8 at approximately 200 units, similar to the phenomenon seen at 0.03 mg/ml ITZ. In contrast, PLGA-ITZ NPs showed a consistent inhibitory effect across the study at fluorescence values near zero, irrespective of size (Appendix B-Table B3).

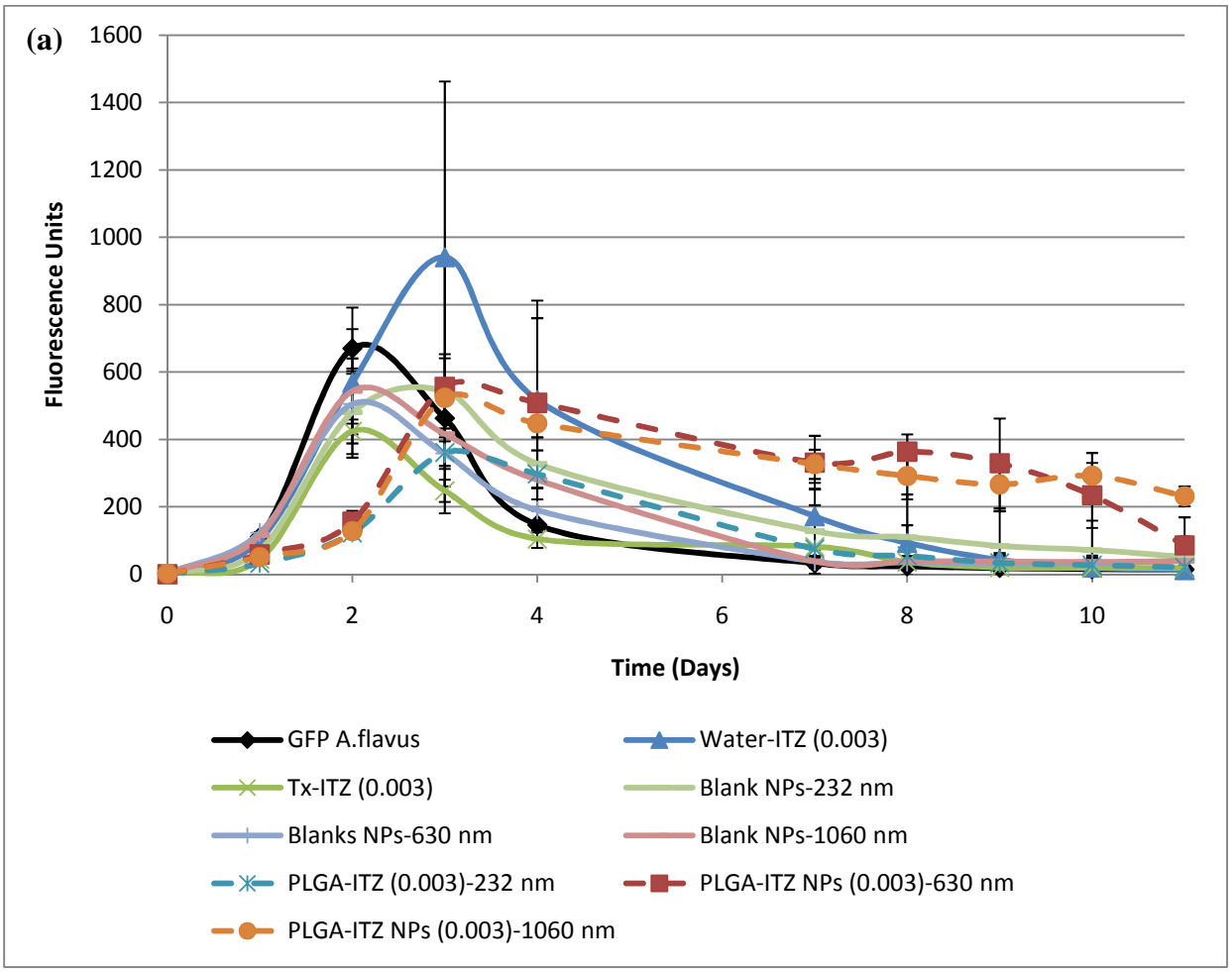

Figure 3.6a: GFP expressing *A.flavus* at 5x10^5 spores/ml, incubated at 37°C with glucose salts media and treated immediately after inoculation. Fluorescence comparison of ITZ in water, Tx-100 ITZ emulsion, and 230 nm, 630 nm, and 1060 nm polylactic-co-glycolic acid nanoparticles with entrapped ITZ at 0.003 mg/ml ITZ (n=3 wells).

www.manaraa.com

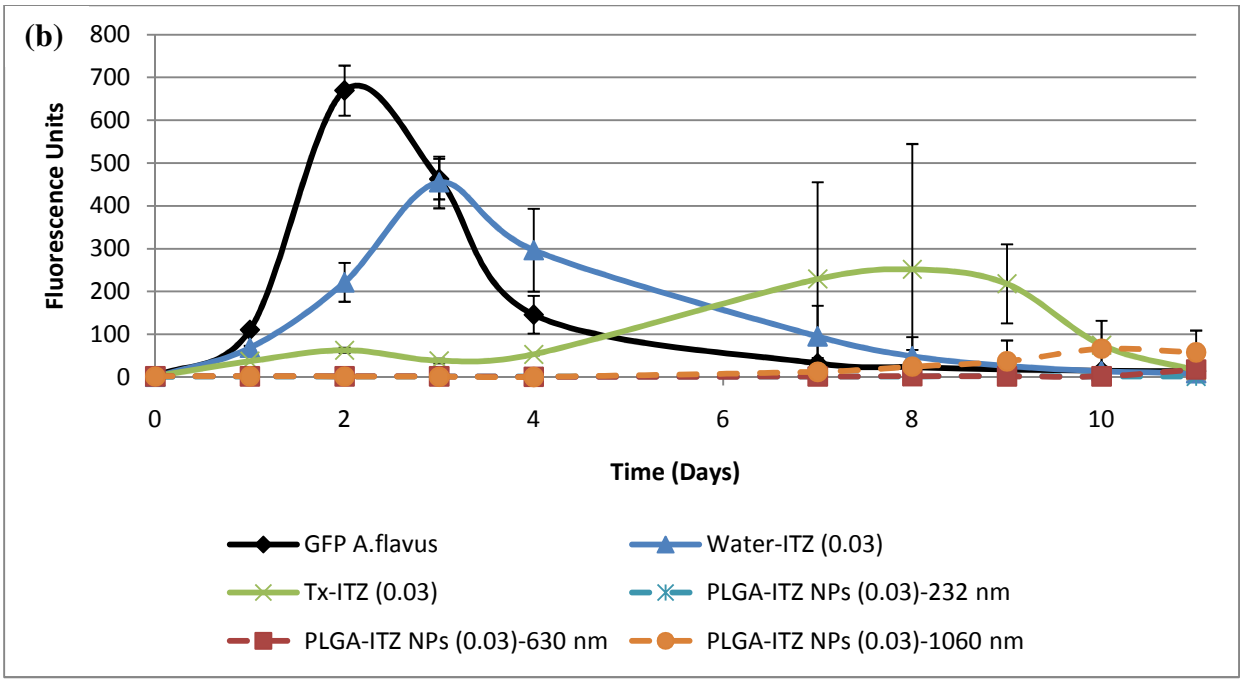

Figure 3.6b: Fluorescence comparison of ITZ in water, Tx-100 ITZ emulsion, and 230 nm, 630 nm, and 1060 nm polylactic-co-glycolic acid nanoparticles with entrapped ITZ at 0.03 mg/ml ITZ (n=3 wells).

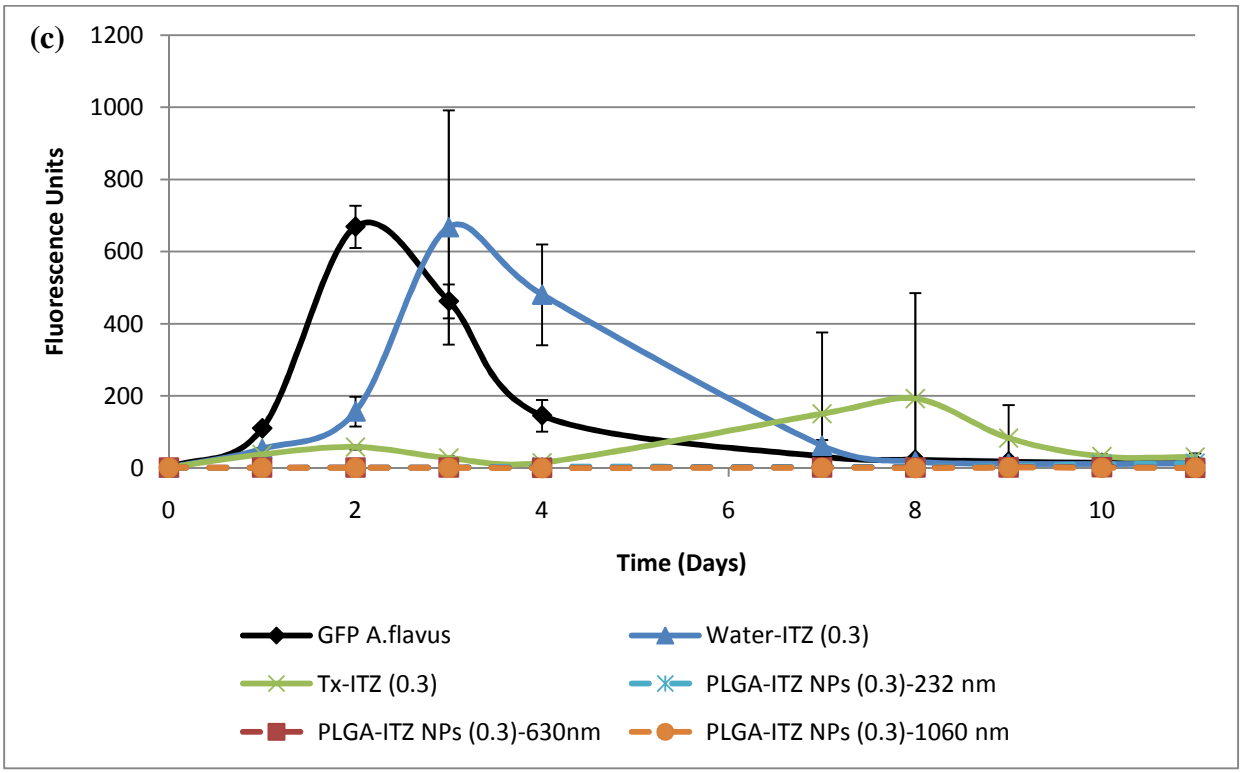

Figure 3.6c: Fluorescence comparison of ITZ in water, Tx-100 ITZ emulsion, and 230 nm, 630 nm, and 1060 nm polylactic-co-glycolic acid nanoparticles with entrapped ITZ at 0.3 mg/ml ITZ (n=3 wells).

www.manaraa.com

3.3.3.2 Antifungal Activity of Treatments 12 hours After *A.flavus* Inoculation

A.flavus was incubated in 96 well plates for 12 hours and then treated to evaluate the antifungal activity after spore germination (Figure 3.7). Water-ITZ again showed minimal inhibition, while Tx-ITZ had substantial antifungal activity. However, PLGA-ITZ NPs maintained a consistent antifungal ability at concentrations of 0.3 and 0.03 mg/ml ITZ at all sizes. The most notable difference in inhibitory activity between the different sized particles occurred at 0.003 mg/ml ITZ, similar to what was seen when treated immediately following inoculation.

Water-ITZ at 0.003 mg/ml ITZ showed no inhibitory effect and fluorescence followed similar trends to those of the control (Figure 3.7a). In comparison, Tx-ITZ inhibited growth to a greater degree during the first three days seen by fluorescence levels of 96, 492, and 306 units, or 71%, 26%, and 20% inhibition, respectively. Decreasing fluorescence was then subsequently seen from the accumulation of waste by-products. Compared to Tx-ITZ, 630 nm and 1060 nm PLGA-ITZ NPs did not show a major effect during the first four days. Leading up to day 2 both particle sizes showed similar activity with a maximum inhibition of only 12% on day 2. Although, in the later days, the 630 nm particle fluorescence was seen declining rapidly compared to Tx-ITZ, whereas 1060 nm particle fluorescence was seen declining much more gradually indicated by fluorescence values as high as 240 units on day 7 compared to 30 units of the control. Largely, 232 nm particles showed a greater inhibitory effect which was seen best during the first 3 days (Appendix B-Table B4).

At 0.03 mg/ml ITZ, water-ITZ showed limited inhibition initially on days 2 and 3 of 46% and 21% relative to the control before declining (Figure 3.7b). Conversely, Tx-ITZ demonstrated significant inhibition seen by fluorescence below 100 units across the study. Both sizes of 630 nm and 1060 nm PLGA-ITZ NPs showed a strong inhibitory effect during the first

www.manaraa.com

four days seen by near zero fluorescence (Appendix B-Table B5). While slight increases were observed towards the end, fluorescence no higher than 60 units was seen in all cases.

At 0.3 mg/ml ITZ, water-ITZ showed an increase in inhibitory action; however this was nominal (Figure 3.7c). On days 1 and 2 fluorescence was recorded at 125 and 525 units, equivalent to 62% and 26% inhibition. Tx-ITZ had significant impact, seen by low fluorescence levels of approximately 20 units consistently throughout the study. Although, PLGA-ITZ NPs maintained fluorescence values near zero over the span of the study, regardless of size (Appendix B-Table B6).

Similar to 232 nm sized particles, mid-range and larger nanoparticles showed an enhanced inhibitory effect when *A.flavus* was treated immediately and 12 hours after inoculation. The most noticeable differences between 630 nm and 1060 nm particles were seen at the lowest ITZ concentration (0.003 mg/ml ITZ) especially in the latter parts of the study, where fluorescence declined much more slowly with larger particles. At the higher ITZ concentration (0.03 mg/ml ITZ), increases in fluorescence were also found with larger nanoparticles, however they were very minimal. The sporadic uptake of ~1000nm nanoparticles seen in Figures 3.4 and 3.5 correlated well with the diminished antifungal activity seen at these sizes at 0.003 mg/ml ITZ, and confirmed that an inverse correlation of size with delivery efficiency existed.

3.4 Discussion

Hyphae exposed to 0.3 mg/ml free dye in 5% alcohol showed minimal dye being internalized (Figure 3.1a). Since coumarin-6 is hydrophobic, some crystallized coumarin-6 could still be seen. In comparison, the emulsion of coumarin-6 (Tx-C6) showed visible accumulation of the dye inside hyphae (Figure 3.1b). This would be expected since the emulsion should facilitate dye entry into the cells. When 203 nm PLGA-C6 nanoparticles were added to pre-grown hyphae, particle uptake was also observed (Figure 3.2). The small fluorescent

www.manaraa.com

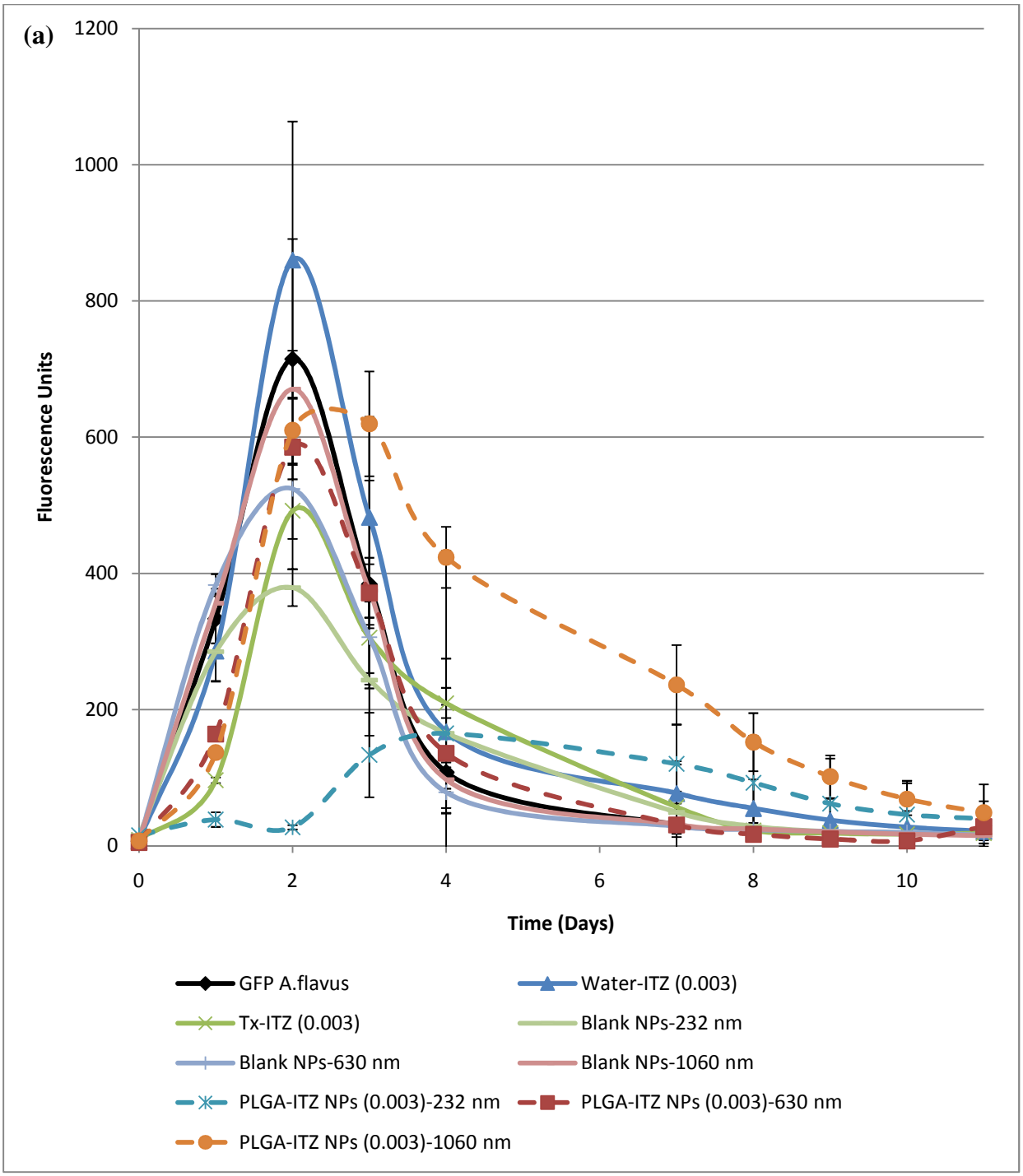

Figure 3.7a: GFP expressing *A.flavus* at 5x10^5 spores/ml, incubated at 37°C with glucose salts media and treated 12 hours after inoculation. Fluorescence comparison of ITZ in water, Tx-100 ITZ emulsion, and 230 nm, 630 nm, and 1060 nm polylactic-co-glycolic acid nanoparticles with entrapped ITZ at 0.003 mg/ml (n=3 wells).

www.manaraa.com

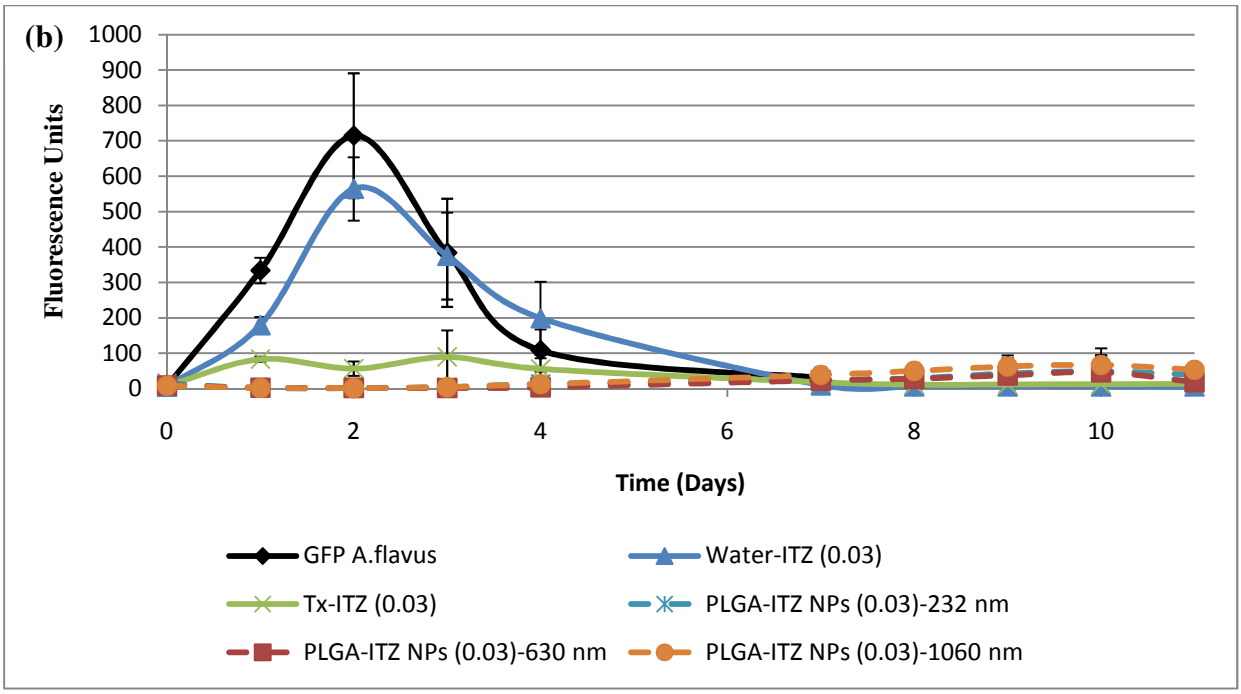

Figure 3.7b: Fluorescence comparison of ITZ in water, Tx-100 ITZ emulsion, and 230 nm, 630 nm, and 1060 nm polylactic-co-glycolic acid nanoparticles with entrapped ITZ at 0.03 mg/ml ITZ (n=3 wells).

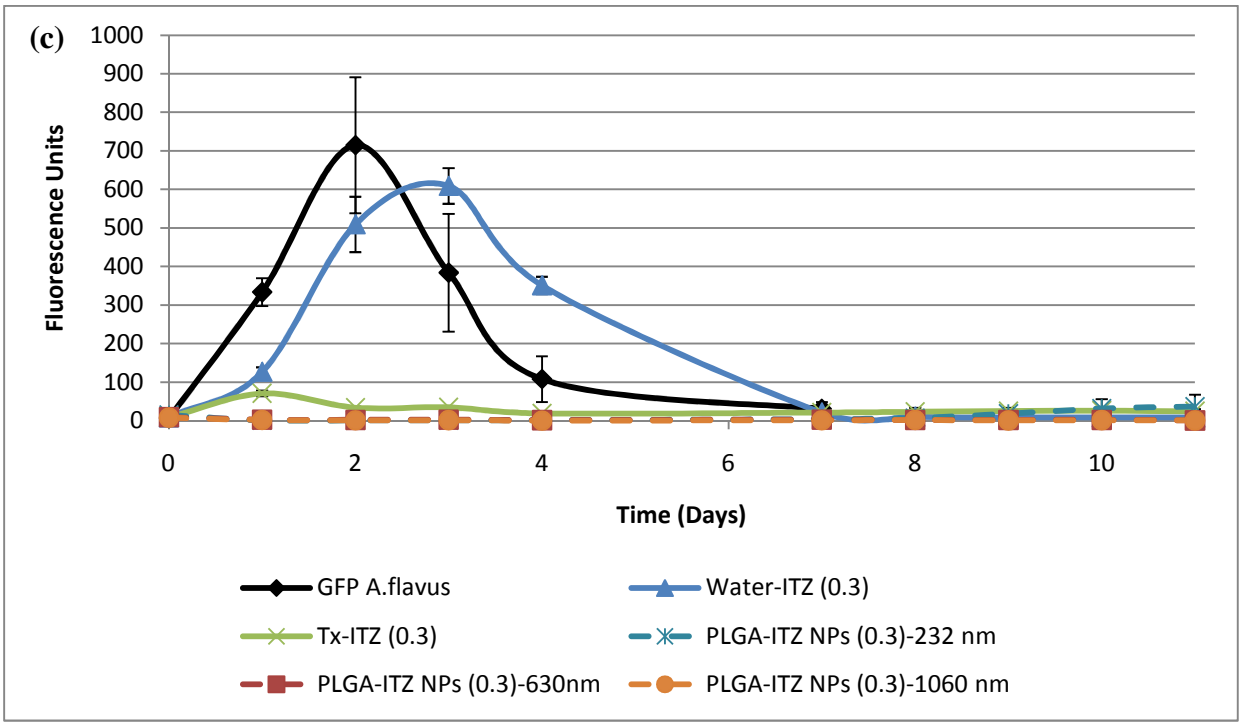

Figure 3.7c: Fluorescence comparison of ITZ in water, Tx-100 ITZ emulsion, and 230 nm, 630 nm, and 1060 nm polylactic-co-glycolic acid nanoparticles with entrapped ITZ at 0.3 mg/ml ITZ (n=3 wells).

www.manaraa.com

vesicles that were seen in the hyphae were believed to be from endosomes which formed once the particles were internalized [34-35]. Coumarin-6 was entrapped in the particle core and no dye leaching or background was observed, indicating that the fluorescence seen inside the hyphae was a result of the PLGA nanoparticles uptake. In addition, the time frame from when the NPs were aliquoted onto the hyphae and photographed was within 2 to 3 minutes, supporting that particle uptake by *A.flavus* was a swift event.

In order to verify if the observed processes were dependent upon the growth stage, PLGA-C6 NPs and *A.flavus* spores were incubated for different times (Figure 3.3). At 0 hours, definitive fluorescent NPs could be seen in the vicinity of the spore, however no activity or dye accumulation was observed (Figure 3.3a). Upon incubation of 1 hour (Figure 3.3b), a physical surface interaction occurred between PGLA-C6 NPs and the spore, and after 12 and 24 hours incubation (Figure 3.3c and 3.3d), hyphae growth became visible along with higher particle density at cell surfaces as well as particle uptake. The cell walls of *A.flavus* are predominantly composed of polysaccharides such as chitin and glucans, with chitin representing a majority of the cell wall composition [36-37]. Chitin is composed of β-1, 4 linked N-acetylglucosamine units and known to contain a strong positive charge. The negative charge of the PLGA nanoparticles from the carboxylic groups provided for an electrostatic interaction between the fungal cells and nanoparticles, which was believed to result in the particles associating with the cell surface. Also, the process of nanoparticle uptake was seen to be related to a vegetative state, explaining why at 0 hours (Figure 3.3a) no activity was seen and as nutrient consumption proceeded particles began attaching to the spore surface (Figure 3.3b). Subsequently, this association with the cell surface could expedite particle and dye entry into the cell, thus yielding a greater accumulation of dye in the hyphae over time.

www.manaraa.com

The study of larger particle (1206 nm) uptake revealed that particle internalization was affected by size. Once PLGA-C6 NPs were added onto the pre-grown hyphae, accumulation of coumarin-6 was still observed inside hyphae (Figure 3.4a), but the event was sporadic compared to 203 nm NPs. The cell walls of *A.flavus* are also known to contain proteins that release hydrolytic enzymes such as phosphatases, amylases, and proteases that assist in transporting larger nutrients in smaller subunits capable of being utilized by the cell, explaining the observed dye accumulation in cells even at larger particle sizes [36, 38-39]. However, in a second photographed location of the same sample, while particle uptake was still observed, fluorescence intensity was visibly lower (Figure 3.4b). This observed difference may be explained by particle density. The fluorescence of 203 nm particles was much more uniformly spread among the sample showing more uniform particle uptake due to a higher NP:cell ratio, when compared to 1206 nm NPs (Figure 3.4). Even so, the particle localization that was still observed for bigger particles on the surface of the fungal cells could also facilitate access of enzymes to particle contents, expediting particle and dye internalization (Figures 3.5a and 3.5b). The size effect on antifungal capability was then studied to see if a correlation could be made between the two studies.

Compared to free ITZ formulations of water-ITZ and Tx-ITZ, PLGA-ITZ NPs of all sizes showed a superior antifungal effect. After immediate treatment and 12 hours post inoculation, higher treatment concentrations of 0.3 and 0.03 mg/ml ITZ did not show any significant difference in antifungal activity between 232, 630, and 1060 nm PLGA-ITZ NPs (Figures 3.6b, 3.6c and Figures 3.7b, 3.7c). Predominantly flat fluorescence profiles were seen compared to Tx-ITZ which showed fluctuating fluorescence profiles. This could be attributed to decreasing drug concentrations from degradation or consumption followed by flourishing of spores that have survived from the intense conditions. Fungal cells also contain active transport

www.manaraa.com

mechanisms to counter exogenous toxicants such as fungicides and remove them [40]. This could also indicate that the particles were mistaken as a food source, endocytosed, and as a result showed improved antifungal ability. The most notable difference in antifungal activity of PLGA-ITZ NPs occurred at 0.003 mg/ml ITZ, seen by a much more gradual decline in fluorescence with 630 and 1060 nm NPs after day 3 compared to smaller sized NPs (Figure 3.6a and Figure 3.7a), possibly due to lower uptake of larger particles (Figures 3.4 and 3.5). At higher ITZ concentrations of 0.3 mg/ml and 0.03 mg/ml, PLGA-ITZ NPs provided a significant enough drug concentration to inhibit growth to the point where no differences were observed in the antifungal effect of nanoparticles of different sizes, while at the lowest ITZ concentration the diminished antifungal ability of larger nanoparticles resulting from the lower particle uptake becomes more apparent. The decreased antifungal effect of larger versus smaller nanoparticles could also be a product of a slower drug release from larger nanoparticles due to their smaller surface to volume ratio [41-44]. Some excessively large particles, such as those seen in Figure 3.5b, that are near the cell surface may slowly release ITZ resulting in a limited antifungal effect, whereas 232 nm particles release ITZ faster yielding a flat fluorescence profile over the span of the study.

Results indicated that PLGA nanoparticle uptake was affected, but not greatly by size in the 200-1000 nm range, and larger particle sizes were correlated with lower drug delivery efficiency at lower ITZ concentrations as indicated in antifungal studies.

3.5 Conclusions

In an attempt to uncover a mechanism of action regarding fungal cells and PLGA-ITZ NP antifungal activity, different sized nanoparticles were tested for particle uptake and antifungal capability. Results revealed that PLGA-C6 nanoparticle uptake at 200 nm was more apparent than 1206 nm. The observed difference was confirmed in GFP quantitative studies. Whereas

www.manaraa.com

200 nm particles showed consistent inhibitory activity across all concentrations compared to free ITZ, larger particles showed weakened antifungal ability at the lowest ITZ concentration of 0.003 mg/ml. NP internalization and cell association seen in the fluorescent studies have been determined as contributing mechanisms of the enhanced antifungal effect of PLGA-ITZ NPs versus free ITZ. While results suggest that other additional mechanisms may also play a role in facilitating ITZ penetration into fungal cells, particle size has proven to be a crucial parameter for drug delivery efficiency.

3.6 Future Perspectives

Finding more potent, less harmful and affordable treatments options is an ongoing effort in medicine today. PLGA nanoparticles have shown to be a valuable and highly effective tool in delivery of a wide variety of bioactive agents, and their applications are consistently expanding. This manuscript has determined that PLGA-ITZ nanoparticles provide for a strong alternative to traditional means of antifungal therapy. The observed activity of PLGA-ITZ NPs has been determined to be linked to nanoparticle uptake by fungal cells and physical association with cell membranes. In general, nanoparticle size showed to be a critical factor that affected nanoparticle uptake and the antifungal efficacy. This study has provided an opportunity to narrow down a mechanism of action of polymeric antifungal nanoparticles. Additional studies focused on release rates of ITZ from different particle sizes and compositions, and nanoparticle interaction with various fungal species at different growth rates are envisioned to provide a more detailed explanation of the enhanced antimicrobial effect observed with antifungal entrapped polymeric nanoparticles.

3.7 References

1. Bala I, Hariharan S, Kumar M: Plga nanoparticles in drug delivery: The state of the art. *Critical Reviews in Therapeutic Drug Carrier Systems* 21(5), 387-422 (2004).

www.manaraa.com

2. Panyam J, Labhasetwar V: Biodegradable nanoparticles for drug and gene delivery to cells and tissue. *Advanced Drug Delivery Reviews* 55(3), 329-347 (2003).

3. Govender T, Stolnik S, Garnett Mc, Illum L, Davis Ss: Plga nanoparticles prepared by nanoprecipitation: Drug loading and release studies of a water soluble drug. *Journal of Controlled Release* 57(2), 171-185 (1999).

4. Patravale Vb, Date Aa, Kulkarni Rm: Nanosuspensions: A promising drug delivery strategy. *Journal of Pharmacy and Pharmacology* 56(7), 827-840 (2004).

5. Nam Ys, Park Jy, Han Sh, Chang Is: Intracellular drug delivery using poly(d,l-lactide-co-glycolide) nanoparticles derivatized with a peptide from a transcriptional activator protein of hiv-1. *Biotechnology Letters* 24(24), 2093-2098 (2002).

6. Cheng J, Teply Ba, Sherifi I *et al.*: Formulation of functionalized plga-peg nanoparticles for in vivo targeted drug delivery. *Biomaterials* 28(5), 869-876 (2007).

7. Song Cx, Labhasetwar V, Murphy H *et al.*: Formulation and characterization of biodegradable nanoparticles for intravascular local drug delivery. *Journal of Controlled Release* 43(2-3), 197-212 (1997).

8. Kumari A, Yadav Sk, Yadav Sc: Biodegradable polymeric nanoparticles based drug delivery systems. *Colloids and Surfaces B: Biointerfaces* 75(1), 1-18 (2010).

9. Song X, Zhao Y, Hou S *et al.*: Dual agents loaded plga nanoparticles: Systematic study of particle size and drug entrapment efficiency. *European Journal of Pharmaceutics and Biopharmaceutics* 69(2), 445-453 (2008).

10. Brannon-Peppas L, Blanchette Jo: Nanoparticle and targeted systems for cancer therapy. *Advanced Drug Delivery Reviews* 56(11), 1649-1659 (2004).

11. Des Rieux A, Fievez V, Garinot M, Schneider Y-J, Préat V: Nanoparticles as potential oral delivery systems of proteins and vaccines: A mechanistic approach. *Journal of Controlled Release* 116(1), 1-27 (2006).

12. Jeong Yi, Na Hs, Seo Dh *et al.*: Ciprofloxacin-encapsulated poly(dl-lactide-co-glycolide) nanoparticles and its antibacterial activity. *International Journal of Pharmaceutics* 352(1-2), 317-323 (2008).

13. Vila A, Sánchez A, Tobío M, Calvo P, Alonso Mj: Design of biodegradable particles for protein delivery. *Journal of Controlled Release* 78(1-3), 15-24 (2002).

14. Debeule K: Itraconazole: Pharmacology, clinical experience and future development. *Int. J. Antimicrob. Agents* 6(3), 175-181 (1996).

www.manaraa.com

15. Willems L, Van Der Geest R, De Beule K: Itraconazole oral solution and intravenous formulations: A review of pharmacokinetics and pharmacodynamics. *J. Clin. Pharm. Ther.* 26(3), 159-169 (2001).

16. Zhang L, Pornpattananangkul D, Hu Cmj, Huang Cm: Development of nanoparticles for antimicrobial drug delivery. *Current Medicinal Chemistry* 17, 585-594 (2010).

17. Choi K-C, Bang J-Y, Kim P-I, Kim C, Song C-E: Amphotericin b-incorporated polymeric micelles composed of poly(d,l-lactide-co-glycolide)/dextran graft copolymer. *International Journal of Pharmaceutics* 355(1-2), 224-230 (2008).

18. Amaral Ac, Bocca Al, Ribeiro Am *et al.*: Amphotericin b in poly(lactic-co-glycolic acid) (plga) and dimercaptosuccinic acid (dmsa) nanoparticles against paracoccidioidomycosis. *J. Antimicrob. Chemother.* 63(3), 526-533 (2009).

19. Nipur R. Patel Kd, Claudia Leonardi and Cristina M. Sabliov: Itraconazole loaded poly(lactic-co-glycolic) acid nanoparticles for improved antifungal activity. *Nanomedicine*, (2010).

20. Nipur Patel Kd, Claudia Leonardi, and Cristina M. Sabliov: Itraconazole loaded poly(lactic-co-glycolic) acid nanoparticles for improved antifungal activity. *Nanomedicine*, (2010).

21. Elamanchili P, Diwan M, Cao M, Samuel J: Characterization of poly(,-lactic-co-glycolic acid) based nanoparticulate system for enhanced delivery of antigens to dendritic cells. *Vaccine* 22(19), 2406-2412 (2004).

22. Gaumet M, Vargas A, Gurny R, Delie F: Nanoparticles for drug delivery: The need for precision in reporting particle size parameters. *European Journal of Pharmaceutics and Biopharmaceutics* 69(1), 1-9 (2008).

23. Desai Mp, Labhasetwar V, Amidon Gl, Levy Rj: Gastrointestinal uptake of biodegradable microparticles: Effect of particle size. *Pharmaceutical Research* 13(12), 1838-1845 (1996).

24. Desai Mp, Labhasetwar V, Walter E, Levy Rj, Amidon Gl: The mechanism of uptake of biodegradable microparticles in caco-2 cells is size dependent. *Pharmaceutical Research* 14, 1568-1573 (1997).

25. Florence At, Hussain N: Transcytosis of nanoparticle and dendrimer delivery systems: Evolving vistas. *Advanced Drug Delivery Reviews* 50(Supplement 1), S69-S89 (2001).

26. Qaddoumi Mg, Ueda H, Yang J, Davda J, Labhasetwar V, Lee Vhl: The characteristics and mechanisms of uptake of plga nanoparticles in rabbit conjunctival epithelial cell layers. *Pharmaceutical Research* 21, 641-648 (2004).

www.manaraa.com

27. Rejman J, Oberle V, Zuhorn Is, Hoekstra D: Size-dependent internalization of particles via the pathways of clathrin-and caveolae-mediated endocytosis. *Biochemical Journal* 377, 159-169 (2004).

28. Yin Win K, Feng S-S: Effects of particle size and surface coating on cellular uptake of polymeric nanoparticles for oral delivery of anticancer drugs. *Biomaterials* 26(15), 2713-2722 (2005).

29. Prabha S, Zhou W-Z, Panyam J, Labhasetwar V: Size-dependency of nanoparticle-mediated gene transfection: Studies with fractionated nanoparticles. *International Journal of Pharmaceutics* 244(1-2), 105-115 (2002).

30. Zauner W, Farrow Na, Haines Amr: In vitro uptake of polystyrene microspheres: Effect of particle size, cell line and cell density. *Journal of Controlled Release* 71(1), 39-51 (2001).

31. Panyam J, Sahoo Sk, Prabha S, Bargar T, Labhasetwar V: Fluorescence and electron microscopy probes for cellular and tissue uptake of poly(d,l-lactide-co-glycolide) nanoparticles. *International Journal of Pharmaceutics* 262(1-2), 1-11 (2003).

32. Pietzonka P, Rothen-Rutishauser B, Langguth P, Wunderli-Allenspach H, Walter E, Merkle Hp: Transfer of lipophilic markers from plga and polystyrene nanoparticles to caco-2 monolayers mimics particle uptake. *Pharmaceutical Research* 19(5), 595-601 (2002).

33. Rajasekaran K, Cary Jw, Cotty Pj, Cleveland Te: Development of a gfp-expressing aspergillus flavus strain to study fungal invasion, colonization, and resistance in cottonseed. *Mycopathologia* 165(2), 89-97 (2008).

34. Higuchi Y, Nakahama T, Shoji J, Arioka M, Kitamoto K: Visualization of the endocytic pathway in the filamentous fungus aspergillus oryzae using an egfp-fused plasma membrane protein. *Biochemical and Biophysical Research Communications* 340(3), 784-791 (2006).

35. Higuchi Y, Shoji Jy, Arioka M, Kitamoto K: Endocytosis is crucial for cell polarity and apical membrane recycling in the filamentous fungus aspergillus oryzae. *Eukaryotic Cell* 8(1), 37-46 (2009).

36. Michael O. Garraway Rce: Fungal nutrition and physiology Krieger Publishing (1992).

37. *The growing fungus.* Neil A.R. Gow Gmg (Ed.^(Eds). Chapman & Hall, London, UK (1995).

38. Griffin Dh: Fungal physiology. (Second Edition). Wiley-Liss, (1994).

www.manaraa.com

39. Alzwei Ao Ak, Elgerbi Am and Candlish Aag: Production of extracellular enzymes and aflatoxins in solid substrate fermentation with aflatoxigenic aspergillus spp. *Mycotoxin Research* 20(2), 87-96 (2004).

40. Del Sorbo G, Schoonbeek Hj, De Waard Ma: Fungal transporters involved in efflux of natural toxic compounds and fungicides. *Fungal Genetics and Biology* 30(1), 1-15 (2000).

41. Jeon H-J, Jeong Y-I, Jang M-K, Park Y-H, Nah J-W: Effect of solvent on the preparation of surfactant-free poly(-lactide-co-glycolide) nanoparticles and norfloxacin release characteristics. *International Journal of Pharmaceutics* 207(1-2), 99-108 (2000).

42. Zweers Mlt, Engbers Ghm, Grijpma Dw, Feijen J: Release of anti-restenosis drugs from poly(ethylene oxide)-poly(dl-lactic-co-glycolic acid) nanoparticles. *Journal of Controlled Release* 114(3), 317-324 (2006).

43. Leroux Jc, Allemann E, Dejaeghere F, Doelker E, Gurny R: Biodegradable nanoparticles - from sustained release formulations to improved site specific drug delivery. *Journal of Controlled Release* 39(2-3), 339-350 (1996).

44. Polakovic M, Görner T, Gref R, Dellacherie E: Lidocaine loaded biodegradable nanospheres: Ii. Modelling of drug release. *Journal of Controlled Release* 60(2-3), 169-177 (1999).

www.manaraa.com

Chapter 4. Conclusions

PLGA nanoparticles as a delivery system for the antifungal drug Itraconazole have proven to be a potent alternative compared to the conventional free or emulsified forms of. Results showed that Itraconazole may provide a steady drug dose for five days and inhibit fungal growth beyond the application point when applied to an inoculated surface, as observed in culture studies. Quantitative inhibitory studies showed an equivalent antifungal effect at 100x less Itraconazole when entrapped in PLGA nanoparticles compared to free Itraconazole formulations. These characteristics can be of great benefit in addressing certain issues with traditional drug forms such as fluctuating drug levels in the blood stream, toxicity from high dosages and excessive related costs. It was determined that smaller PLGA-ITZ NPs compared to larger particles were able to penetrate *A.flavus* cells more efficiently, resulting in a superior antifungal effect, especially at lower drug concentrations. A definite mechanism of action has not be determined, however the current study has provided great insight that links the observed superior antifungal activity of the entrapped ITZ with the ability of PLGA nanoparticles to be efficiently uptaken by fungal cells. Other studies are required to fully investigate and understand the mechanism of action and factors involved in the observed activity of PLGA-ITZ NPs.

www.manaraa.com

Appendix A

Table S1: Least square means of fluorescence unit natural log (FULN) at 0.003 mg/ml Itraconazole (ITZ) concentration treated immediately after inoculation (0 h).

Treatment[1]	Day	FULN	SE[2]	Letter group[3]
Blank_NPs	1	4.2784	0.1309	J
Blank_NPs	2	6.1507	0.1309	BC
Blank_NPs	3	6.2835	0.1309	AB
Blank_NPs	4	5.6971	0.1309	DEF
PLGA-ITZ NPs	1	3.4545	0.1309	K
PLGA-ITZ NPs	2	4.8051	0.1309	I
PLGA-ITZ NPs	3	5.8597	0.1309	CDE
PLGA-ITZ NPs	4	5.6438	0.1309	EFG
Tx_ITZ	1	4.0504	0.1309	J
Tx_ITZ	2	5.1505	0.1309	HI
Tx_ITZ	3	5.8545	0.1309	CDE
Tx_ITZ	4	5.3927	0.1309	FGH
W_ITZ	1	4.1878	0.1309	J
W_ITZ	2	6.3845	0.1309	AB
W_ITZ	3	6.0260	0.1309	BCD
W_ITZ	4	5.2757	0.1309	GH
control	1	4.3301	0.1309	J
control	2	6.6333	0.1309	A
control	3	6.2766	0.1309	AB
control	4	5.3333	0.1309	FGH

[1]Treatment: Blank_NPs = blank nanoparticles; PLGA-ITZ NPs = polylactic-*co*-glycolic acid nanoparticles with Itraconazole; Tx_ITZ = Itraconazole emulsion in Triton X-100; W_ITZ = Itraconazole in water; control = *A.flavus* alone.
[2]SEM: standard error of the mean.
[3]Letter group: means with different letters are significantly different ($P < 0.05$). Least square means were compared among treatments over time when a significant treatment by time interaction ($P < 0.0001$) was observed using *Tukey* post-hoc multiple comparison adjustment.

www.manaraa.com

Table S2: Least square means of fluorescence unit natural log (FULN) at 0.03 mg/ml Itraconazole (ITZ) concentration treated immediately after inoculation (0 h).

Treatment[1]	Day	FULN	SE[2]	Letter group[3]
Blank_NPs	1	4.2784	0.1834	DEF
Blank_NPs	2	6.1507	0.1834	ABC
Blank_NPs	3	6.2835	0.1834	AB
Blank_NPs	4	5.6971	0.1834	ABC
PLGA-ITZ NPs	1	0.4621	0.1834	G
PLGA-ITZ NPs	2	0.2310	0.1834	G
PLGA-ITZ NPs	3	0.2310	0.1834	G
PLGA-ITZ NPs	4	0.2310	0.1834	G
Tx_ITZ	1	3.7926	0.1834	F
Tx_ITZ	2	4.2420	0.1834	EF
Tx_ITZ	3	5.2192	0.1834	CD
Tx_ITZ	4	5.1587	0.1834	CDE
W_ITZ	1	3.9949	0.1834	F
W_ITZ	2	6.2997	0.1834	AB
W_ITZ	3	6.1562	0.1834	ABC
W_ITZ	4	5.7026	0.1834	ABC
control	1	4.3301	0.1834	DEF
control	2	6.6333	0.1834	A
control	3	6.2766	0.1834	A
control	4	5.3333	0.1834	BC

[1]Treatment: Blank_NPs = blank nanoparticles; PLGA-ITZ NPs = polylactic-*co*-glycolic acid nanoparticles with Itraconazole; Tx_ITZ = Itraconazole emulsion in Triton X-100; W_ITZ = Itraconazole in water; control = *A.flavus*.
[2]SEM: standard error of the mean.
[3]Letter group: means with different letters are significantly different ($P < 0.05$). Least square means were compared among treatments over time when a significant treatment by time interaction ($P < 0.0001$) was observed using *Tukey* post-hoc multiple comparison adjustment.

www.manaraa.com

Table S3: Least square means of fluorescence unit natural log (FULN) at 0.3 mg/ml Itraconazole (ITZ) concentration treated immediately after inoculation (0 h).

Treatment[1]	Day	FULN	SE[2]	Letter group[3]
Blank_NPs	1	4.2784	0.3579	CDE
Blank_NPs	2	6.1507	0.3579	AB
Blank_NPs	3	6.2835	0.3579	AB
Blank_NPs	4	5.6971	0.3579	ABC
PLGA-ITZ NPs	1	2.11E-15	0.3579	F
PLGA-ITZ NPs	2	0.2310	0.3579	F
PLGA-ITZ NPs	3	0.3662	0.3579	F
PLGA-ITZ NPs	4	0.9986	0.3579	F
Tx_ITZ	1	3.6919	0.3579	DE
Tx_ITZ	2	3.7559	0.3579	CDE
Tx_ITZ	3	3.8203	0.3579	CDE
Tx_ITZ	4	5.1582	0.3579	ABCDE
W_ITZ	1	3.6107	0.3579	E
W_ITZ	2	5.5047	0.3579	ABCD
W_ITZ	3	6.7174	0.3579	A
W_ITZ	4	6.3728	0.3579	A
control	1	4.3301	0.3579	BCDE
control	2	6.6333	0.3579	A
control	3	6.2766	0.3579	A
control	4	5.3333	0.3579	ABCDE

[1]Treatment: Blank_NPs = blank nanoparticles; PLGA-ITZ NPs = polylactic-*co*-glycolic acid nanoparticles with Itraconazole; Tx_ITZ = Itraconazole emulsion in Triton X-100; W_ITZ = Itraconazole in water; control = *A.flavus*.
[2]SEM: standard error of the mean.
[3]Letter group: means with different letters are significantly different ($P < 0.05$). Least square means were compared among treatments over time when a significant treatment by time interaction ($P = 0.0002$) was observed using *Tukey* post-hoc multiple comparison adjustment.

www.manaraa.com

Table S4: Least square means of fluorescence unit natural log (FULN) at 0.003 mg/ml Itraconazole (ITZ) concentration treated 12 h after inoculation (12 h).

Treatment[1]	Day	FULN	SE[2]	Letter group[3]
Blank_NPs	0	2.7296	0.2314	MN
Blank_NPs	1	5.6453	0.2314	CDEF
Blank_NPs	2	5.9359	0.2314	BCD
Blank_NPs	3	5.4603	0.2314	CDEFGH
Blank_NPs	4	4.9754	0.2314	GHI
PLGA-ITZ NPs	0	2.7511	0.2314	MN
PLGA-ITZ NPs	1	3.6314	0.2314	KL
PLGA-ITZ NPs	2	3.3037	0.2314	LM
PLGA-ITZ NPs	3	4.8163	0.2314	HIJ
PLGA-ITZ NPs	4	5.0841	0.2314	FGHI
Tx_ITZ	0	2.7066	0.2314	MN
Tx_ITZ	1	4.1643	0.2314	JK
Tx_ITZ	2	4.6073	0.2314	IJ
Tx_ITZ	3	5.8694	0.2314	BCDE
Tx_ITZ	4	6.9556	0.2314	A
W_ITZ	0	2.6374	0.2314	N
W_ITZ	1	5.0174	0.2314	FGHI
W_ITZ	2	6.0616	0.2314	BC
W_ITZ	3	5.6429	0.2314	CDEF
W_ITZ	4	5.2977	0.2314	DEFGH
control	0	2.4508	0.2314	N
control	1	5.5647	0.2314	CDEFG
control	2	6.4132	0.2314	AB
control	3	5.7689	0.2314	BCDE
control	4	5.2321	0.2314	EFGHI

[1]Treatment: Blank_NPs = blank nanoparticles; PLGA-ITZ NPs = polylactic-*co*-glycolic acid nanoparticles with Itraconazole; Tx_ITZ = Itraconazole emulsion in Triton X-100; W_ITZ = Itraconazole in water; control = *A.flavus*.
[2]SEM: standard error of the mean.
[3]Letter group: means with different letters are significantly different ($P < 0.05$). Least square means were compared among treatments over time when a significant treatment by time interaction ($P < 0.0001$) was observed using *Tukey* post-hoc multiple comparison adjustment.

www.manaraa.com

Table S5: Least square means of fluorescence unit natural log (FULN) at 0.03 mg/ml Itraconazole (ITZ) concentration treated 12 h after inoculation (12 h).

Treatment[1]	Day	FULN	SE[2]	Letter group[3]
Blank_NPs	0	2.7296	0.4126	DEFGH
Blank_NPs	1	5.6453	0.4126	ABC
Blank_NPs	2	5.9359	0.4126	AB
Blank_NPs	3	5.4603	0.4126	ABC
Blank_NPs	4	4.9754	0.4126	ABCD
PLGA-ITZ NPs	0	2.7066	0.4126	EFGH
PLGA-ITZ NPs	1	0.2310	0.4126	I
PLGA-ITZ NPs	2	0.6931	0.4126	HI
PLGA-ITZ NPs	3	1.1552	0.4126	HI
PLGA-ITZ NPs	4	1.8783	0.4126	GHI
Tx_ITZ	0	2.6819	0.4126	EFGH
Tx_ITZ	1	4.0669	0.4126	BCDEFG
Tx_ITZ	2	3.4904	0.4126	CDEFG
Tx_ITZ	3	4.1698	0.4126	ABCDEF
Tx_ITZ	4	6.0189	0.4126	AB
W_ITZ	0	2.5817	0.4126	FGH
W_ITZ	1	4.8697	0.4126	ABCDE
W_ITZ	2	6.0405	0.4126	AB
W_ITZ	3	6.0070	0.4126	AB
W_ITZ	4	5.8715	0.4126	AB
control	0	2.4508	0.4126	FGHI
control	1	5.5647	0.4126	ABC
control	2	6.4132	0.4126	A
control	3	5.7689	0.4126	AB
control	4	5.2321	0.4126	ABC

[1]Treatment: Blank_NPs = blank nanoparticles; PLGA-ITZ NPs = polylactic-*co*-glycolic acid nanoparticles with Itraconazole; Tx_ITZ = Itraconazole emulsion in Triton X-100; W_ITZ = Itraconazole in water; control = *A.flavus*.
[2]SEM: standard error of the mean.
[3]Letter group: means with different letters are significantly different ($P < 0.05$). Least square means were compared among treatments over time when a significant treatment by time interaction ($P < 0.0001$) was observed using *Tukey* post-hoc multiple comparison adjustment.

www.manaraa.com

Table S6: Least square means of fluorescence unit natural log (FULN) at 0.3 mg/ml Itraconazole (ITZ) concentration treated 12 h after inoculation (12 h).

Treatment[1]	Day	FULN	SE[2]	Letter group[3]
Blank_NPs	0	2.7296	0.1891	DEF
Blank_NPs	1	5.6453	0.1891	ABC
Blank_NPs	2	5.9359	0.1891	AB
Blank_NPs	3	5.4603	0.1891	ABC
Blank_NPs	4	4.9754	0.1891	C
PLGA-ITZ NPs	0	2.7066	0.1891	DEF
PLGA-ITZ NPs	1	-244E-17	0.1891	H
PLGA-ITZ NPs	2	-244E-17	0.1891	H
PLGA-ITZ NPs	3	-211E-17	0.1891	H
PLGA-ITZ NPs	4	0.2310	0.1891	H
Tx_ITZ	0	2.6107	0.1891	EG
Tx_ITZ	1	3.4399	0.1891	DF
Tx_ITZ	2	2.9407	0.1891	DEF
Tx_ITZ	3	2.7673	0.1891	DEF
Tx_ITZ	4	2.6177	0.1891	EG
W_ITZ	0	2.5383	0.1891	FG
W_ITZ	1	3.6387	0.1891	DE
W_ITZ	2	5.6166	0.1891	ABC
W_ITZ	3	6.0206	0.1891	ABC
W_ITZ	4	6.0253	0.1891	AB
control	0	2.4508	0.1891	FG
control	1	5.5647	0.1891	BC
control	2	6.4132	0.1891	A
control	3	5.7689	0.1891	ABC
control	4	5.2321	0.1891	BC

[1]Treatment: Blank_NPs = blank nanoparticles; PLGA_ITZ = polylactic-*co*-glycolic acid nanoparticles with Itraconazole; Tx_ITZ = Itraconazole emulsion in Triton X-100; W_ITZ = Itraconazole in water; control = *A.flavus*.
[2]SEM: standard error of the mean.
[3]Letter group: means with different letters are significantly different ($P < 0.05$). Least square means were compared among treatments over time when a significant treatment by time interaction ($P < 0.0001$) was observed using *Tukey* post-hoc multiple comparison adjustment.

www.manaraa.com

Appendix B

Table B1: Least square means of fluorescence unit natural log (FULN) at 0.003 mg/ml Itraconazole (ITZ) concentration treated immediately after inoculation (0 h).

Treatment[1]	Day	FULN	SE[2]	Letter group[3]
B10_0	0	0.3109	0.1816	P
B10_0	1	4.7514	0.1816	HIJKMN
B10_0	2	6.2880	0.1816	ABC
B10_0	3	6.0111	0.1816	ABCDE
B10_0	4	5.5581	0.1816	BCDEFG
B2_0	0	-2.3026	0.1641	Q
B2_0	1	4.2798	0.1641	JKNO
B2_0	2	6.1509	0.1641	ABC
B2_0	3	6.2836	0.1641	AB
B2_0	4	5.6974	0.1641	ABCDEFH
B6_0	0	0.7419	0.1142	P
B6_0	1	4.8183	0.1142	GIJKM
B6_0	2	6.2145	0.1142	AB
B6_0	3	5.8775	0.1142	ABCE
B6_0	4	5.2001	0.1142	DFGHIL
P10_0.003	0	0.5264	0.1230	P
P10_0.003	1	3.9329	0.1230	NO
P10_0.003	2	4.8487	0.1230	GIJKM
P10_0.003	3	6.2454	0.1230	AB
P10_0.003	4	6.0936	0.1230	ABC
P2_0.003	0	0.09531	0.1348	P
P2_0.003	1	3.4576	0.1348	O
P2_0.003	2	4.8059	0.1348	GIJKM
P2_0.003	3	5.8600	0.1348	ABCDE
P2_0.003	4	5.6442	0.1348	BCDEFH
P6_0.003	0	-2.3026	0.2053	Q
P6_0.003	1	4.0735	0.2053	KNO
P6_0.003	2	5.0342	0.2053	EFGHIJL
P6_0.003	3	6.1838	0.2053	ABC
P6_0.003	4	6.1581	0.2053	ABCD
T0.003	0	0.7419	0.08123	P
T0.003	1	3.8008	0.08123	O
T0.003	2	6.0475	0.08123	AB
T0.003	3	5.5064	0.08123	CDEFH
T0.003	4	4.6292	0.08123	IJK
W0.003	0	-0.4884	0.5042	PQ
W0.003	1	4.6191	0.5042	ABCDEFGHIJKNO
W0.003	2	6.2974	0.5042	ABCDEFGHIJK
W0.003	3	6.7052	0.5042	ABCDEFGHI
W0.003	4	6.0810	0.5042	ABCDEFGHIJK
control	0	0.5264	0.1268	P
control	1	4.7041	0.1268	GIJKM
control	2	6.5038	0.1268	A
control	3	6.1338	0.1268	AB
control	4	4.9558	0.1268	FGHIJK

[1]Treatment: B10_0, B6_0, B2_0= blank nanoparticles at 1060nm, 630nm, 230 nm; P_10, P_6, P_2= polylactic-*co*-glycolic acid nanoparticles with Itraconazole at 1060nm, 630nm, 230nm.; T = Itraconazole emulsion in Triton X-100; W = Itraconazole in water; control = *A.flavus* alone.
[2]SEM: standard error of the mean.
[3]Letter group: means with different letters are significantly different ($P < 0.05$). Least square means were compared among treatments over time when a significant treatment by time interaction ($P < 0.0001$) was observed using *Tukey* post-hoc multiple comparison adjustment.

www.manaraa.com

Table B2: Least square means of fluorescence unit natural log (FULN) at 0.03 mg/ml Itraconazole (ITZ) concentration treated immediately after inoculation (0 h).

Treatment[1]	Day	FULN	SE[2]	Letter group[3]
B10_0	0	0.3109	0.1816	LM
B10_0	1	4.7514	0.1816	FHIJK
B10_0	2	6.2880	0.1816	AB
B10_0	3	6.0111	0.1816	ABCD
B10_0	4	5.5581	0.1816	BCDEG
B2_0	0	-2.3026	0.1641	N
B2_0	1	4.2798	0.1641	HIJK
B2_0	2	6.1509	0.1641	ABC
B2_0	3	6.2836	0.1641	AB
B2_0	4	5.6974	0.1641	ABCDEF
B6_0	0	0.7419	0.1142	L
B6_0	1	4.8183	0.1142	GHI
B6_0	2	6.2145	0.1142	AB
B6_0	3	5.8775	0.1142	ABC
B6_0	4	5.2001	0.1142	DEFG
P10_0.03	0	0.4407	0.4012	LM
P10_0.03	1	0.7419	0.4012	LM
P10_0.03	2	0.3109	0.4012	LM
P10_0.03	3	0.09531	0.4012	LM
P10_0.03	4	-1.5033	0.4012	MN
P2_0.03	0	0.09531	0.1928	LM
P2_0.03	1	0.5264	0.1928	L
P2_0.03	2	0.3109	0.1928	LM
P2_0.03	3	0.3109	0.1928	LM
P2_0.03	4	0.3109	0.1928	LM
P6_0.03	0	0.7419	0.1351	L
P6_0.03	1	0.7419	0.1351	L
P6_0.03	2	0.6562	0.1351	L
P6_0.03	3	0.7419	0.1351	L
P6_0.03	4	0.09531	0.1351	LM
T0.03	0	0.7419	0.2169	L
T0.03	1	3.6129	0.2169	K
T0.03	2	4.1415	0.2169	HIJK
T0.03	3	3.6383	0.2169	K
T0.03	4	3.7859	0.2169	JK
W0.03	0	0.09531	0.1150	LM
W0.03	1	4.2293	0.1150	IJK
W0.03	2	5.3883	0.1150	CDEFG
W0.03	3	6.1148	0.1150	ABC
W0.03	4	5.6505	0.1150	BCDE
control	0	0.5264	0.1268	L
control	1	4.7041	0.1268	GHIJ
control	2	6.5038	0.1268	A
control	3	6.1338	0.1268	AB
control	4	4.9558	0.1268	EFGH

[1]Treatment: B10_0, B6_0, B2_0= blank nanoparticles at 1060nm, 630nm, 230 nm; P_10, P_6, P_2= polylactic-*co*-glycolic acid nanoparticles with Itraconazole at 1060nm, 630nm, 230nm.; T = Itraconazole emulsion in Triton X-100; W = Itraconazole in water; control = *A.flavus* alone.
[2]SEM: standard error of the mean.
[3]Letter group: means with different letters are significantly different ($P < 0.05$). Least square means were compared among treatments over time when a significant treatment by time interaction ($P < 0.0001$) was observed using *Tukey* post-hoc multiple comparison adjustment.

www.manaraa.com

Table B3: Least square means of fluorescence unit natural log (FULN) at 0.3 mg/ml Itraconazole (ITZ) concentration treated immediately after inoculation (0 h).

Treatment[1]	Day	FULN	SE[2]	Letter group[3]
B10_0	0	0.3109	0.1816	QR
B10_0	1	4.7514	0.1816	FIJKL
B10_0	2	6.2880	0.1816	AB
B10_0	3	6.0111	0.1816	ABCD
B10_0	4	5.5581	0.1816	BCDEG
B2_0	0	-2.3026	0.1641	S
B2_0	1	4.2798	0.1641	IJLM
B2_0	2	6.1509	0.1641	AB
B2_0	3	6.2836	0.1641	AB
B2_0	4	5.6974	0.1641	ABCDEF
B6_0	0	0.7419	0.1142	Q
B6_0	1	4.8183	0.1142	GIJK
B6_0	2	6.2145	0.1142	AB
B6_0	3	5.8775	0.1142	ABD
B6_0	4	5.2001	0.1142	CEFGH
P10_0.3	0	0.3109	0.5146	QR
P10_0.3	1	-0.7040	0.5146	QRS
P10_0.3	2	0.09531	0.5146	QR
P10_0.3	3	0.09531	0.5146	QR
P10_0.3	4	-1.5033	0.5146	RS
P2_0.3	0	-0.7040	0.4976	QRS
P2_0.3	1	0.09531	0.4976	QR
P2_0.3	2	0.3109	0.4976	QR
P2_0.3	3	0.4407	0.4976	QR
P2_0.3	4	1.0499	0.4976	PQR
P6_0.3	0	0.7419	0.4142	QR
P6_0.3	1	0.7419	0.4142	QR
P6_0.3	2	0.7419	0.4142	QR
P6_0.3	3	0.7419	0.4142	QR
P6_0.3	4	-0.4884	0.4142	QRS
T0.3	0	0.5264	0.1163	QR
T0.3	1	3.6400	0.1163	MN
T0.3	2	4.0701	0.1163	LM
T0.3	3	3.3229	0.1163	NO
T0.3	4	2.7101	0.1163	OP
W0.3	0	0.6562	0.2038	QR
W0.3	1	3.9839	0.2038	JLMN
W0.3	2	5.0377	0.2038	DEFGHI
W0.3	3	6.4307	0.2038	AB
W0.3	4	6.1501	0.2038	ABC
control	0	0.5264	0.1268	QR
control	1	4.7041	0.1268	GIJKL
control	2	6.5038	0.1268	A
control	3	6.1338	0.1268	AB
control	4	4.9558	0.1268	EFGIJ

[1]Treatment: B10_0, B6_0, B2_0= blank nanoparticles at 1060nm, 630nm, 230 nm; P_10, P_6, P_2= polylactic-*co*-glycolic acid nanoparticles with Itraconazole at 1060nm, 630nm, 230nm.; T = Itraconazole emulsion in Triton X-100; W = Itraconazole in water; control = *A.flavus* alone.
[2]SEM: standard error of the mean.
[3]Letter group: means with different letters are significantly different ($P < 0.05$). Least square means were compared among treatments over time when a significant treatment by time interaction ($P < 0.0001$) was observed using *Tukey* post-hoc multiple comparison adjustment.

www.manaraa.com

Table B4: Least square means of fluorescence unit natural log (FULN) at 0.003 mg/ml Itraconazole (ITZ) concentration treated 12 h after inoculation (12 h).

Treatment[1]	Day	FULN	SE[2]	Letter group[3]
B10_0	0	2.0479	0.06539	QR
B10_0	1	5.8750	0.06539	CGK
B10_0	2	6.5061	0.06539	AD
B10_0	3	5.9227	0.06539	BCGK
B10_0	4	4.5671	0.06539	M
B2_0	0	2.7361	0.1814	PQ
B2_0	1	5.6457	0.1814	BCFGHIJ
B2_0	2	5.9362	0.1814	ABCGH
B2_0	3	5.4607	0.1814	CGHIJ
B2_0	4	4.9762	0.1814	IJMN
B6_0	0	2.0919	0.1228	QR
B6_0	1	5.9477	0.1228	BCDGK
B6_0	2	6.2554	0.1228	ABCG
B6_0	3	5.7144	0.1228	CGHI
B6_0	4	4.3109	0.1228	M
P10_0.003	0	2.0040	0.05207	QR
P10_0.003	1	4.9207	0.05207	J
P10_0.003	2	6.4115	0.05207	ADEF
P10_0.003	3	6.4240	0.05207	ADE
P10_0.003	4	6.0453	0.05207	BCG
P2_0.003	0	0.09531	0.1348	S
P2_0.003	1	3.4576	0.1348	OP
P2_0.003	2	4.8059	0.1348	JM
P2_0.003	3	5.8600	0.1348	BCEGIKL
P2_0.003	4	5.6442	0.1348	CGHI
P6_0.003	0	1.6292	0.09923	R
P6_0.003	1	5.1000	0.09923	HJN
P6_0.003	2	6.3717	0.09923	AB
P6_0.003	3	5.9111	0.09923	BCGK
P6_0.003	4	4.8691	0.09923	JM
T0.003	0	2.1695	0.3535	PQR
T0.003	1	4.5682	0.3535	HIJKMO
T0.003	2	6.1884	0.3535	ABCGHIJ
T0.003	3	5.7043	0.3535	ABCGHIJM
T0.003	4	4.8362	0.3535	GHIJMO
W0.003	0	2.0040	0.1476	QR
W0.003	1	5.6480	0.1476	BCGHI
W0.003	2	6.7396	0.1476	A
W0.003	3	6.1478	0.1476	ABCG
W0.003	4	5.0723	0.1476	HIJLM
control	0	1.9601	0.1935	QR
control	1	5.8063	0.1935	ABCGHI
control	2	6.5530	0.1935	ABC
control	3	5.8997	0.1935	ABCGHI
control	4	4.5735	0.1935	JM

[1]Treatment: B10_0, B6_0, B2_0= blank nanoparticles at 1060nm, 630nm, 230 nm; P_10, P_6, P_2= polylactic-*co*-glycolic acid nanoparticles with Itraconazole at 1060nm, 630nm, 230nm.; T = Itraconazole emulsion in Triton X-100; W = Itraconazole in water; control = *A.flavus* alone.
[2]SEM: standard error of the mean.
[3]Letter group: means with different letters are significantly different ($P < 0.05$). Least square means were compared among treatments over time when a significant treatment by time interaction ($P < 0.0001$) was observed using *Tukey* post-hoc multiple comparison adjustment.

www.manaraa.com

Table B5: Least square means of fluorescence unit natural log (FULN) at 0.03 mg/ml Itraconazole (ITZ) concentration treated 12 h after inoculation (12 h).

Treatment[1]	Day	FULN	SE[2]	Letter group[3]
B10_0	0	2.0479	0.06539	LM
B10_0	1	5.8750	0.06539	BC
B10_0	2	6.5061	0.06539	A
B10_0	3	5.9227	0.06539	BC
B10_0	4	4.5671	0.06539	H
B2_0	0	2.7361	0.1814	JKL
B2_0	1	5.6457	0.1814	BCDEF
B2_0	2	5.9362	0.1814	ABC
B2_0	3	5.4607	0.1814	BCDEFG
B2_0	4	4.9762	0.1814	DEFGH
B6_0	0	2.0919	0.1228	LM
B6_0	1	5.9477	0.1228	ABC
B6_0	2	6.2554	0.1228	AB
B6_0	3	5.7144	0.1228	BCDE
B6_0	4	4.3109	0.1228	HI
P10_0.03	0	2.0867	0.8292	GHIJKLMNO
P10_0.03	1	0.5264	0.8292	JKLMNO
P10_0.03	2	0.3109	0.8292	KLMNO
P10_0.03	3	1.1062	0.8292	IJKLMNO
P10_0.03	4	1.1152	0.8292	IJKLMNO
P2_0.03	0	0.09531	0.1928	O
P2_0.03	1	0.5264	0.1928	O
P2_0.03	2	0.3109	0.1928	O
P2_0.03	3	0.3109	0.1928	O
P2_0.03	4	0.3109	0.1928	O
P6_0.03	0	2.2083	0.3182	KLMN
P6_0.03	1	0.8718	0.3182	MNO
P6_0.03	2	0.7419	0.3182	MNO
P6_0.03	3	0.5264	0.3182	NO
P6_0.03	4	0.7608	0.3182	MNO
T0.03	0	2.1307	0.2944	LMN
T0.03	1	4.4217	0.2944	EFGHI
T0.03	2	3.9963	0.2944	HIJ
T0.03	3	4.2735	0.2944	FGHI
T0.03	4	3.8818	0.2944	HIJK
W0.03	0	1.7486	0.1931	LMN
W0.03	1	5.1841	0.1931	CDEFGH
W0.03	2	6.3273	0.1931	AB
W0.03	3	5.8856	0.1931	ABCD
W0.03	4	5.1797	0.1931	CDEFGH
control	0	1.9601	0.1935	LMN
control	1	5.8063	0.1935	ABCDE
control	2	6.5530	0.1935	AB
control	3	5.8997	0.1935	ABCD
control	4	4.5735	0.1935	FGHI

[1]Treatment: B10_0, B6_0, B2_0= blank nanoparticles at 1060nm, 630nm, 230 nm; P_10, P_6, P_2= polylactic-*co*-glycolic acid nanoparticles with Itraconazole at 1060nm, 630nm, 230nm.; T = Itraconazole emulsion in Triton X-100; W = Itraconazole in water; control = *A.flavus* alone.
[2]SEM: standard error of the mean.
[3]Letter group: means with different letters are significantly different ($P < 0.05$). Least square means were compared among treatments over time when a significant treatment by time interaction ($P < 0.0001$) was observed using *Tukey* post-hoc multiple comparison adjustment.

www.manaraa.com

Table B6: Least square means of fluorescence unit natural log (FULN) at 0.3 mg/ml Itraconazole (ITZ) concentration treated 12 h after inoculation (12 h).

Treatment[1]	Day	FULN	SE[2]	Letter group[3]
B10_0	0	2.0479	0.1215	MNO
B10_0	1	5.8750	0.1215	ABCD
B10_0	2	6.5061	0.1215	A
B10_0	3	5.9227	0.1215	ABCD
B10_0	4	4.5671	0.1215	FIJ
B2_0	0	2.7361	0.1215	LM
B2_0	1	5.6457	0.1215	CDG
B2_0	2	5.9362	0.1215	ABCD
B2_0	3	5.4607	0.1215	DEH
B2_0	4	4.9762	0.1215	EFI
B6_0	0	2.0919	0.1215	MNO
B6_0	1	5.9477	0.1215	ABCD
B6_0	2	6.2554	0.1215	ABC
B6_0	3	5.7144	0.1215	BCDG
B6_0	4	4.3109	0.1215	IJ
P10_0.3	0	2.0919	0.1215	MNO
P10_0.3	1	0.5264	0.1215	RS
P10_0.3	2	0.09531	0.1215	RS
P10_0.3	3	0.3109	0.1215	RS
P10_0.3	4	-2.3026	0.1215	T
P2_0.3	0	-0.7040	0.2753	S
P2_0.3	1	0.09531	0.2753	RS
P2_0.3	2	0.3109	0.2753	RS
P2_0.3	3	0.4407	0.2753	QRS
P2_0.3	4	1.0499	0.2753	NOPQR
P6_0.3	0	2.2083	0.2753	LMNO
P6_0.3	1	0.8718	0.2753	OPQRS
P6_0.3	2	0.7419	0.2753	PQRS
P6_0.3	3	1.0016	0.2753	NOPQR
P6_0.3	4	0.3109	0.2753	RS
T0.3	0	2.1695	0.2753	MNOP
T0.3	1	4.2607	0.2753	FHIJK
T0.3	2	3.5273	0.2753	JKL
T0.3	3	3.5551	0.2753	JKL
T0.3	4	2.9488	0.2753	KLM
W0.3	0	2.1695	0.1215	MN
W0.3	1	4.8395	0.1215	EFI
W0.3	2	6.2264	0.1215	ABC
W0.3	3	6.4100	0.1215	AB
W0.3	4	5.8597	0.1215	ABCD
control	0	1.9601	0.2753	LMNOPQ
control	1	5.8063	0.2753	ABCDEF
control	2	6.5530	0.2753	ABCD
control	3	5.8997	0.2753	ABCDE
control	4	4.5735	0.2753	EFGIJ

[1]Treatment: B10_0, B6_0, B2_0= blank nanoparticles at 1060nm, 630nm, 230 nm; P_10, P_6, P_2= polylactic-*co*-glycolic acid nanoparticles with Itraconazole at 1060nm, 630nm, 230nm.; T = Itraconazole emulsion in Triton X-100; W = Itraconazole in water; control = *A.flavus* alone.
[2]SEM: standard error of the mean.
[3]Letter group: means with different letters are significantly different ($P < 0.05$). Least square means were compared among treatments over time when a significant treatment by time interaction ($P < 0.0001$) was observed using *Tukey* post-hoc multiple comparison adjustment.

www.manaraa.com

Vita

Nipur Patel received his Bachelor of Science in biological and agricultural engineering in December 2007 from Louisiana State University. During his undergraduate studies, he worked at Pennington Biomedical Research center in the Dr. Hansel Laboratory for Cancer Prevention, conducting tests of potential cancer therapeutic compounds. After graduating from LSU, he worked for two years at Esperance Pharmaceuticals as a research associate on the development and testing of proteins intended for targeted cancer therapies. He is an active member of The American Association for the Advancement of Science (AAAS). He joined the Biological and Agricultural Engineering Department in the fall semester of 2009. Since, Nipur has published one paper on studies conducted on this project and will be publishing a follow up paper shortly. Nipur Patel will be awarded the degree of Master of Science in Biological and Agricultural Engineering from LSU in August 2010.

www.manaraa.com